COMPETITION BETWEEN FUSION AND QUASIFISSION IN THE FORMATION OF SUPERHEAVY ELEMENTS

D.J. Hinde

Department of Nuclear Physics
Research School of Physics and Engineering
Australian National University
Canberra, ACT 2601,
Australia

15 MV NEC 14UD tandem electrostatic accelerator
(David Weisser, Trevor Ophel)

Superconducting Linac (6 MV)
(Nikolai Lobanov, Tibor Kibedi)

FUSION17 Conference 20-24 Feb 2017

Hobart, Tasmania, Australia (summer)
http://fusion17.anu.edu.au/

(Nanda Dasgupta)

NCRIS
National Research Infrastructure for Australia
An Australian Government Initiative

Australian National University

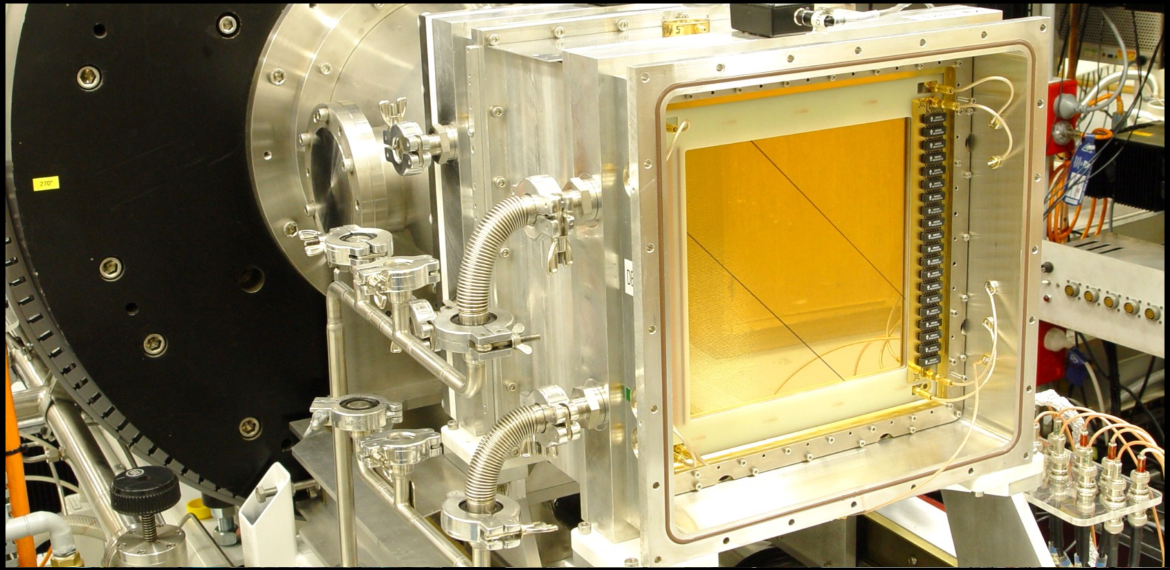

SOLITAIRE

8T superconducting solenoid

E.R. detectors

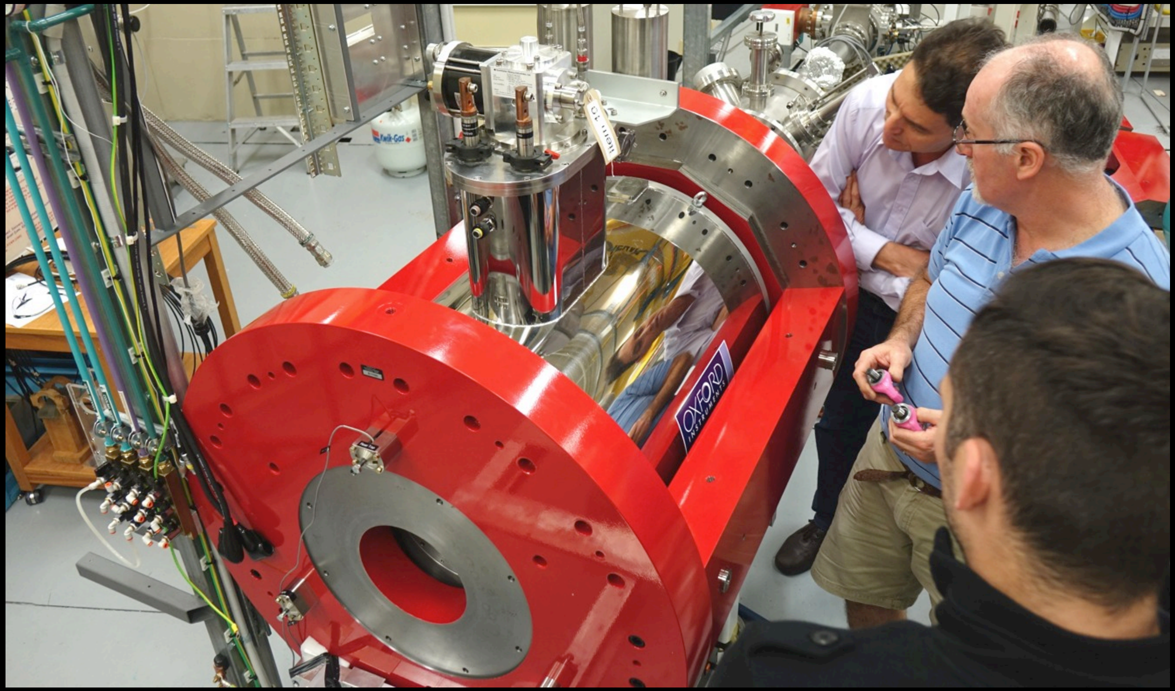

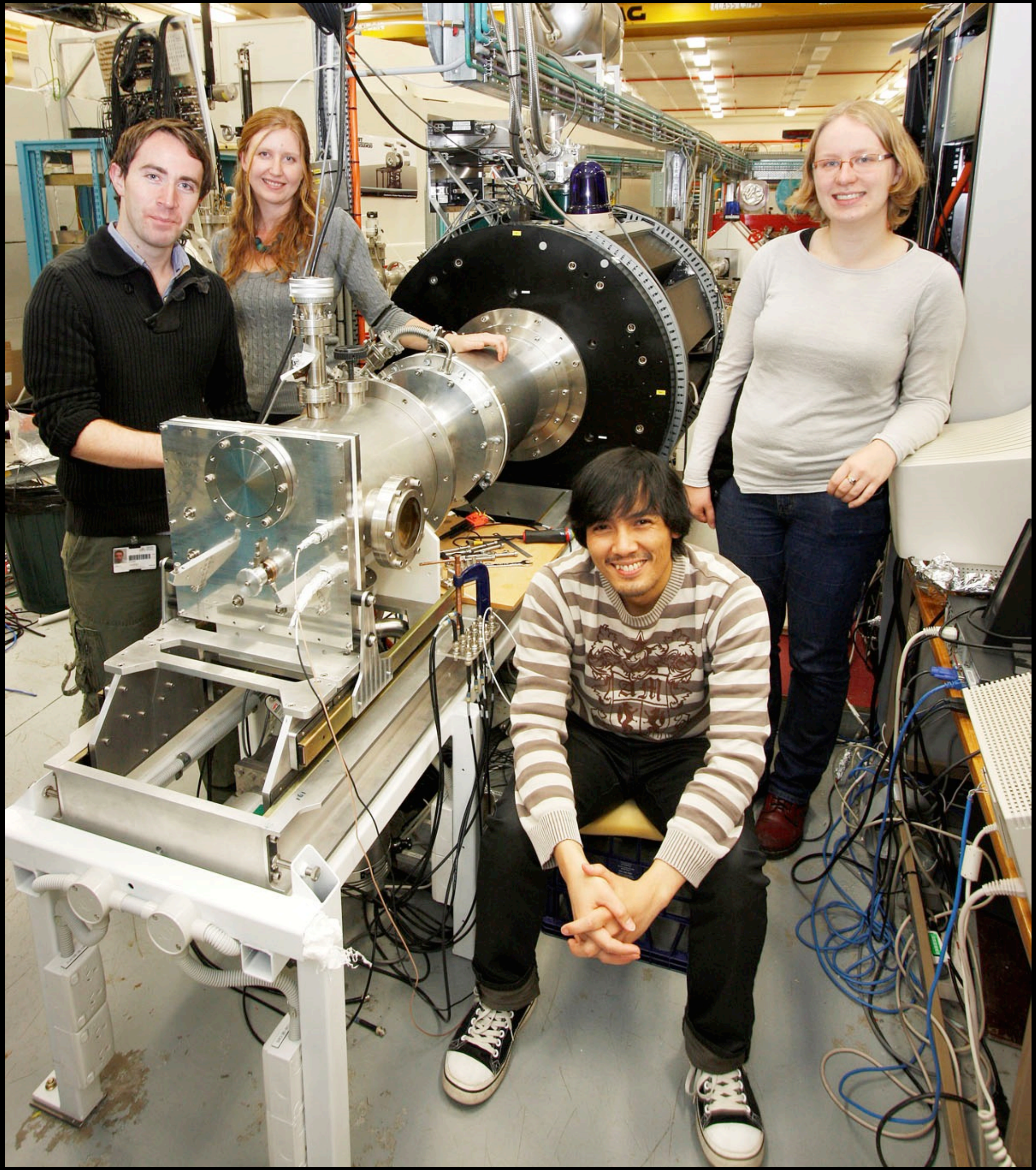

RIB: SOLEROO 6.5T s/c solenoid and tracking detectors

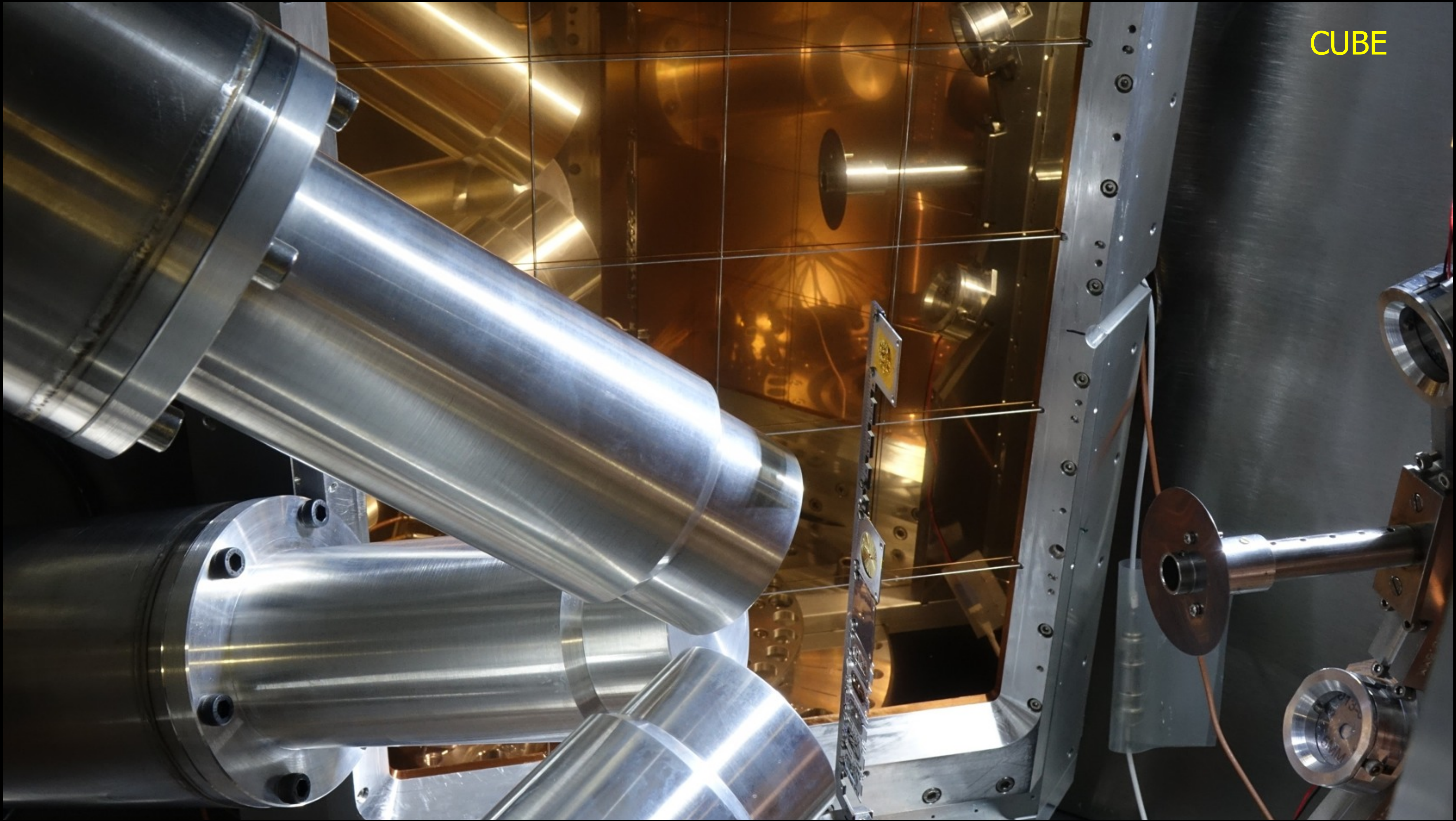
CUBE

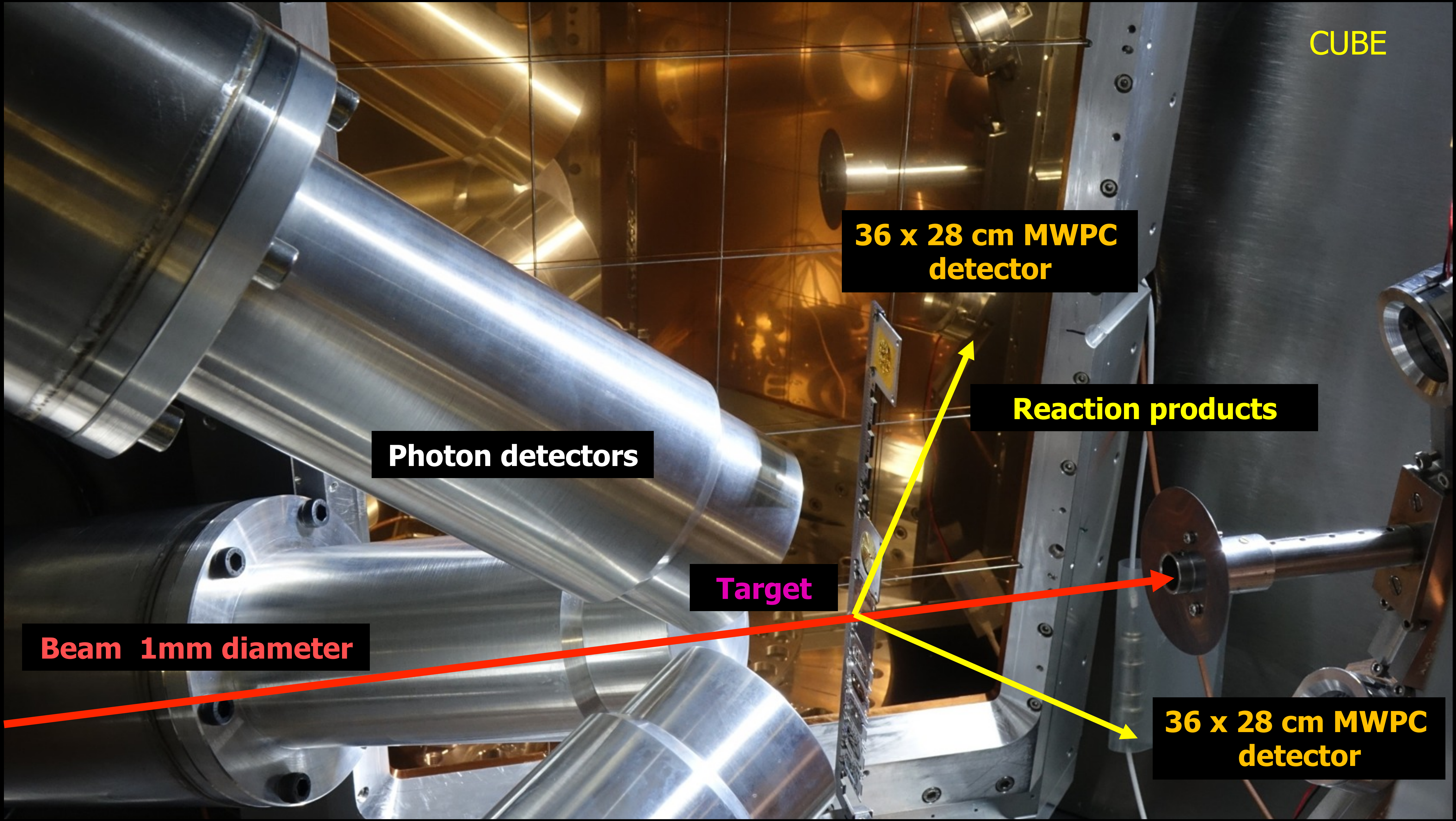
CUBE
36 x 28 cm MWPC detector
Reaction products
Photon detectors
Target
Beam 1mm diameter
36 x 28 cm MWPC detector

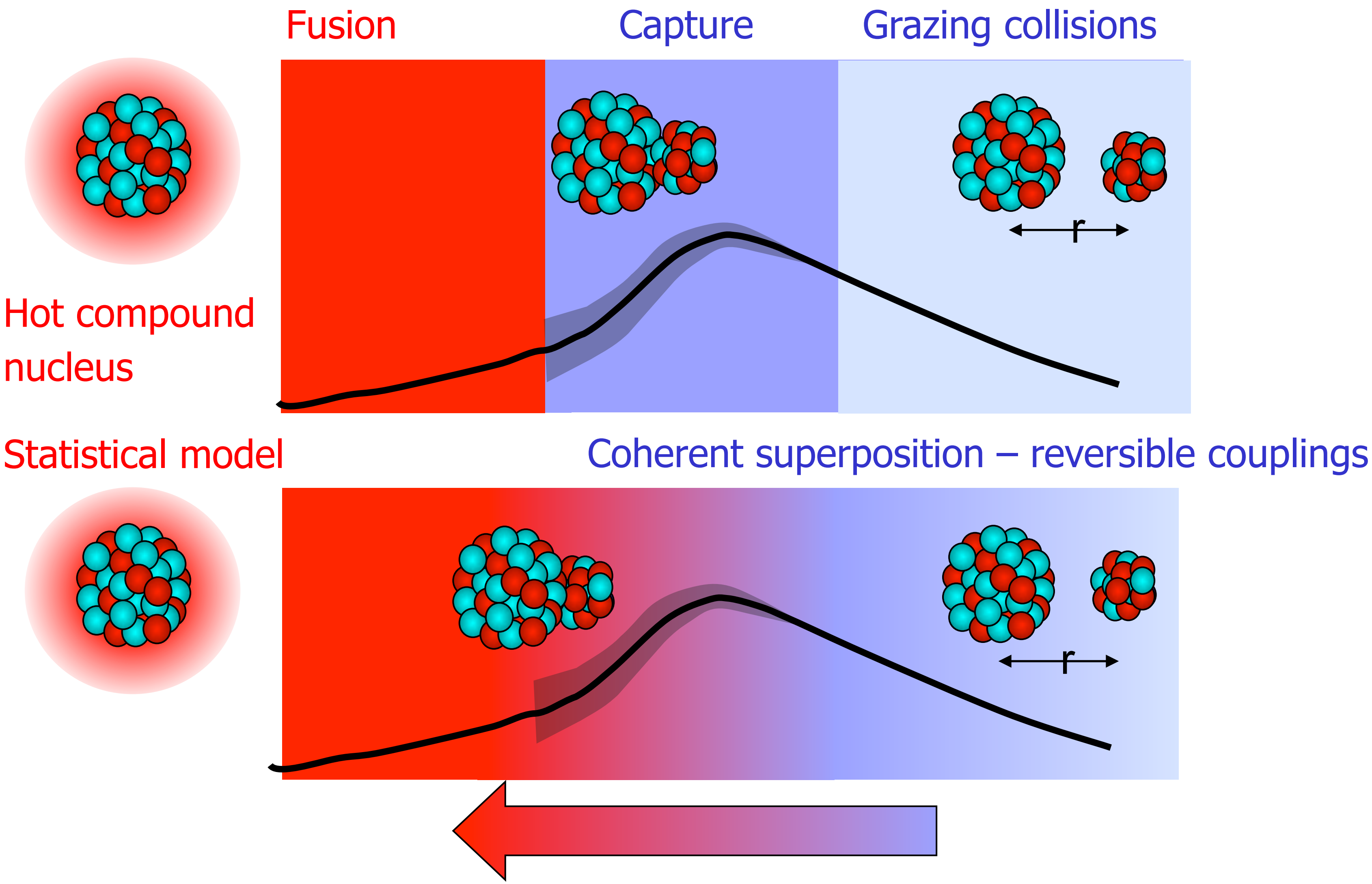

Microscopic understanding of the complex non-equilibrium interactions of two nuclei

Nuclear fusion forming superheavy elements

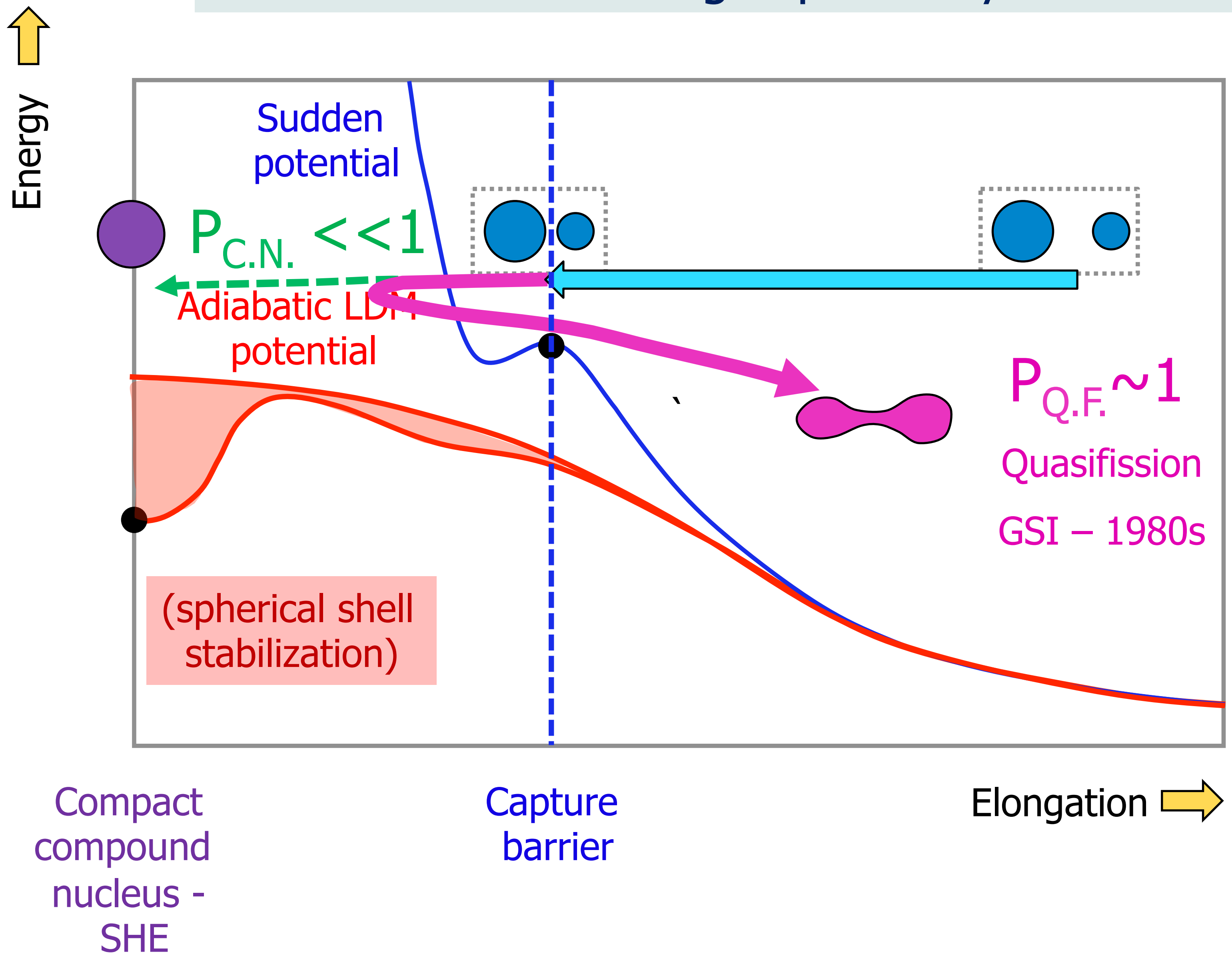

Nuclear fusion forming superheavy elements

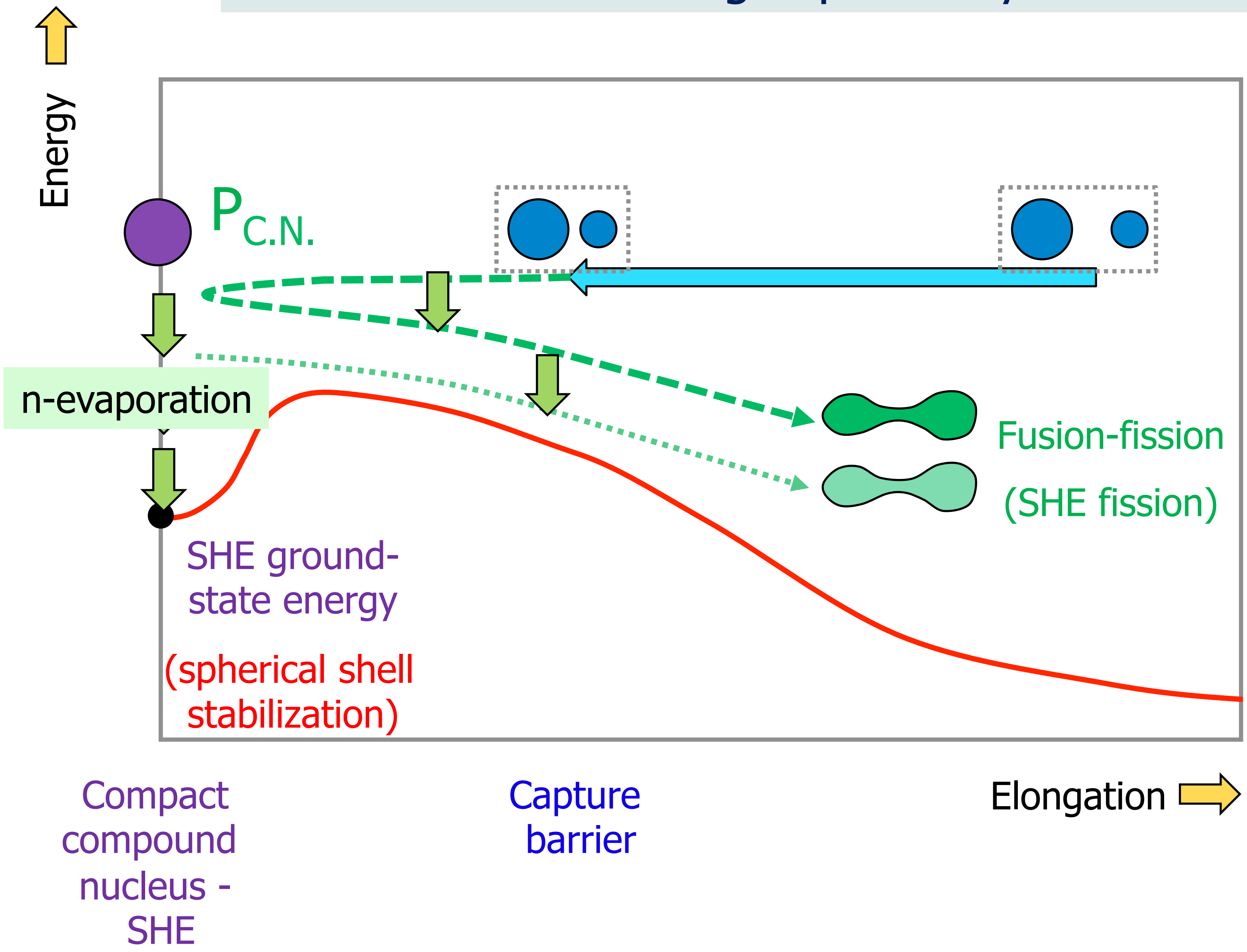

Reaction to form element 112 (Copernicium)

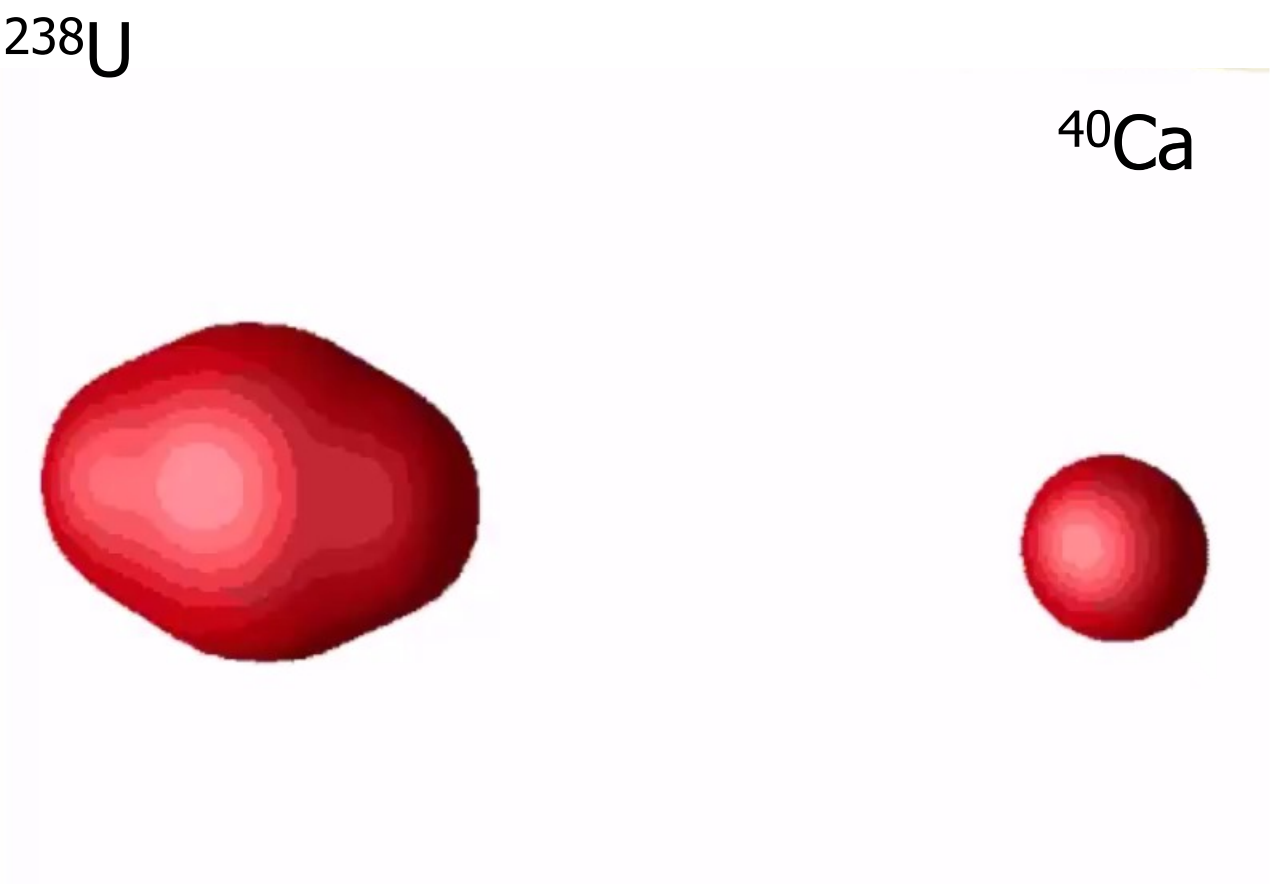

TDHF calculation of $^{40}Ca+^{238}U$ reaction (Cedric Simenel, Aditya Wakhle)

A. Wakhle et al., PRL **113** (2014) 182502

$$P_{CN} + P_{QF} = 1$$

PSHE=Pcapture. PCN . P fission survival

(E, L)

Quasifission: non-equilibrium process

Sticking time: a key characteristic

Dependence of quasifission probability and characteristics (time scale) on collision variables (related to P_{CN}):

- Compound nucleus fissility (Z^2/A);
- Entrance channel Coulomb repulsion (Z_1Z_2);
- Angular momentum;
- Nuclear structure of the colliding nuclei:
  - static deformation
  - closed shells (magic numbers)

Many variables!

Dependence of quasifission probability and characteristics (time scale) on collision variables (related to P_{CN}):

- Compound nucleus fissility (Z^2/A);
- Coulomb repulsion (Z_1Z_2);
- Angular momentum;
- Nuclear structure of the colliding nuclei:
  - deformation
  - closed shells (magic numbers)

Many variables!

Analogy between QF dynamics and nuclear masses

- Smooth liquid drop dynamics (Coulomb, nuclear, viscosity)
- Modification of dynamics due to shell structure (PES and viscosity)

Ultimate goal: reliable model including all relevant physics to predict P_{CN}

Model should predict QF characteristics, as QF is most likely outcome

MAD – time scales of mass-equilibration and rotation (GSI)

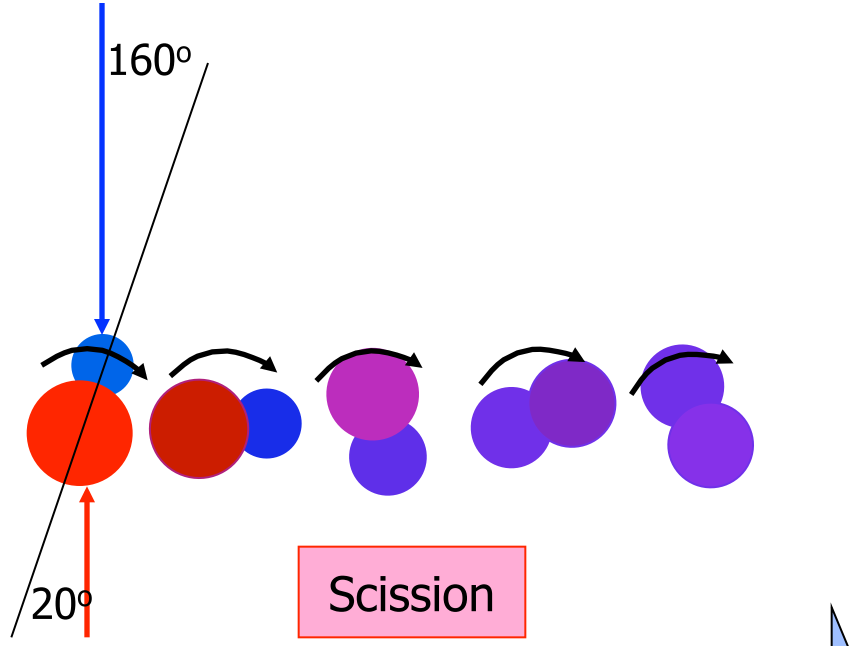

R. Bock et al., NP **A388** (1982) 334
J. Toke et al., NP **A440** (1985) 327
W.Q. Shen at al., PRC **36** (1987) 115
B.B. Back et al., PRC **53** (1996) 1734

Miminal mass-angle correlation

Strong mass-angle correlation

Mass-angle distributions – MAD

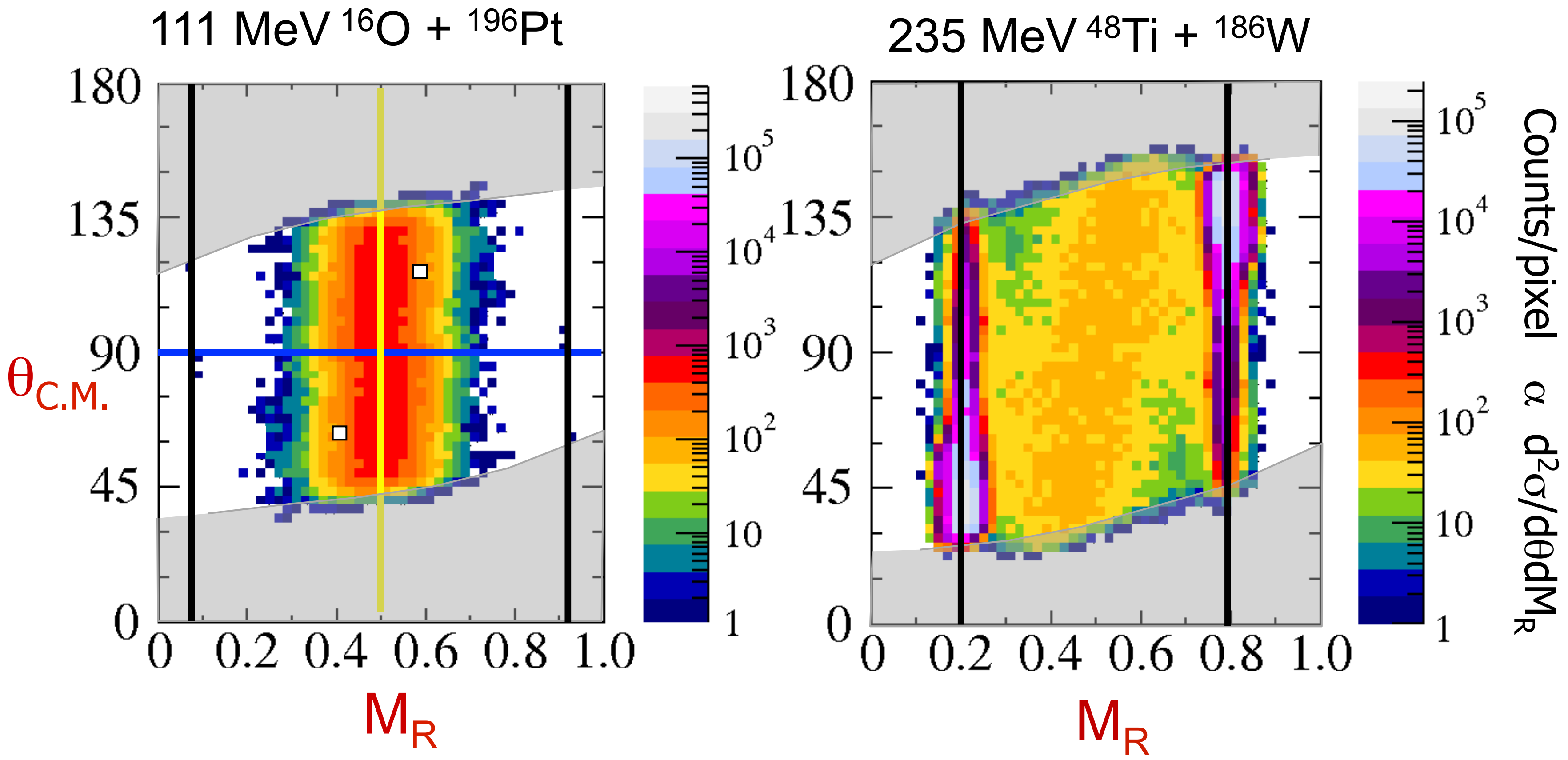

MAD – mass-equilibration and rotation (GSI 1980's)

R. Bock et al., NP **A388** (1982) 334
J. Toke et al., NP **A440** (1985) 327
W.Q. Shen at al., PRC **36** (1987) 115
B.B. Back et al., PRC **53** (1996) 1734

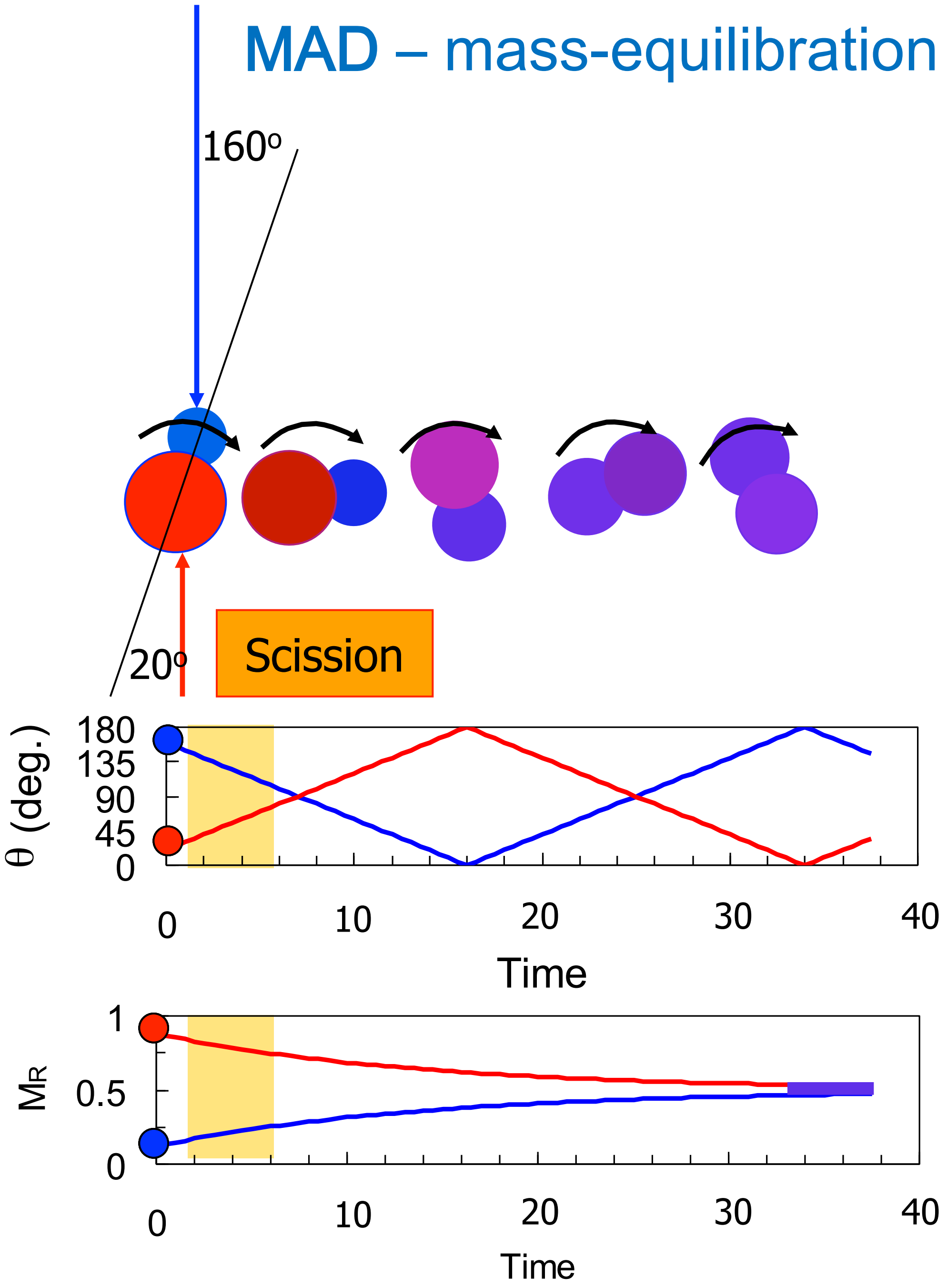

Little mass and angle evolution

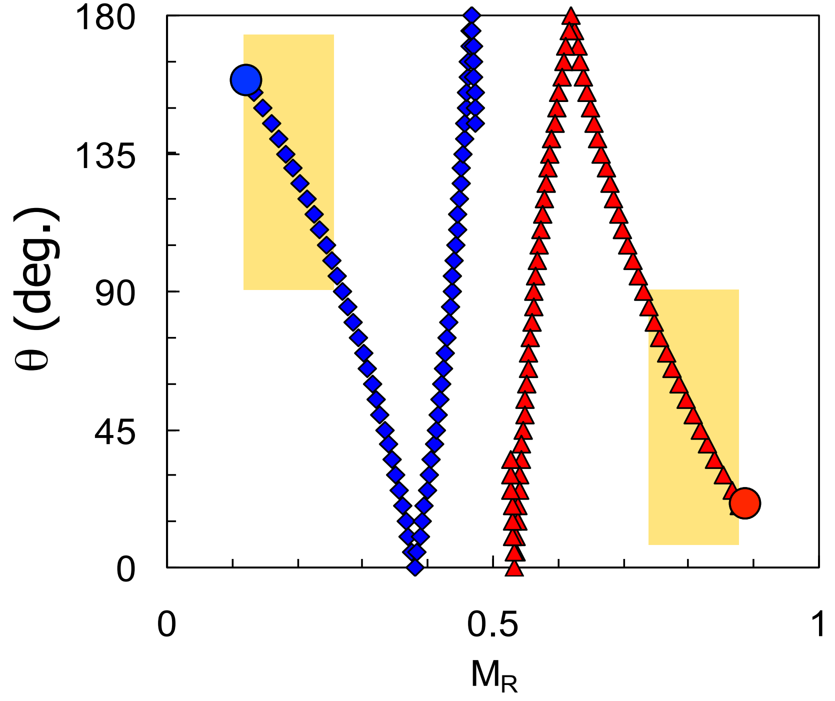

QF Timescales from MAD

Experimental MAD

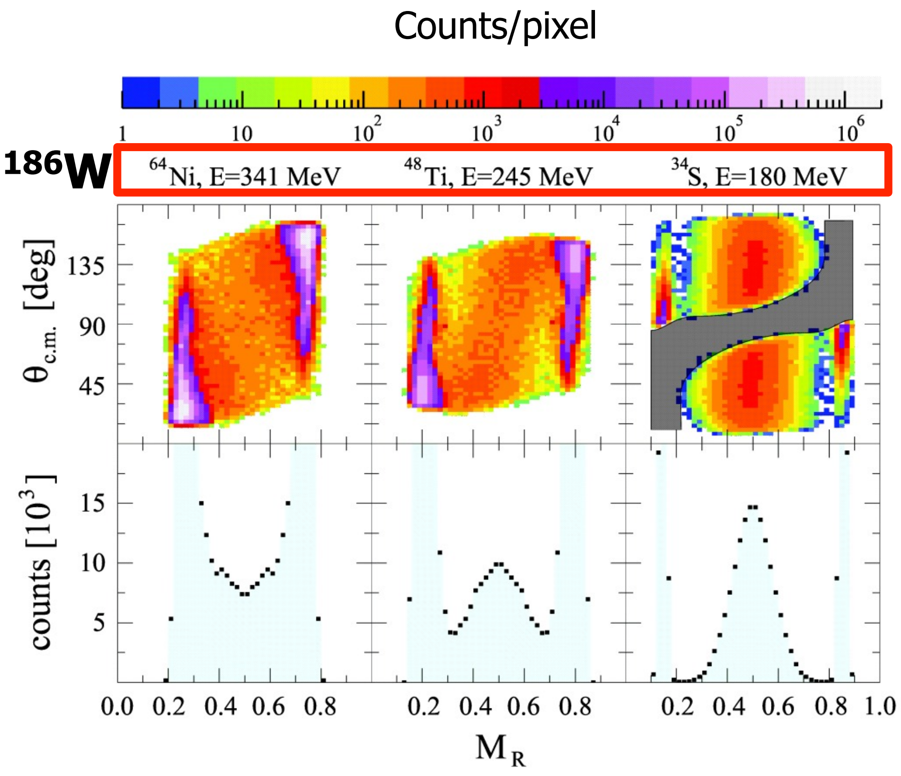

R. du Rietz et al. PRL **106** (2011) 052701

Defining smooth liquid drop QF dynamics

- minimise shell effects – high Ex – high E/V_b
- minimise effects of angular momentum – low E/V_b
- Compromise: choose E/V_b = 1.05-1.10
  - effects of spherical magic numbers attenuated by Ex
  - effects of deformation alignment averaged out
  - in angular momentum regime relevant to SHE production

Defining smooth liquid drop QF dynamics

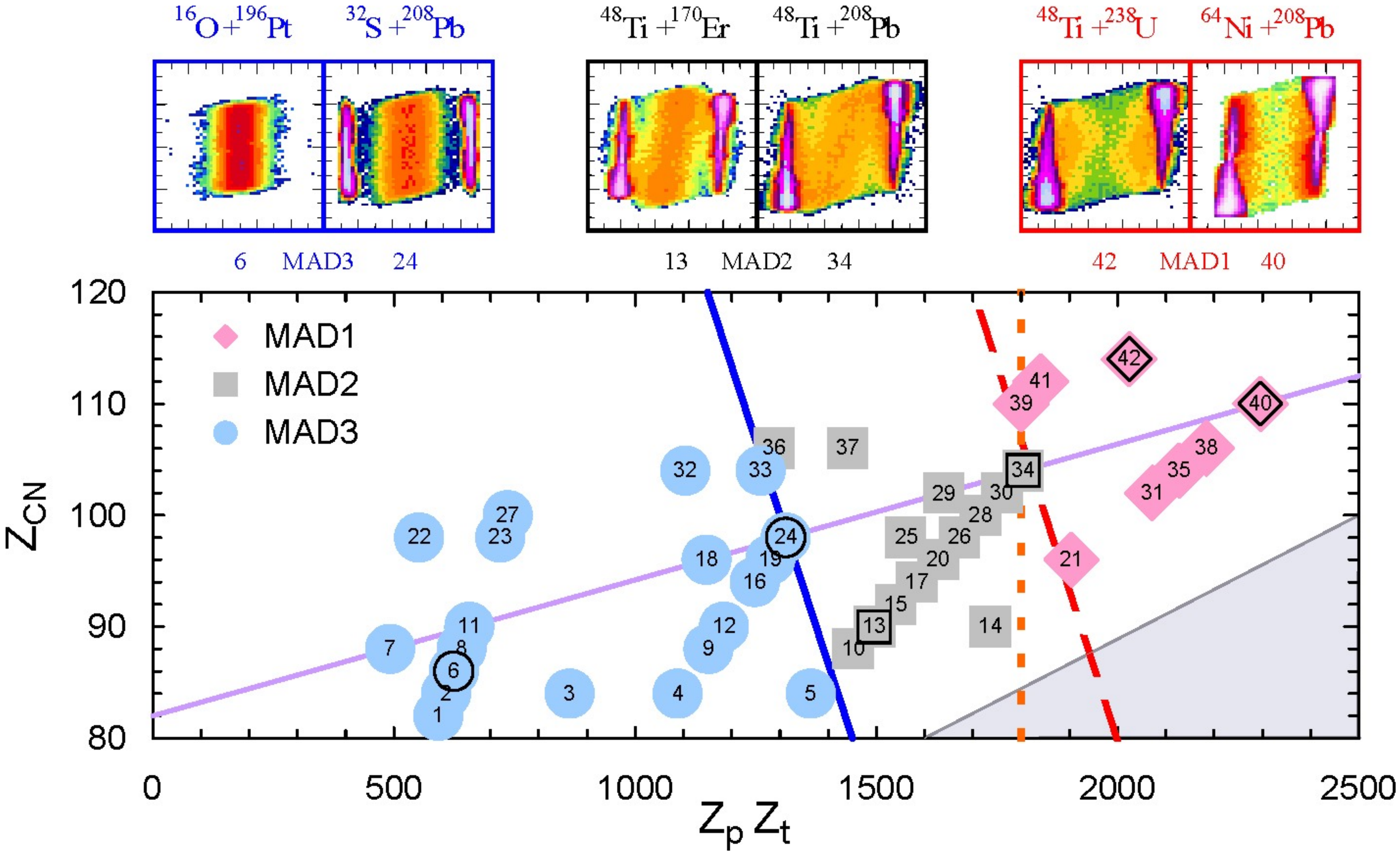

R. du Rietz et al., PRC **88** (2013) 054618

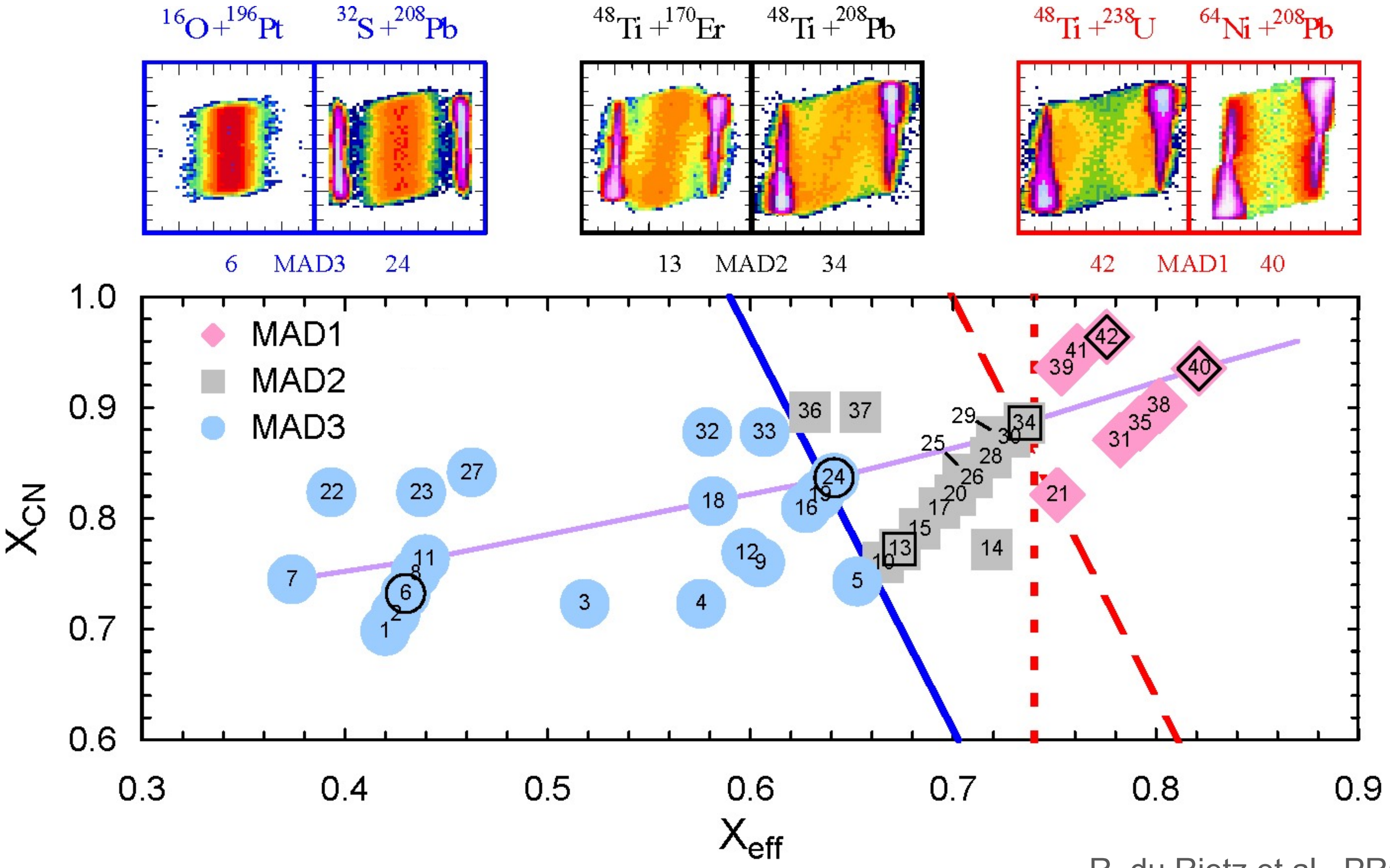

R. du Rietz et al., PRC **88** (2013) 054618

$$x_{CN} = \frac{(Z^2/A)}{(Z^2/A)_{crit}} \qquad (Z^2/A)_{crit} = 50.883\,(1 - 1.7826\,I^2)$$

$$I = (A - 2Z)/A$$

$$x_{eff} = \frac{4Z_1 Z_2/\left[A_1^{1/3} A_2^{1/3}\left(A_1^{1/3} + A_2^{1/3}\right)\right]}{(Z^2/A)_{crit}}$$

W. J. Swiatecki, Phys. Scr. **24, 113 (1981)**

Nuclear structure effects: (i) deformation alignment

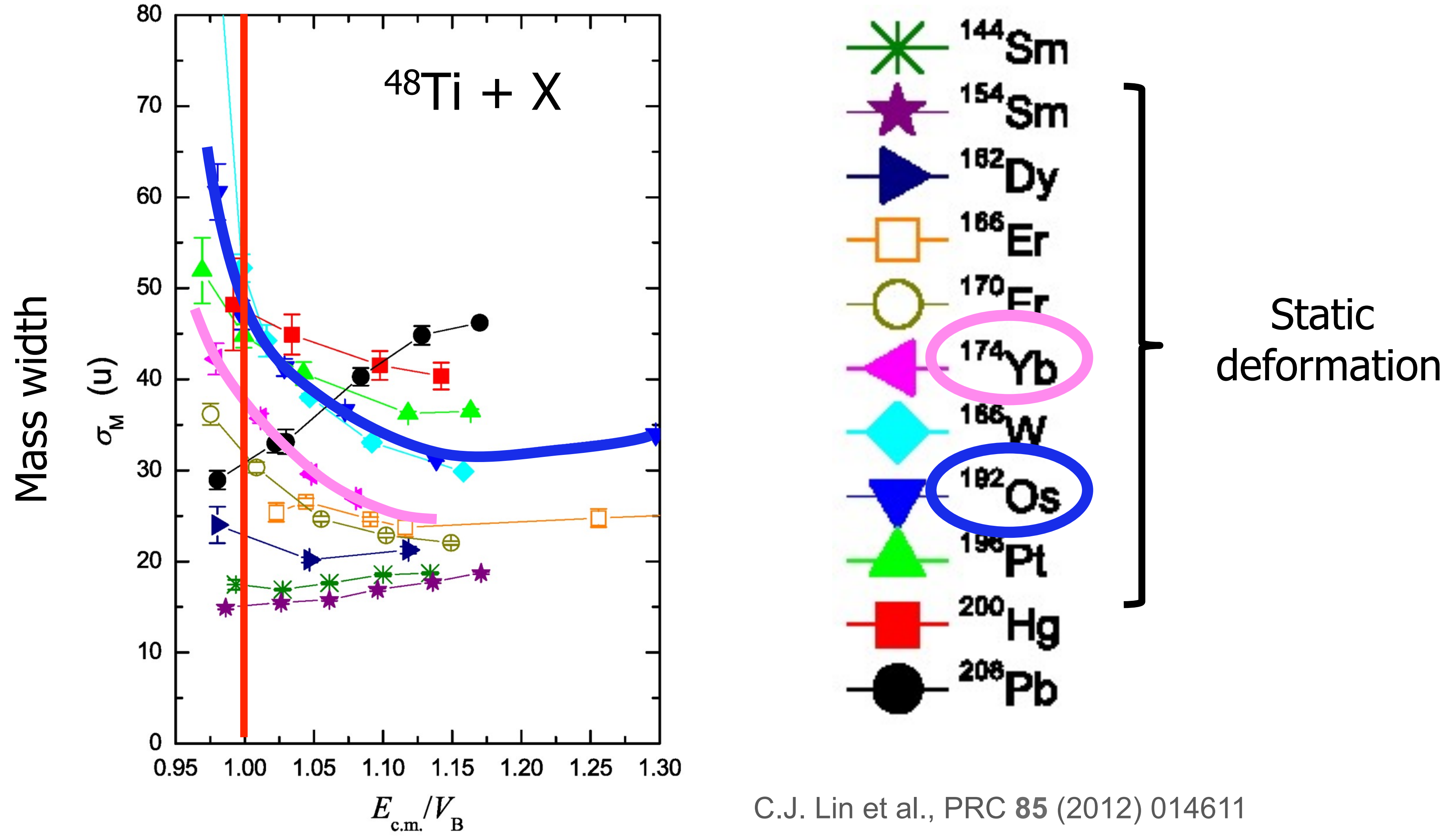

C.J. Lin et al., PRC **85** (2012) 014611

Consistent with measurements showing no/small ER σ sub-barrier

Nuclear structure effects: (i) deformation alignment

Static deformation alignment

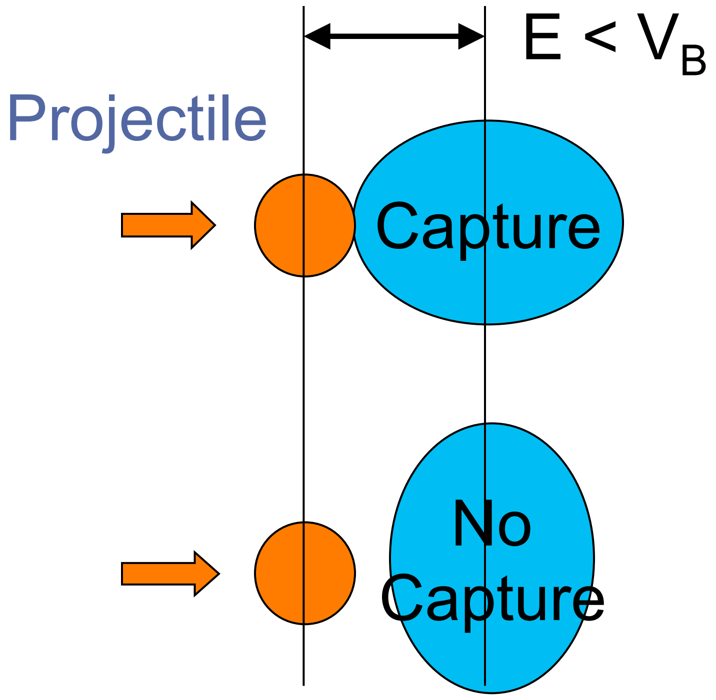

Hinde et al., PRL **74** (1995) 1295; Hinde et al., PRC **53** (1996) 1290

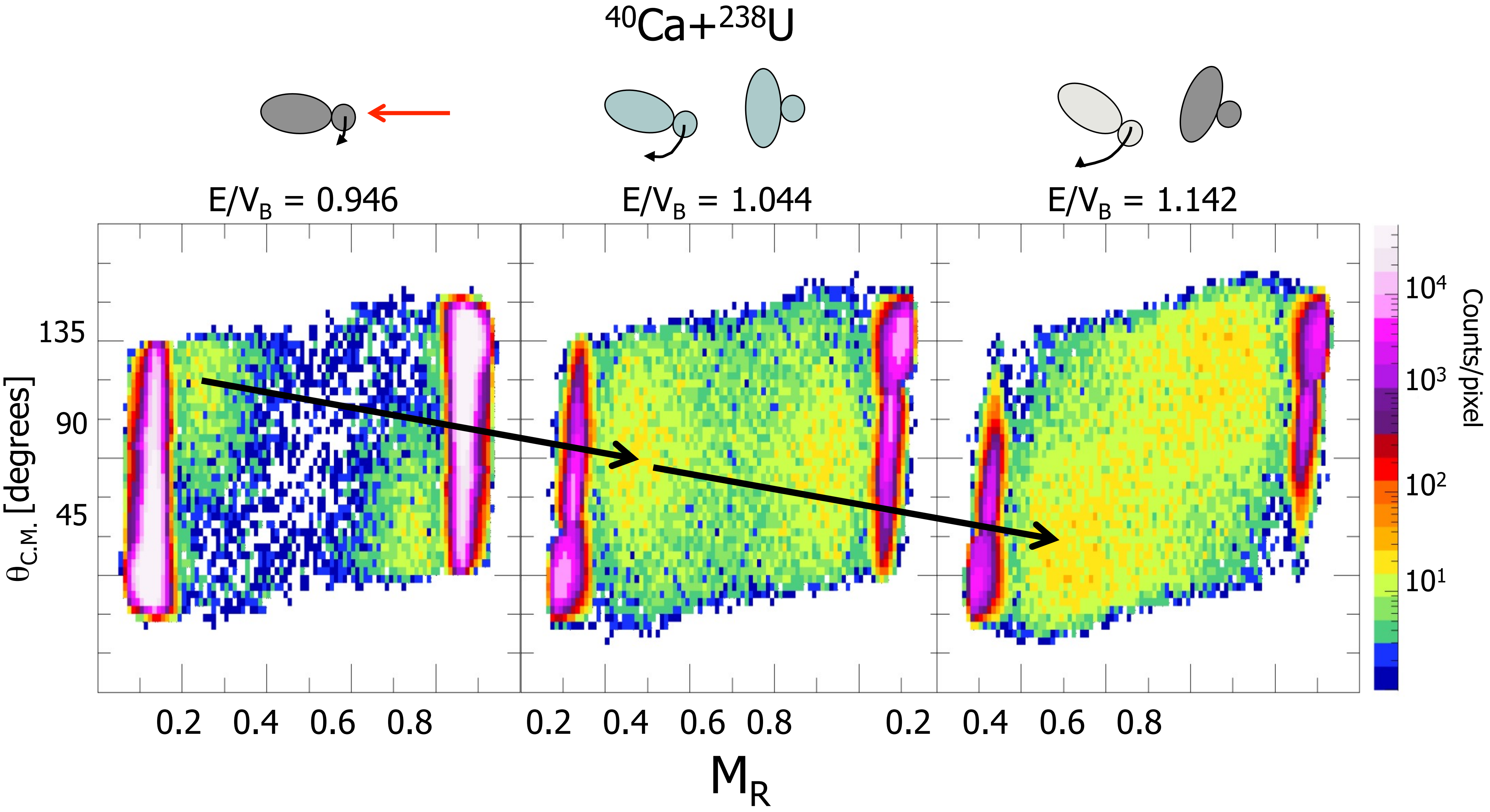

A. Wakhle et al., PRL **113** (2014) 182502

Deformation alignment

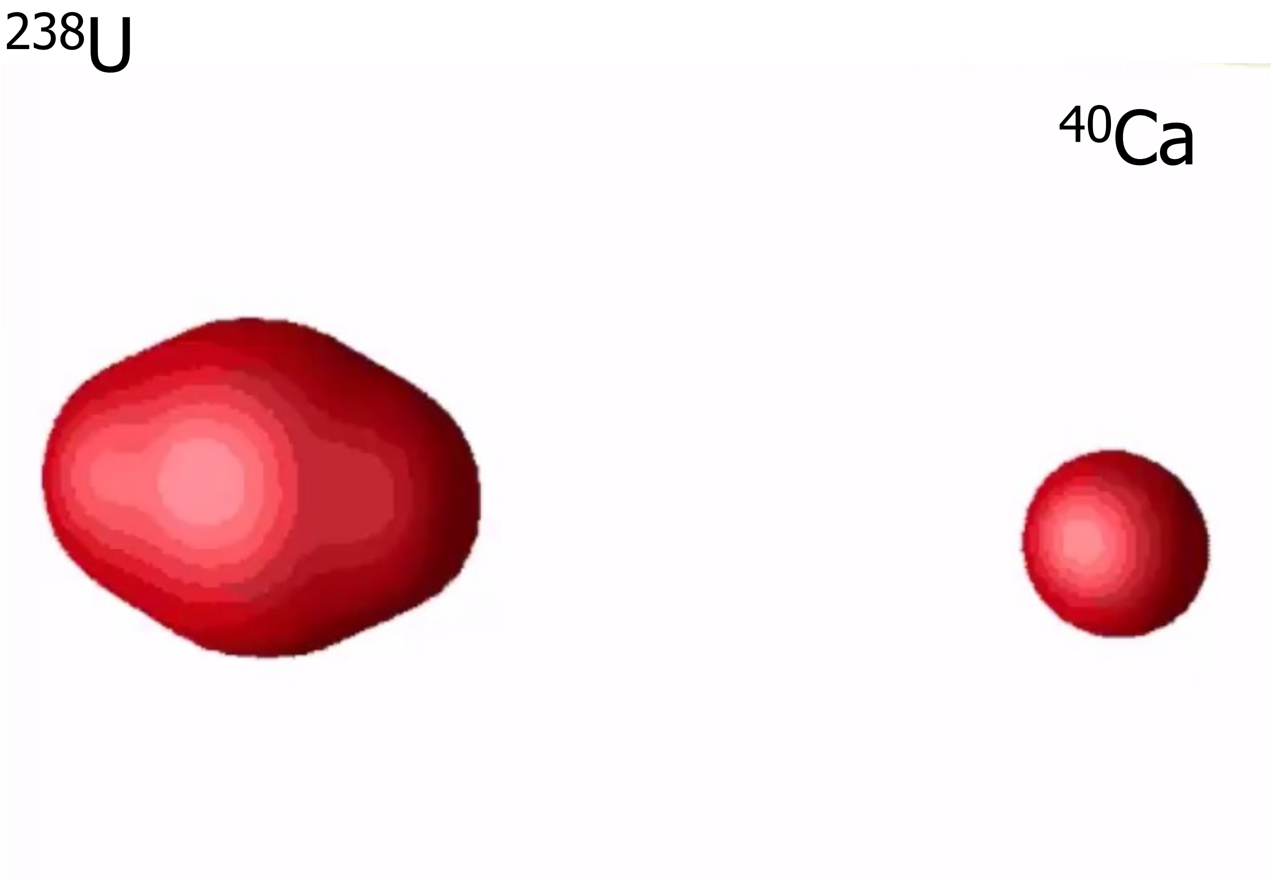

TDHF calculation of ^{40}Ca+^{238}U reaction (Cedric Simenel, Aditya Wakhle)

A. Wakhle et al., PRL **113** (2014) 182502

Deformation alignment – experiment vs. TDHF $^{40}Ca+^{238}U$

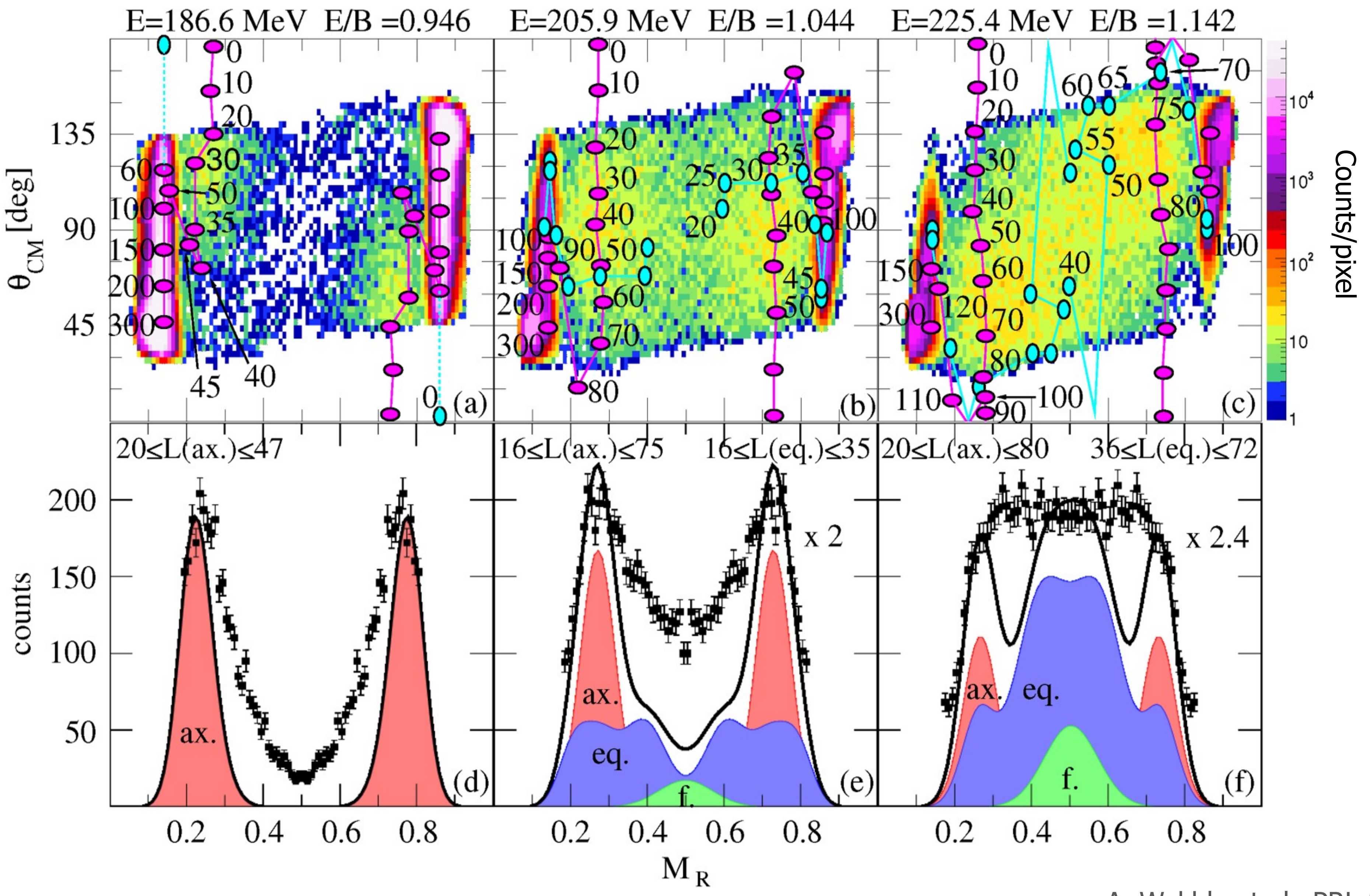

A. Wakhle et al., PRL **113** (2014) 182502

$^{54}Cr + ^{238}U$ (Z = 116; ^{292}Lv)

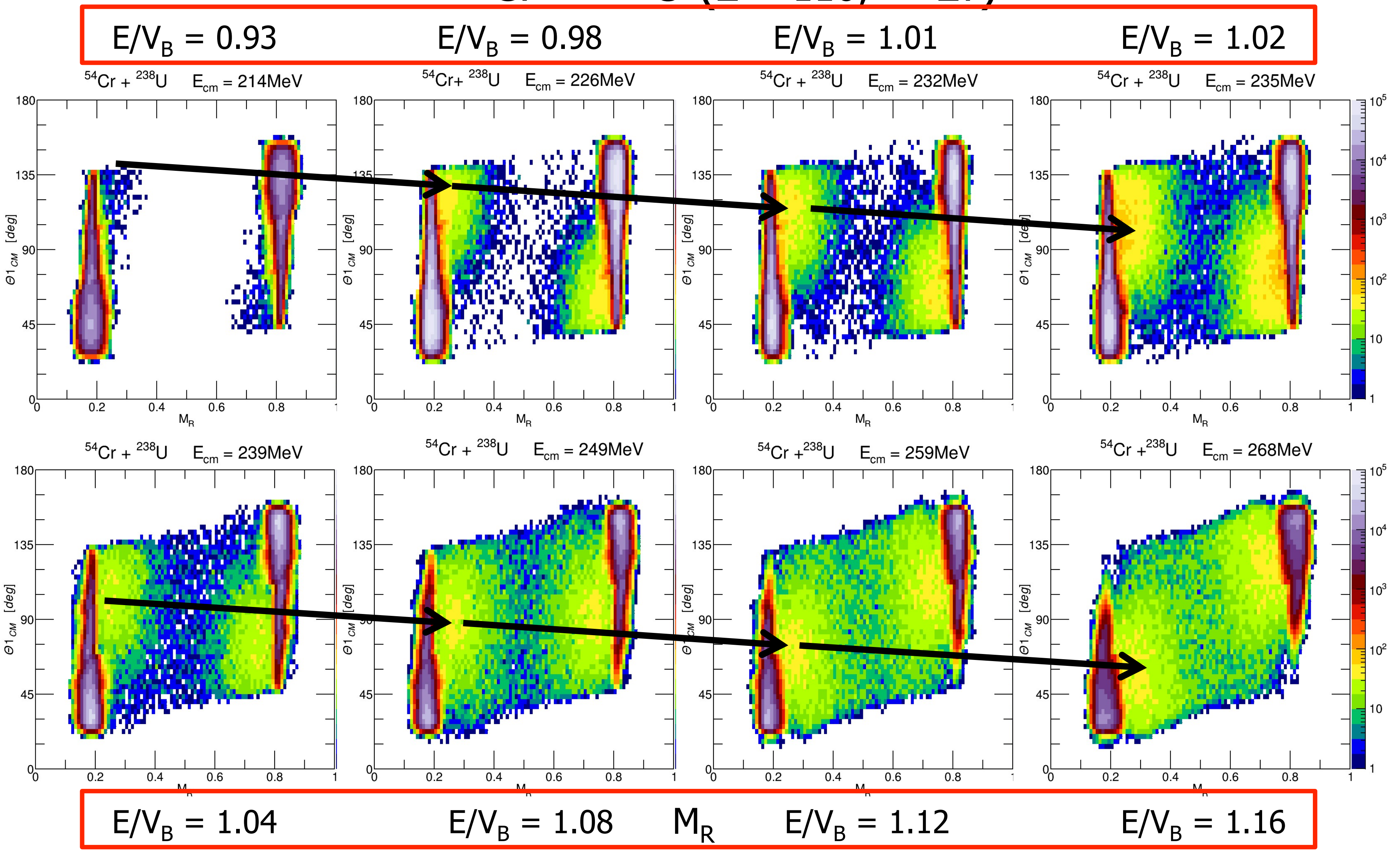

+ other measurements with ^{48}Ca, ^{50}Ti, ^{54}Cr, ^{58}Fe and ^{64}Ni beams bombarding ^{232}Th, ^{238}U, ^{244}Pu, ^{248}Cm, ^{249}Cf targets forming Z up to 120 (thanks to Mainz radiochem., GSI targetlab)

2016-2017

Nuclear structure effects: (ii) magic numbers

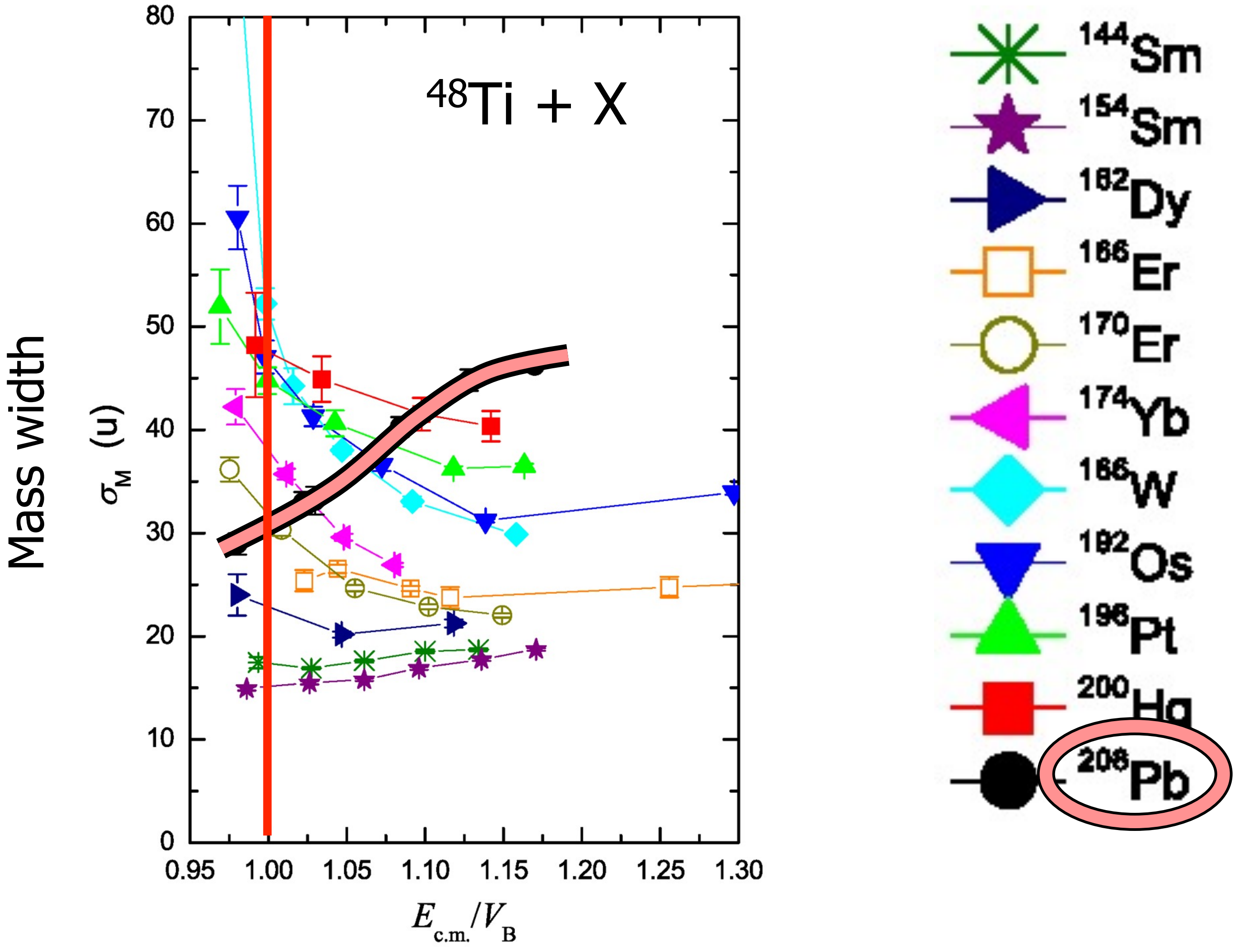

C.J. Lin et al., PRC **85** (2012) 014611

Spherical magic nuclei – multiple magic numbers

C. Simenel et al., PLB710 (2012) 607

E. Prokhorova et al., NPA802(2008)45

$E/V_B = 0.98$

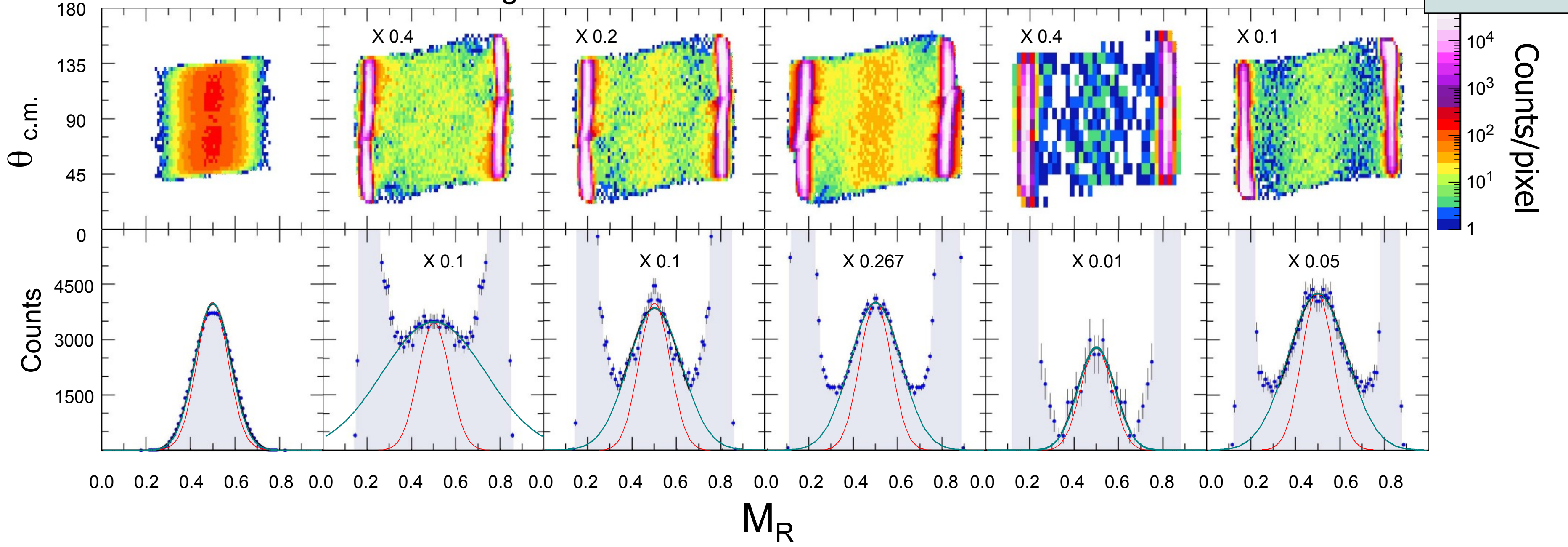

	$^{254}_{100}Fm$ ($^{16}O + ^{238}U$)	$^{248}_{102}No$ ($^{48}Ti + ^{200}Hg$)	$^{256}_{104}Db$ ($^{48}Ti + ^{208}Pb$)	$^{248}_{102}No$ ($^{44}Ca + ^{204}Pb$)	$^{252}_{102}No$ ($^{48}Ca + ^{204}Pb$)	$^{248}_{102}No$ ($^{40}Ca + ^{208}Pb$)	$^{256}_{102}No$ ($^{48}Ca + ^{208}Pb$)
σ_{MR}	0.081	0.237	0.120	0.114	0.084	0.126	0.068
err	0.001	0.018	0.003	0.002	0.006	0.004	0.002
N_{magic}	2	0	2	2	3	4	4

Entrance channel closed shells and N/Z mismatch

N/Z equilibration will cause early energy damping as nuclei overlap:
- more elongated “entry point” to diffusive motion

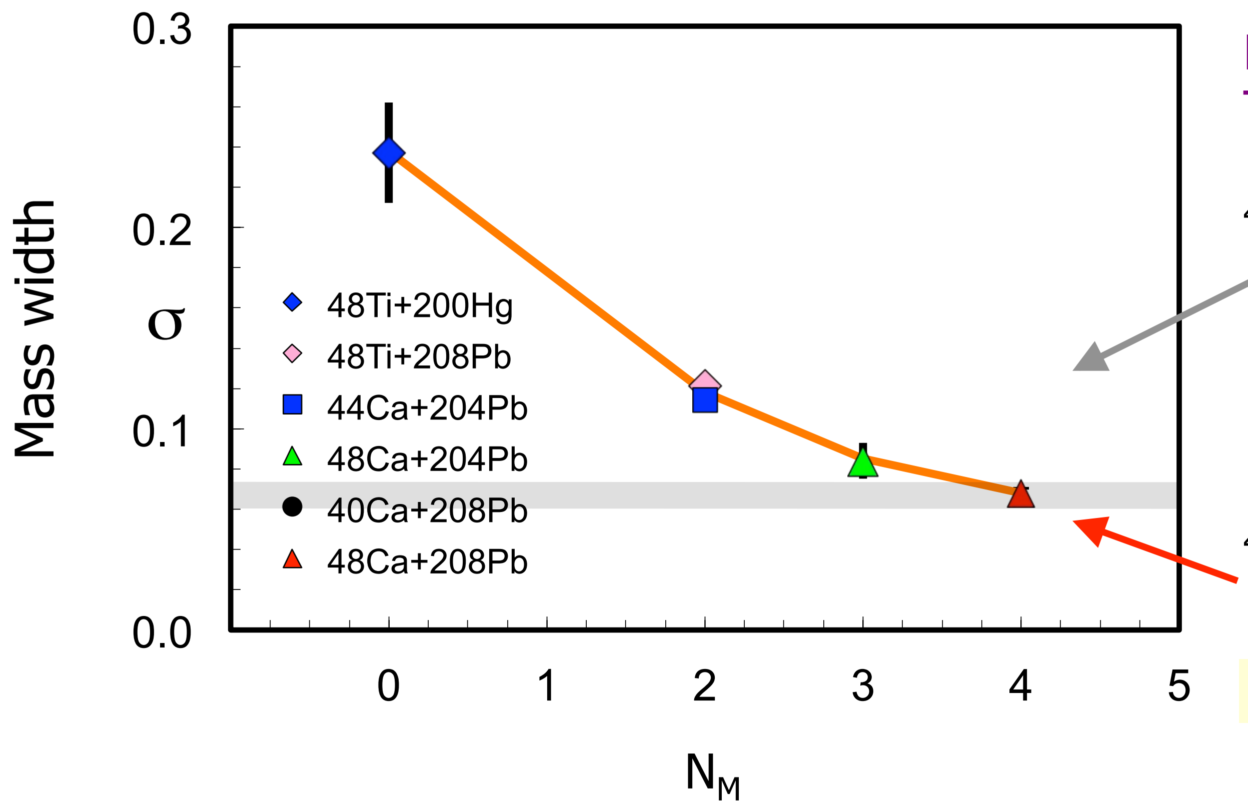

Fast N/Z equilibration.
TDHF calculated outcomes:

$^{40}Ca+^{208}Pb$
P(no transfer) ~ 10^{-4}

Average transfer outcome:
$^{42}Ar+ ^{206}Po$ $N_m = 0$

$^{48}Ca+^{208}Pb$
P(no transfer) ~ 0.5

C. Simenel et al., PLB 710 (2012) 607

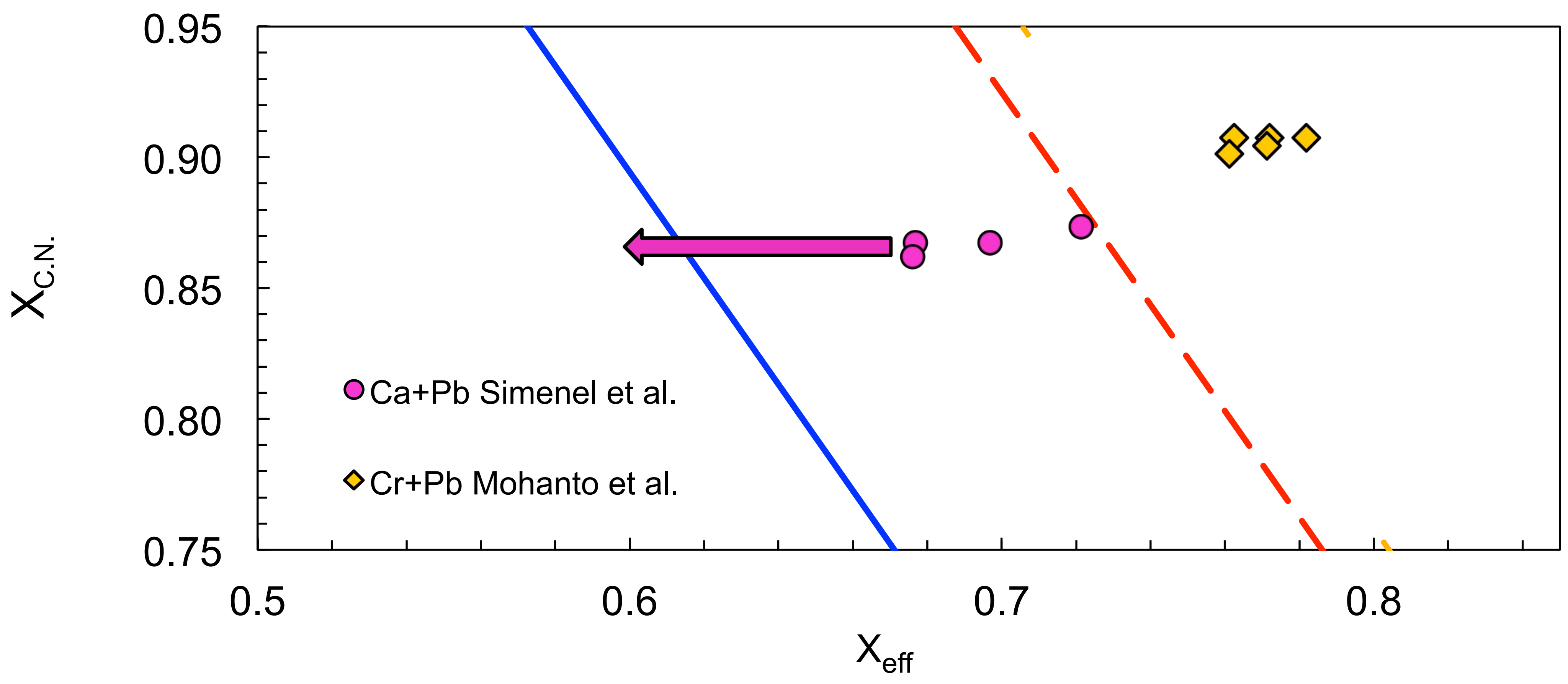

C. Simenel et al., PLB **710** (2012) 607

G. Mohanto et al., ANU, in preparation

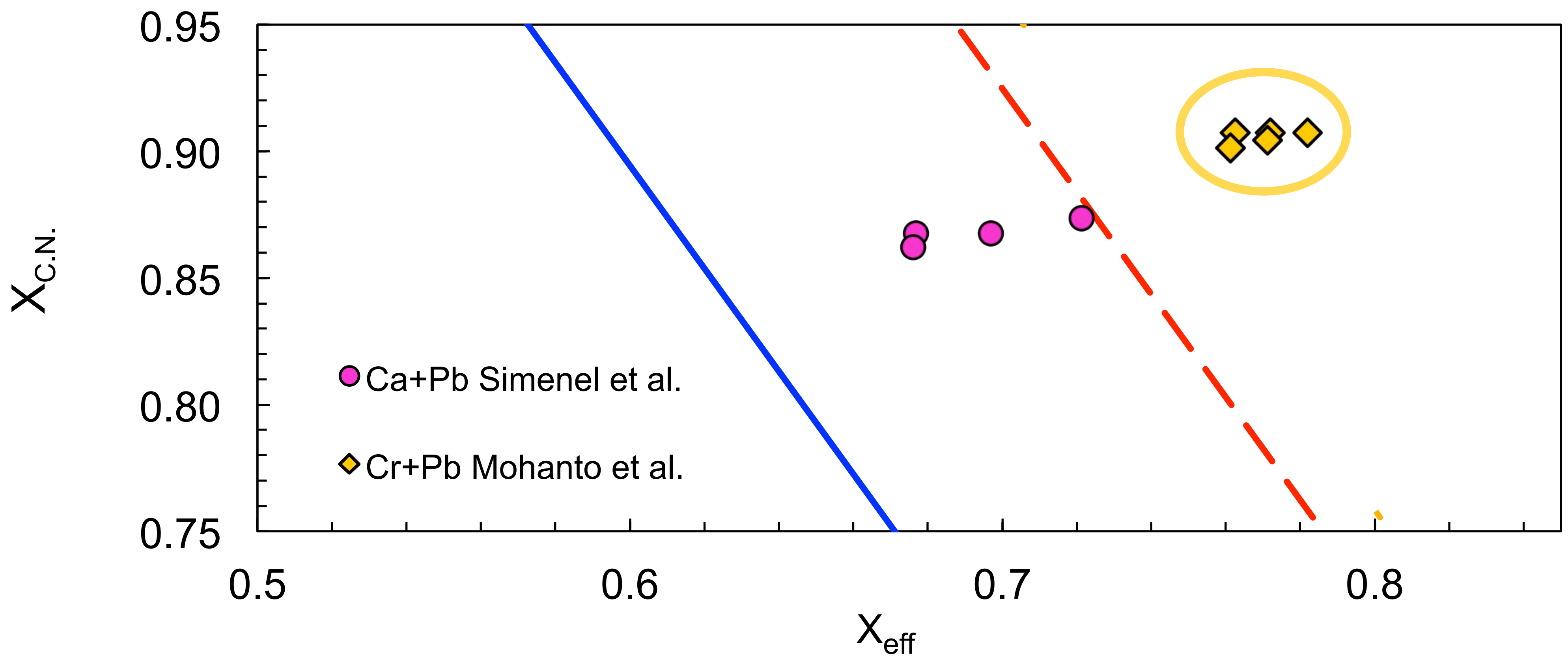

$^{50,52,54}Cr + {}^{208,206,204}Pb \rightarrow {}^{258,260,262}Sg$ (Z=106)

C. Simenel et al., PLB **710** (2012) 607

G. Mohanto et al., ANU, in preparation

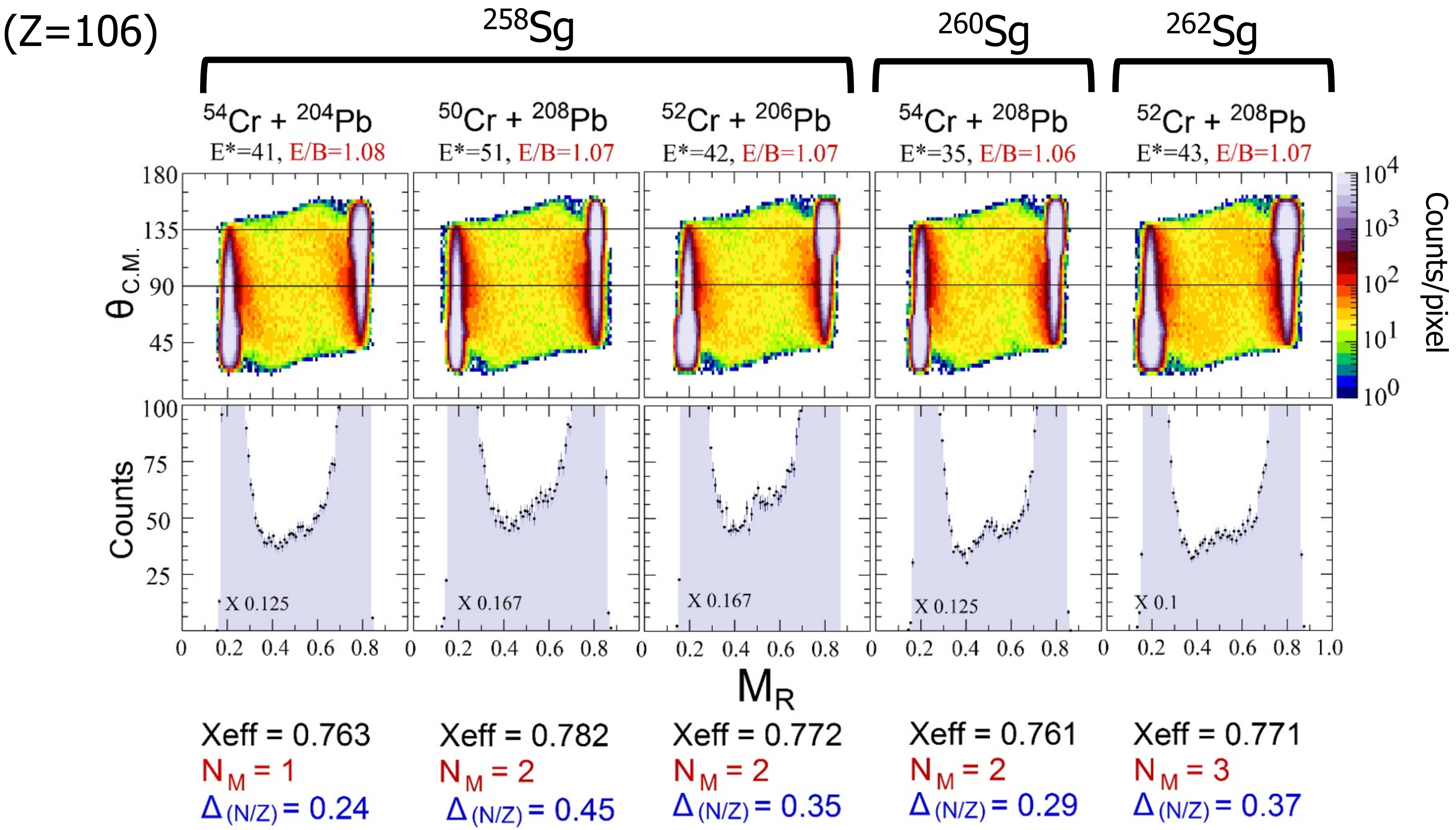

Energy well above-barrier: magic numbers, N/Z matching – little effect

G. Mohanto et al., ANU, in preparation

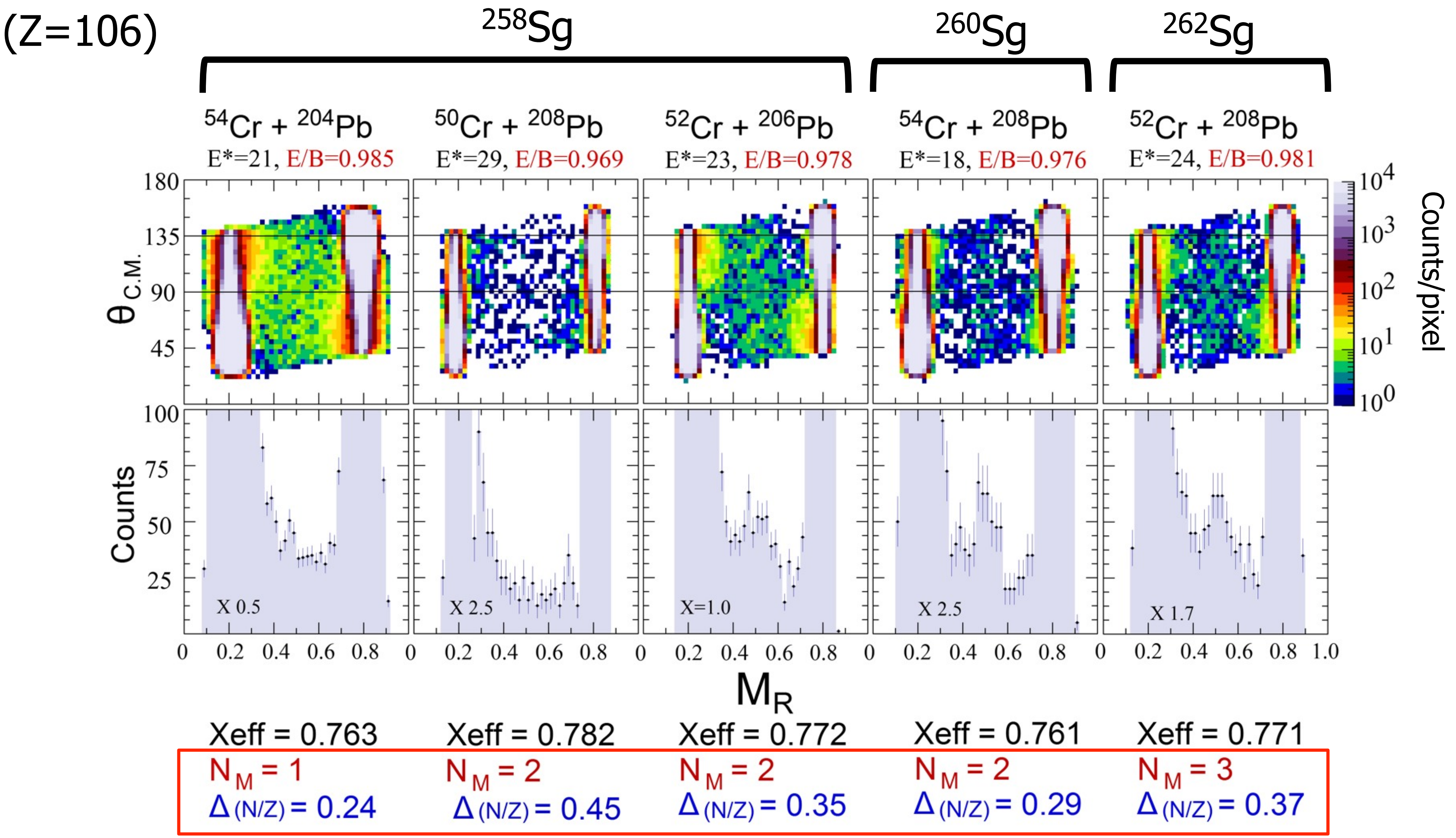

Sub-barrier energy: magic numbers, adequate N/Z matching – fusion-fission?

G. Mohanto et al., ANU, in preparation

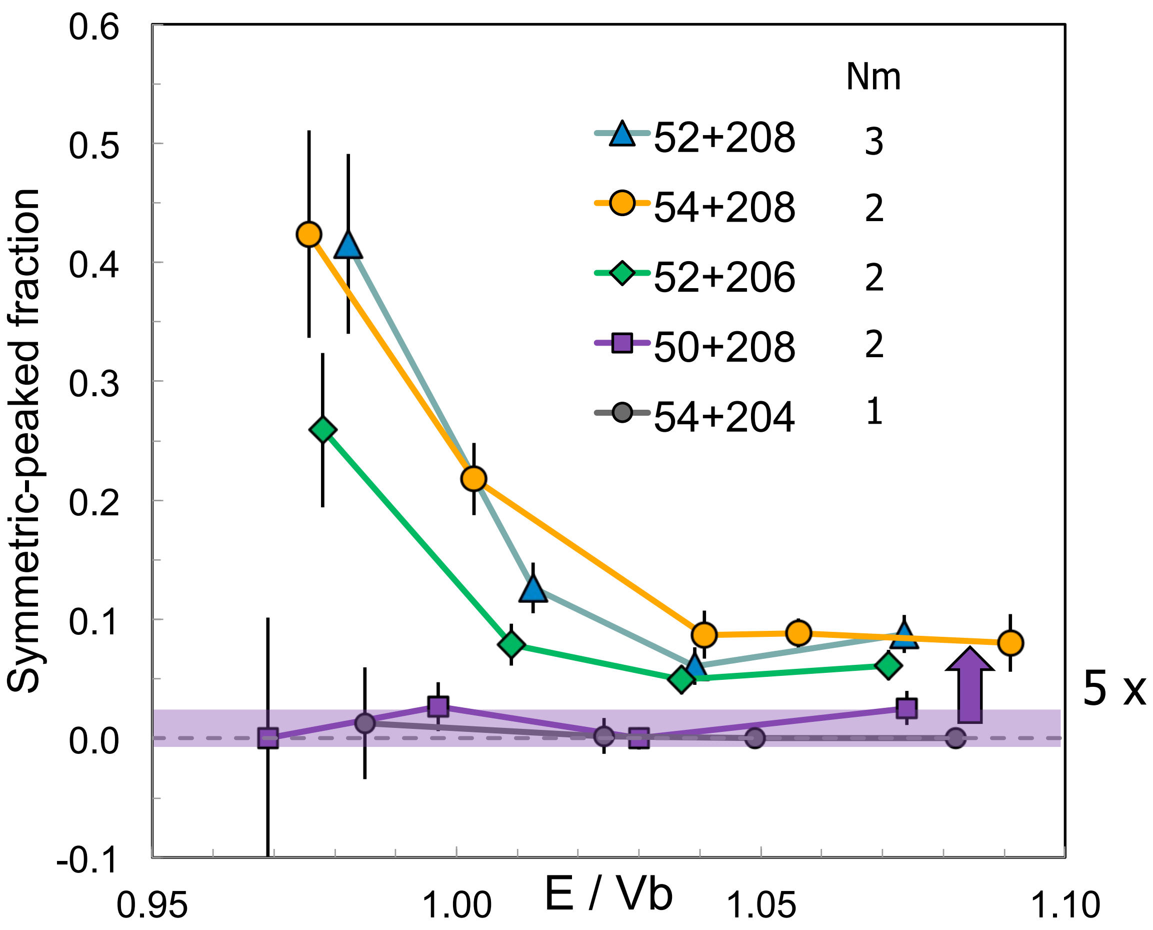

Trajectory bifurcation – slow mass-symmetric and fast mass-asymmetric

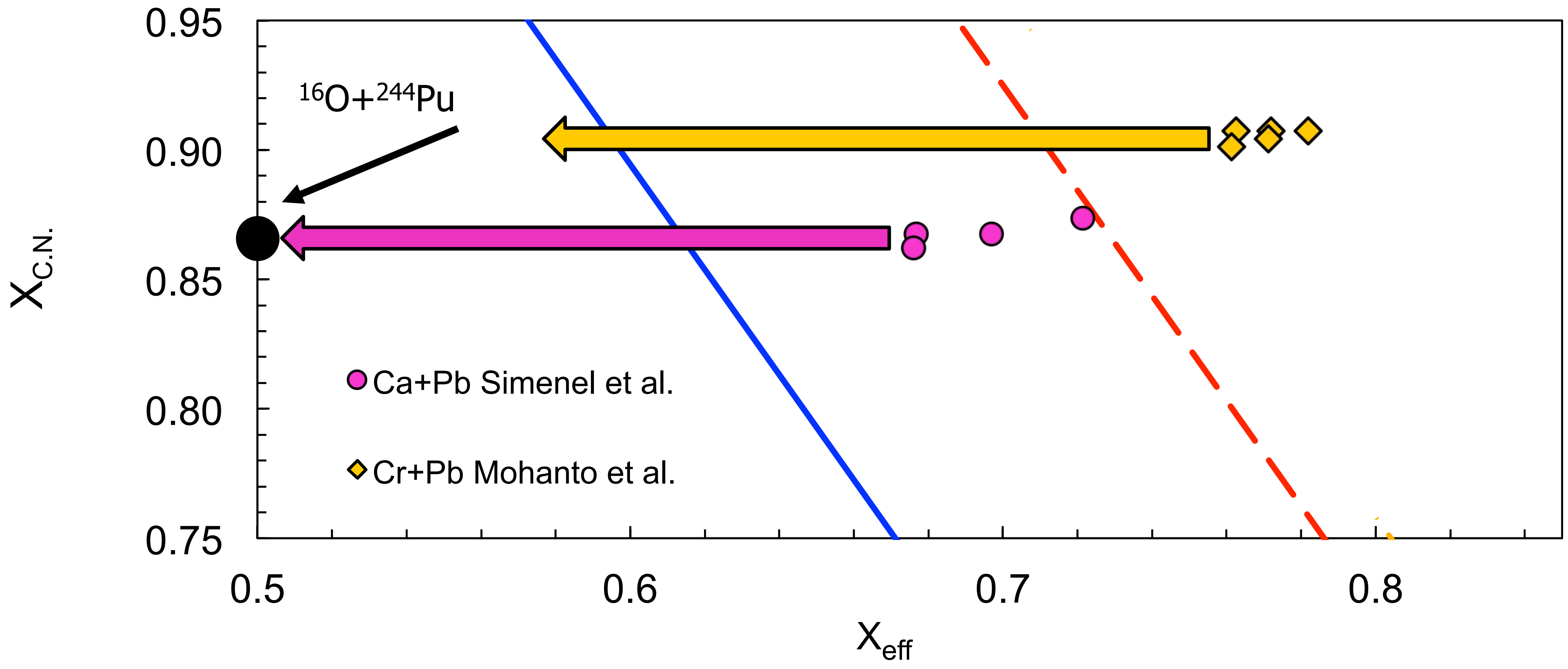

Nuclear structure of the projectile and target can play a very significant role

C. Simenel et al., PLB **710** (2012) 607

G. Mohanto et al., ANU, in preparation

M. Dasgupta
C. Simenel
E. Williams
D.Y. Jeung
E. Prasad
R. Rafiei
A. Wakhle (ANU, MSU)
R.G. Thomas (ANU, BARC)
R. du Rietz (ANU, Malmo)
C.J. Lin (ANU, CIAE)
G. Mohanto (ANU, BARC)
J. Khuyagbaatar (GSI)
Ch.E. Düllmann (GSI/Mainz)
H. David (GSI) .....
Z. Kohley (MSU)
K. Hammerton (MSU) .....
M. Morjean (GANIL)
D. Jacquet (Orsay) ......
+ many ANU students and postdocs running the ANU accelerator

Conclusions

- Determination of smooth trends of Mass-Angle Distributions allows to quantify the effects on sticking times of:
  - deformation alignment
  - entrance channel closed shells, N/Z matching
- Deformation alignment – "tip collisions" - short sticking times
  - fast QF below-barrier (agrees with small P_{CN} from σ_{xn})
- Magic numbers, N/Z matching important in cold fusion reactions
  - more magic numbers are better – $^{48}Ca+^{208}Pb$ – sub-barrier F-F
  - trajectory bifurcation $^{52,54}Cr$ + $^{206,208}Pb$ – fast QF + F-F
- Actinide collisions (U, Pu, Cm)
  - New systematic MAD measurements for ^{48}Ca, ^{50}Ti, ^{54}Cr, ^{64}Ni
  - Sticking times; mass evolution towards symmetry, fusion-fission
- Challenge for models: reproduce quasifission observables!

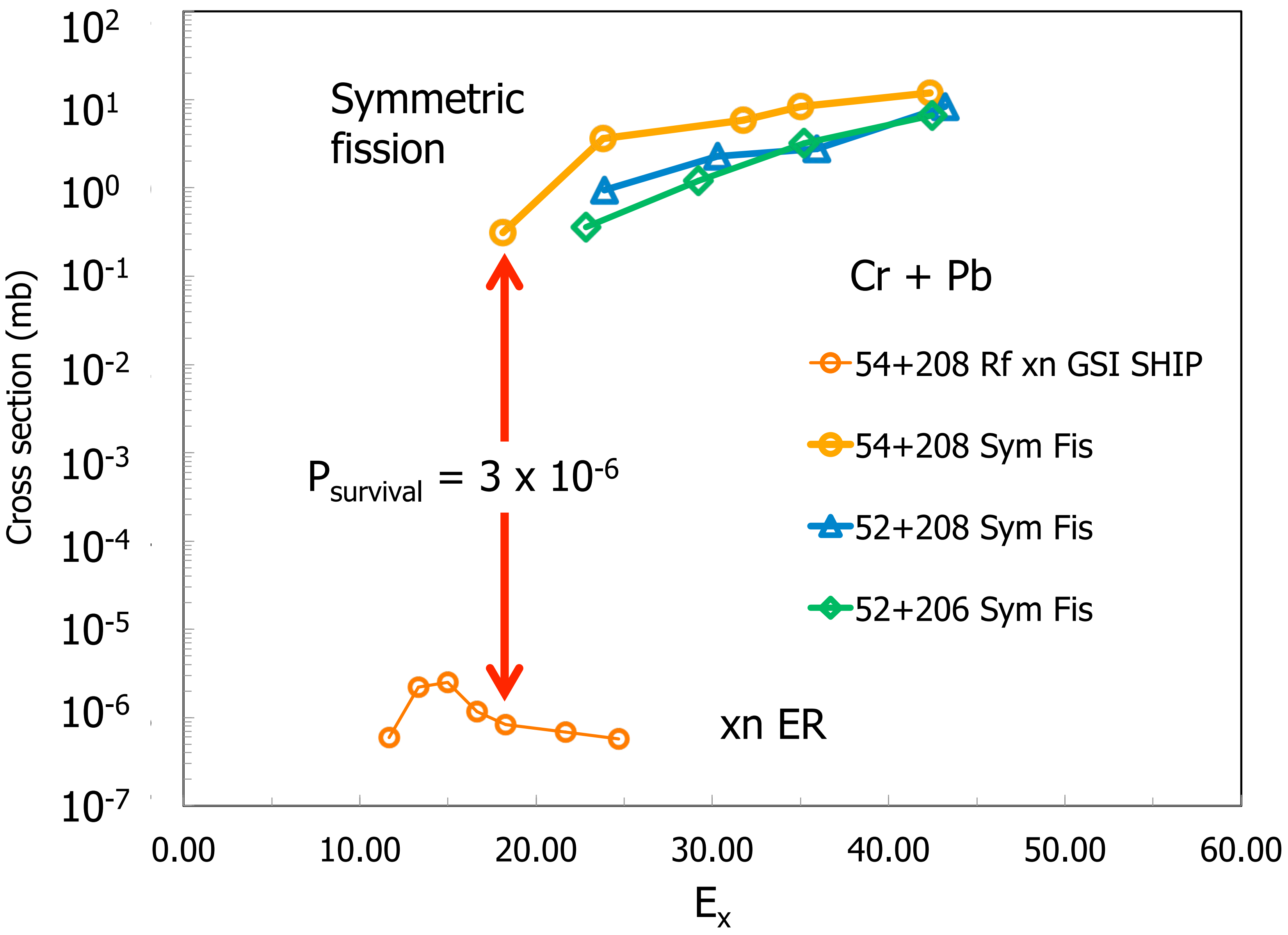

Symmetric fission
Cr + Pb
54+208 Rf xn GSI SHIP
54+208 Sym Fis
52+208 Sym Fis
52+206 Sym Fis
P_survival = 3 x 10^-6
xn ER
Cross section (mb)
10^2
10^1
10^0
10^-1
10^-2
10^-3
10^-4
10^-5
10^-6
10^-7
0.00
10.00
20.00
30.00
40.00
50.00
60.00
E_x

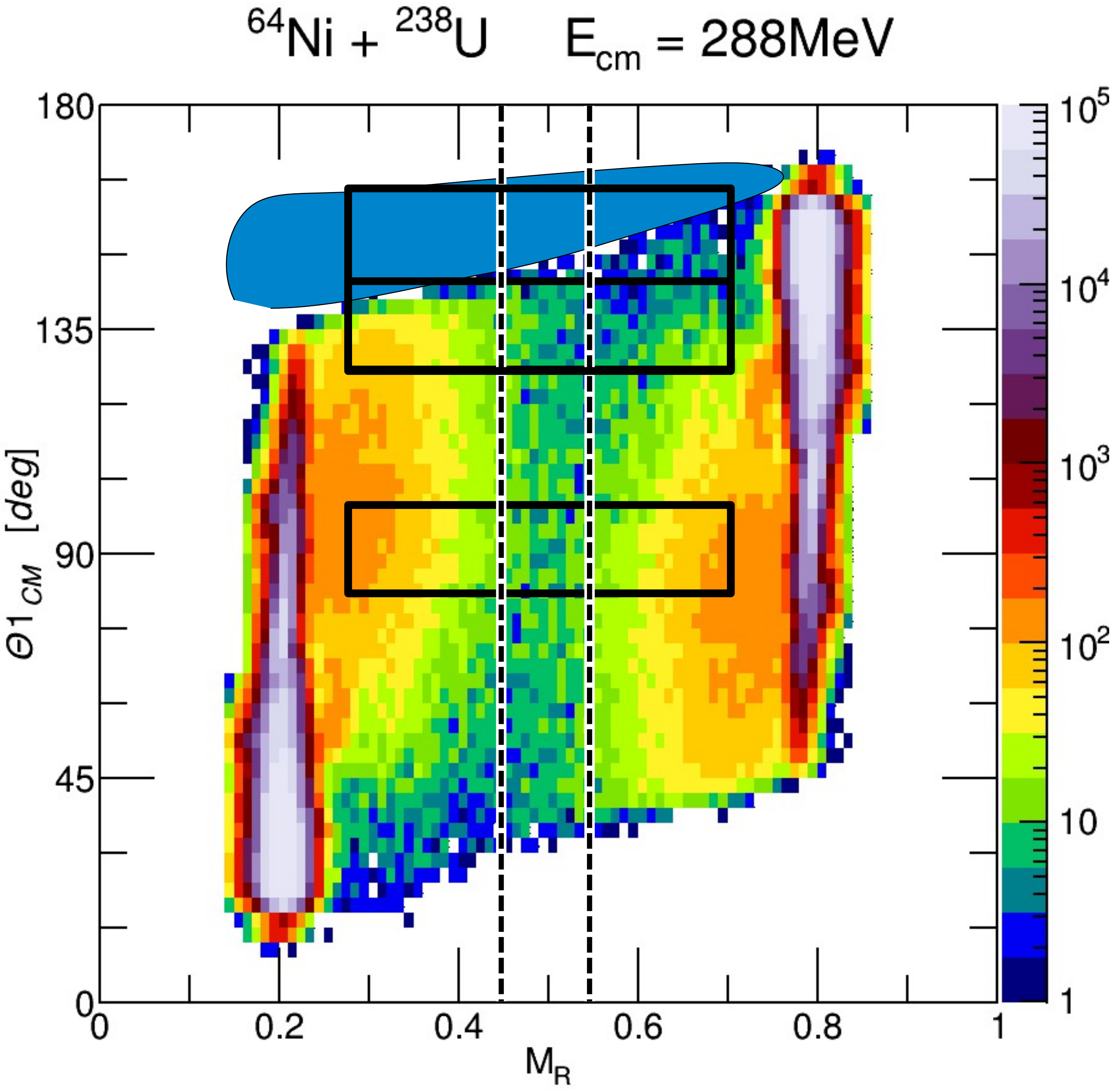

64Ni + 238U Ecm = 288MeV
Θ1CM [deg]
MR
180
135
90
45
0
0
0.2
0.4
0.6
0.8
1
10^5
10^4
10^3
10^2
10
1

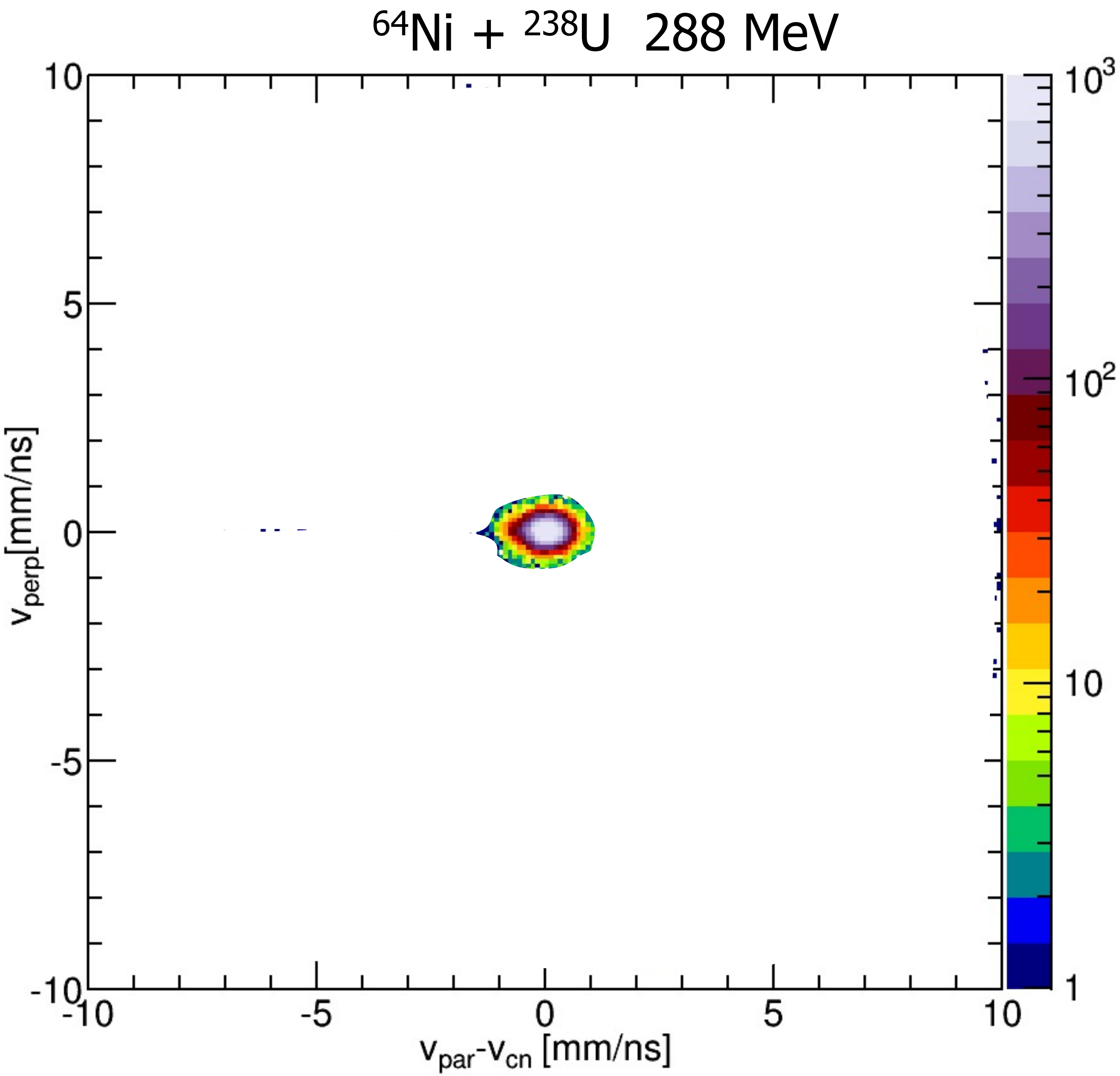

64Ni + 238U 288 MeV
10
5
0
-5
-10
-10
-5
0
5
10
vperp[mm/ns]
vpar-vcn [mm/ns]
10^3
10^2
10
1

$^{54}Cr + ^{238}U$

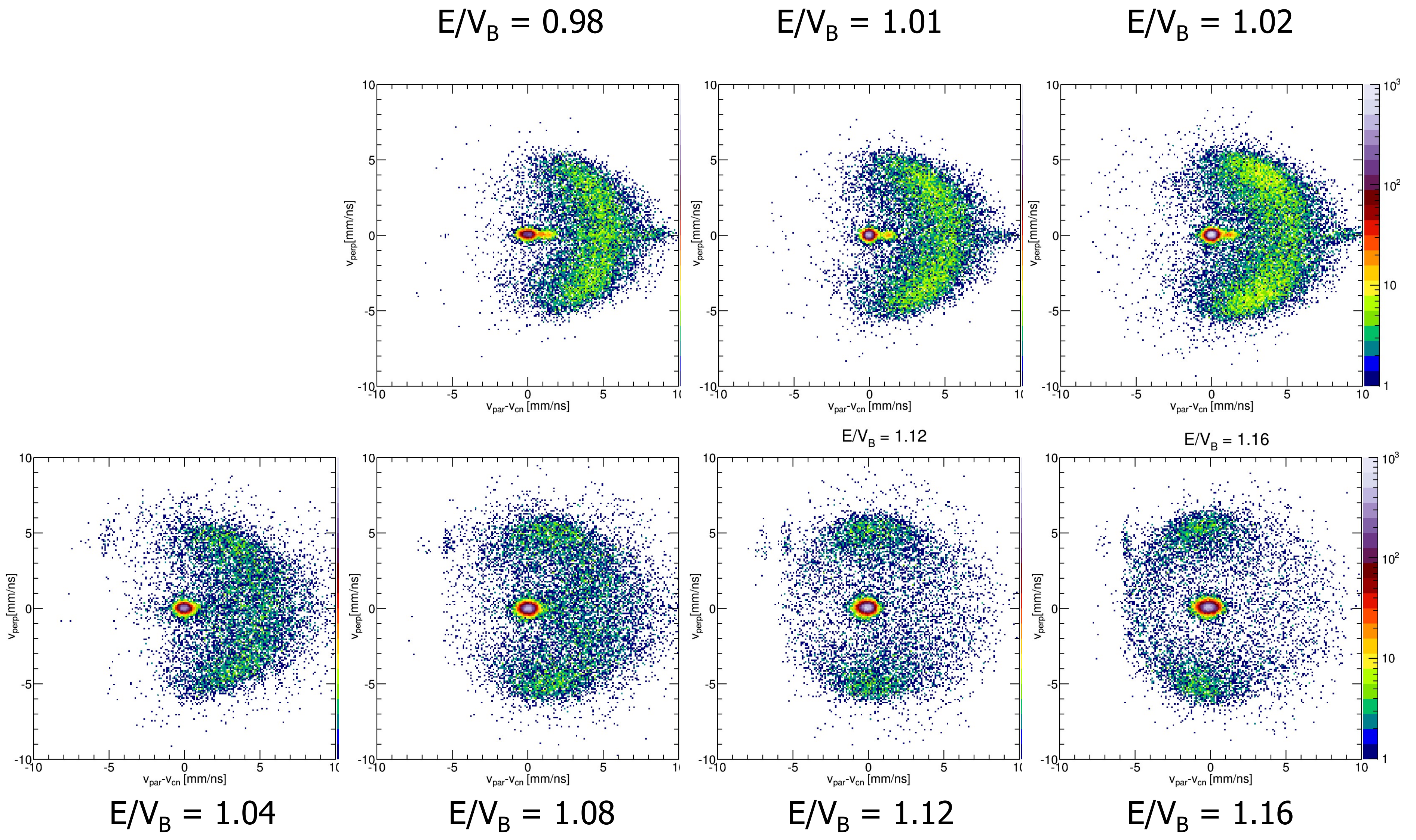
E/V_B = 0.98
E/V_B = 1.01
E/V_B = 1.02
E/V_B = 1.12
E/V_B = 1.16
v_perp [mm/ns]
v_par-v_cn [mm/ns]
10
5
0
-5
-10
10^3
10^2
10
1
E/V_B = 1.04
E/V_B = 1.08
E/V_B = 1.12
E/V_B = 1.16

$^{48}Ca+^{238}U$ $^{50}Ti+^{238}U$ $^{54}Cr+^{238}U$ $^{58}Fe+^{238}U$ $^{64}Ni+^{238}U$

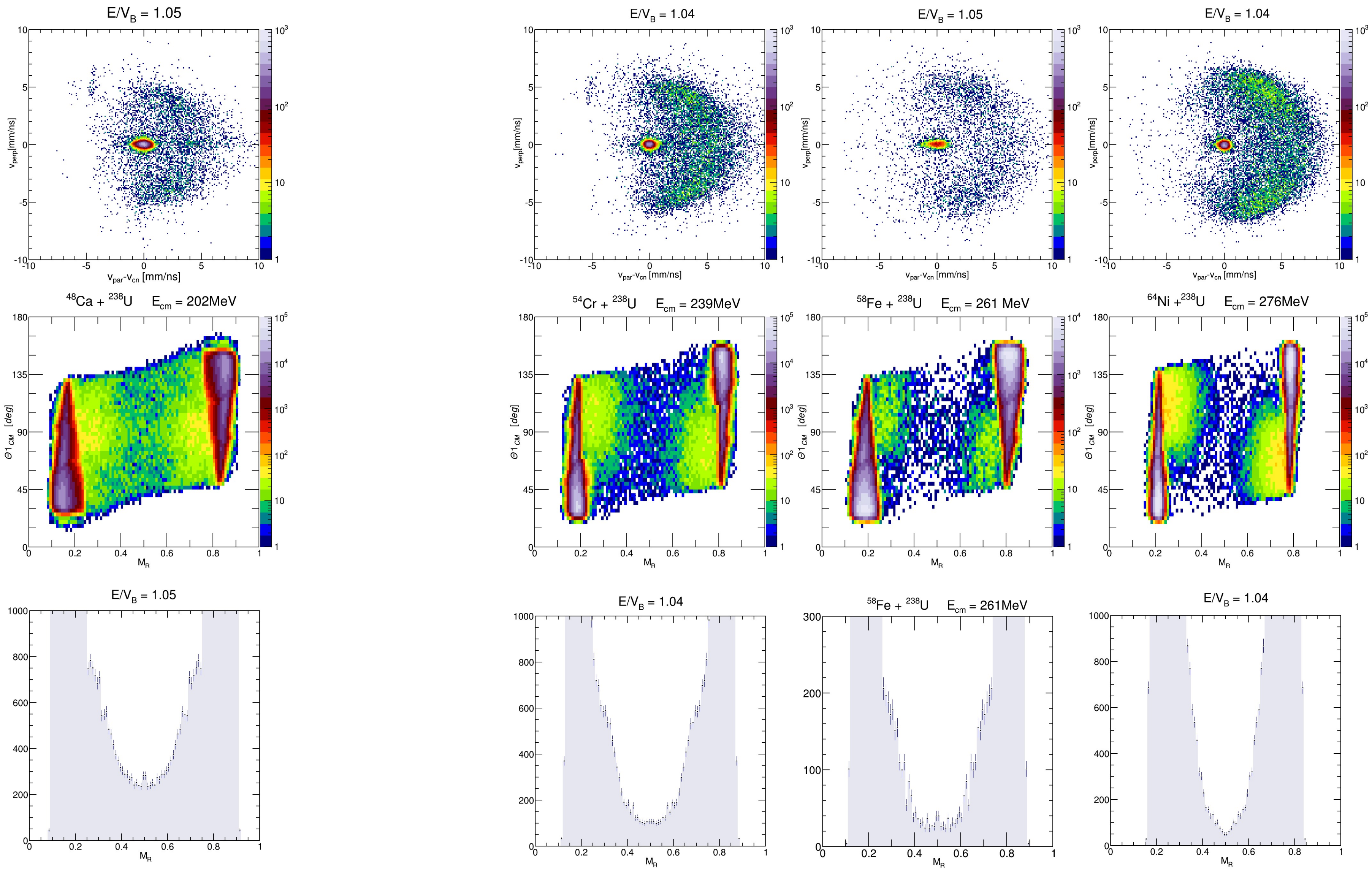

+ measurements with ^{244}Pu, ^{248}Cm targets (thanks to Mainz radiochemistry, GSI targetlab)

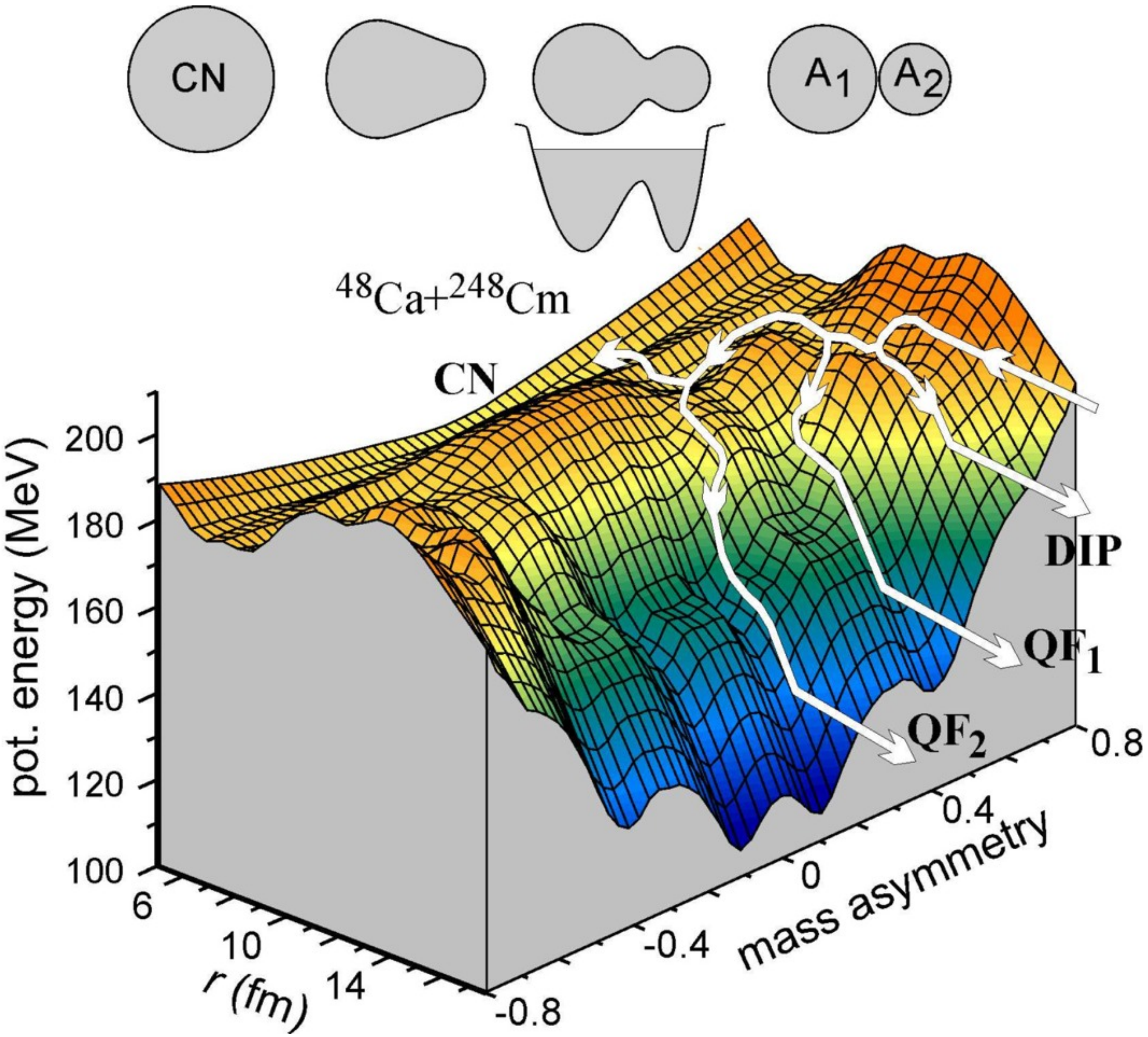
CN
A_1
A_2
$^{48}Ca+^{248}Cm$
CN
DIP
QF_1
QF_2
pot. energy (MeV)
200
180
160
140
120
100
6
10
14
r (fm)
-0.8
-0.4
0
0.4
0.8
mass asymmetry

High P_{CN} for $^{48}Ca+^{208}Pb$

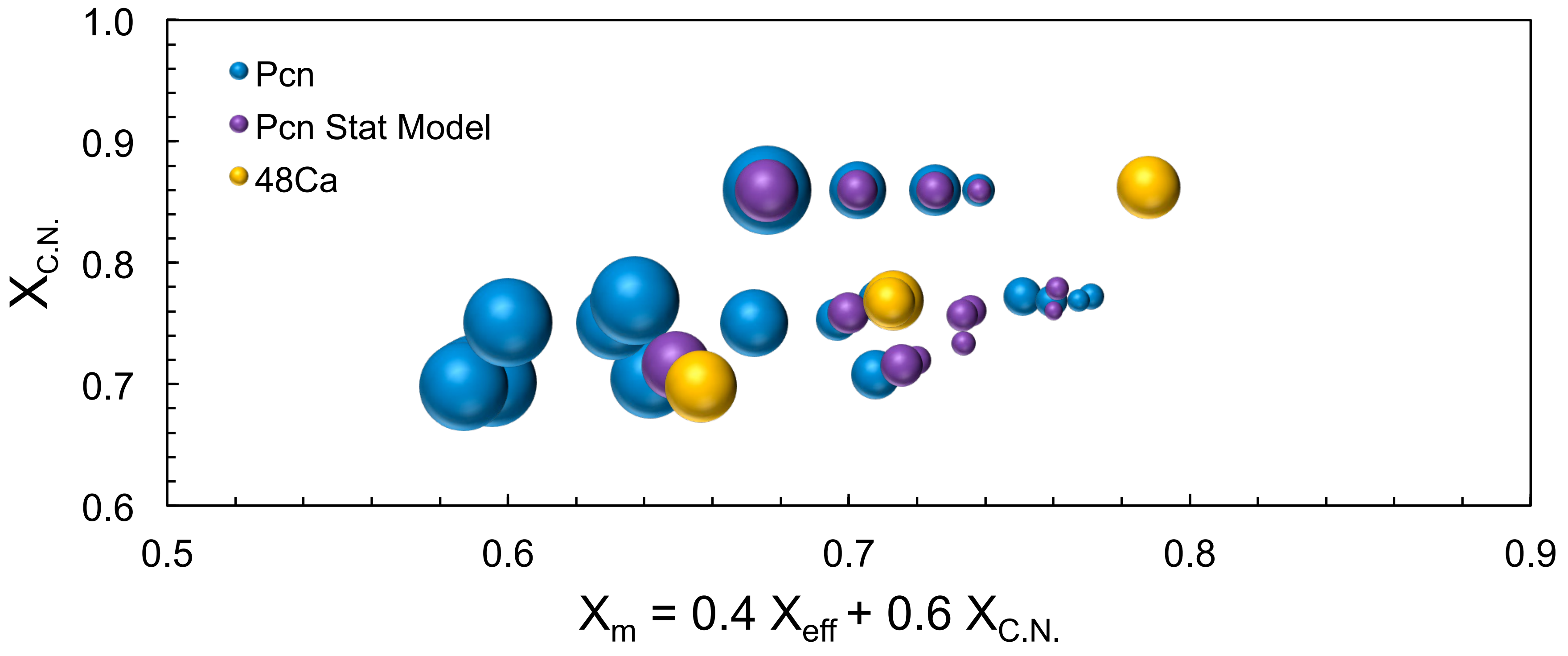

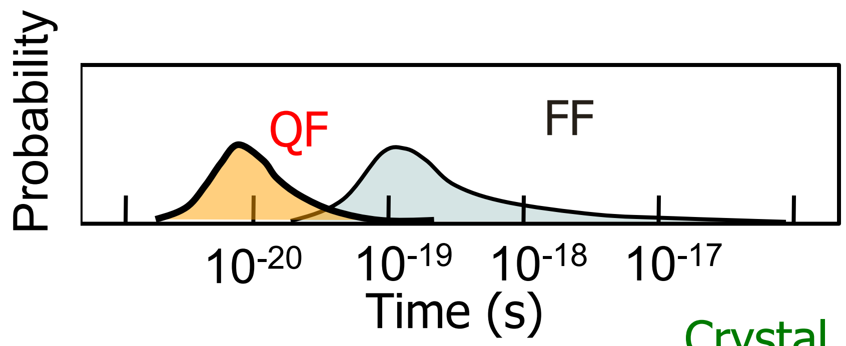

Crystal blocking: 10%-20% fusion-fission

X-rays: 53% fusion-fission

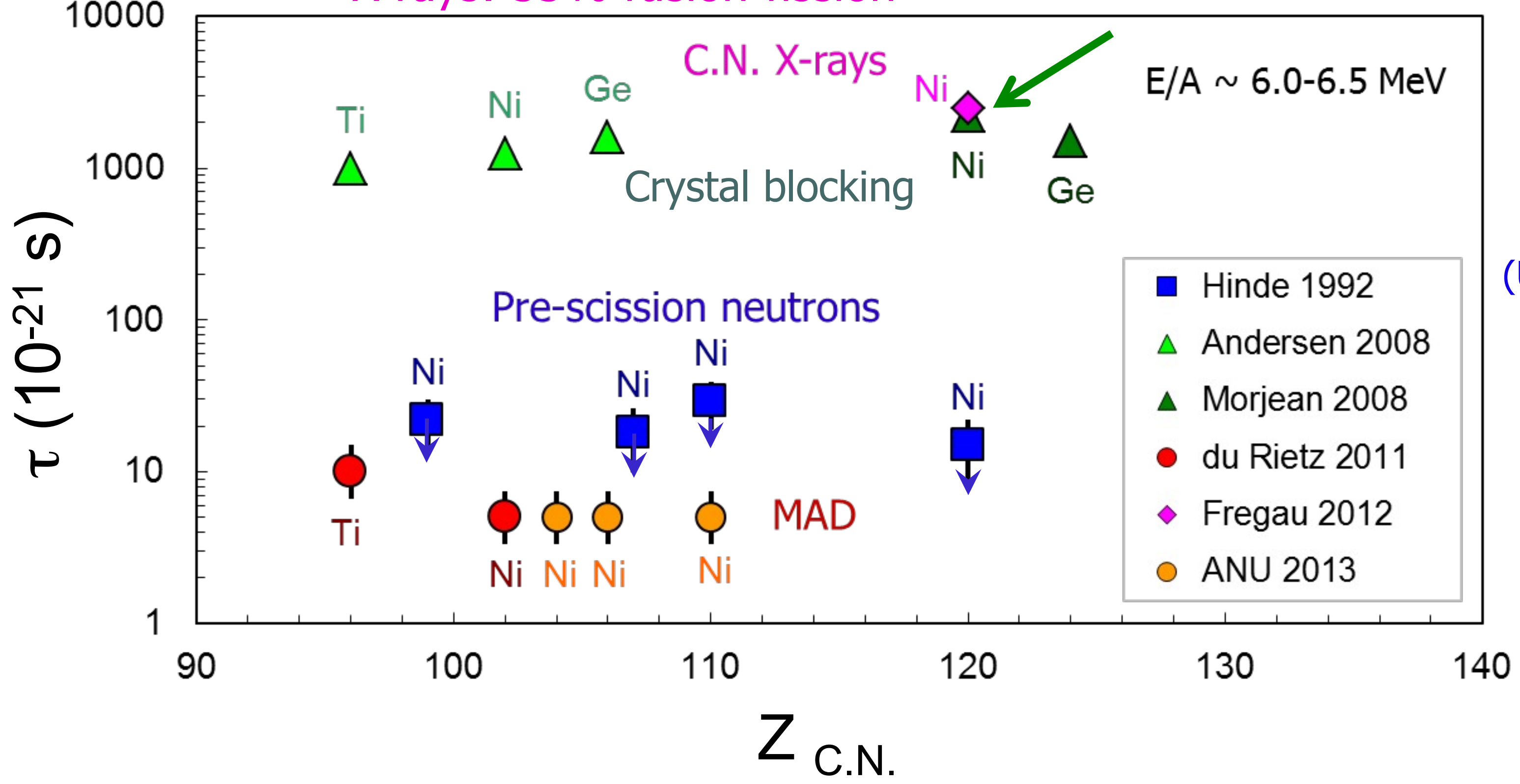

(Upper limit)

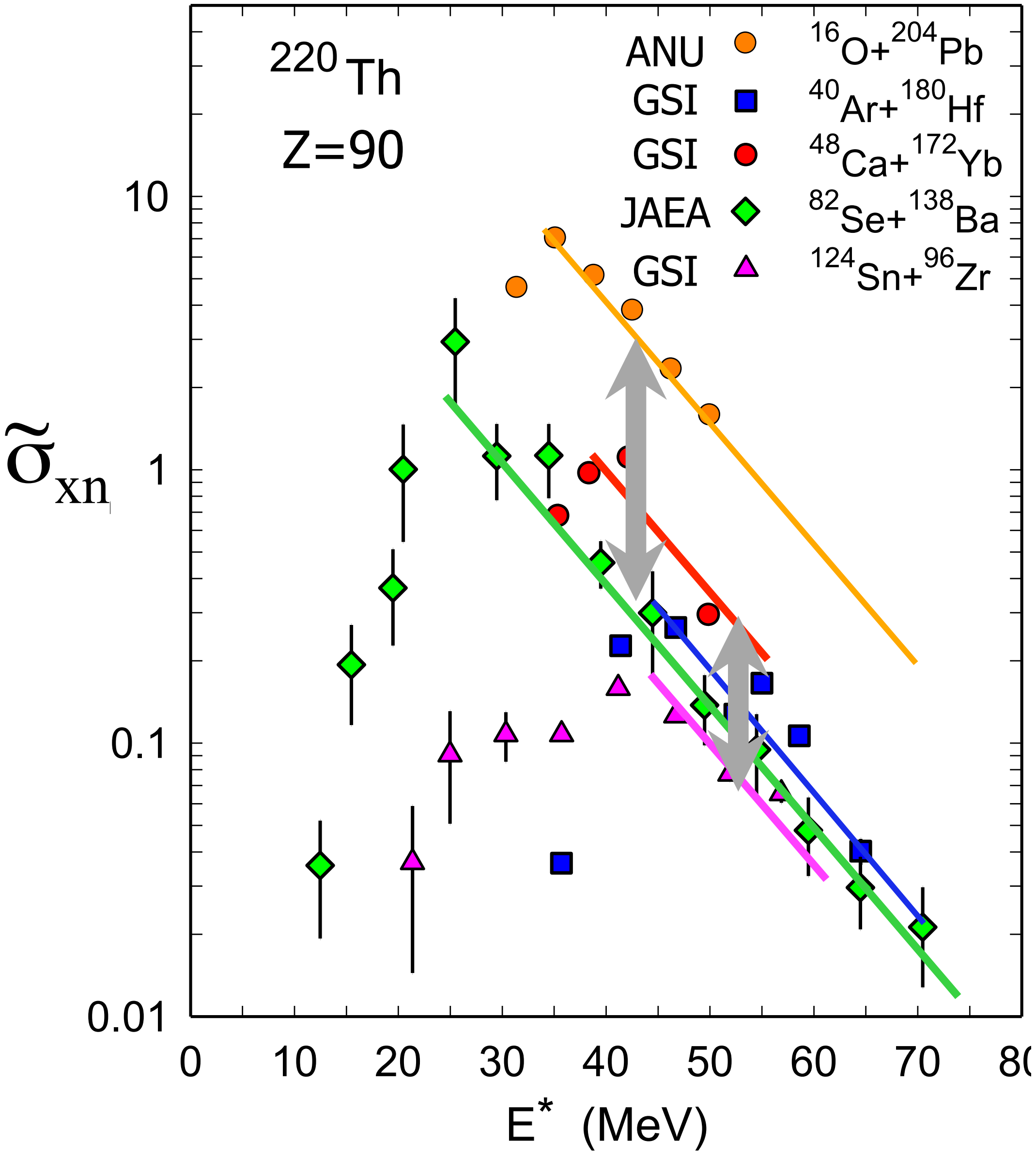

More mass-symmetric reactions:

P_{xn} only ~10% of that for ^{16}O

Weak dependence on mass asymmetry for more symmetric reactions

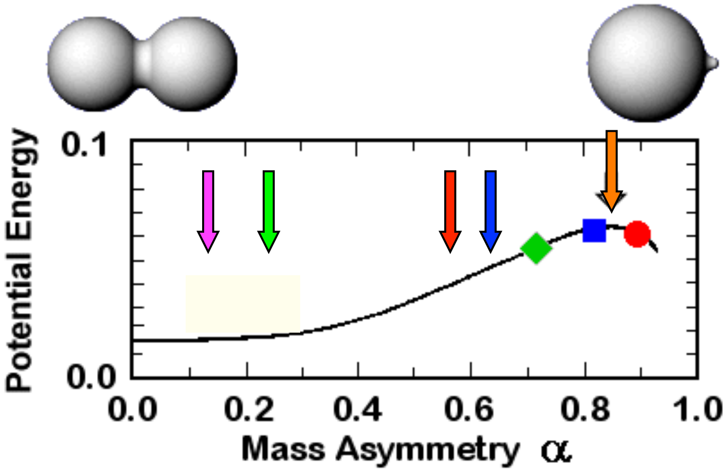

Hinde, Dasgupta, Mukherjee Phys. Rev. Lett. 89 (2002) 272701

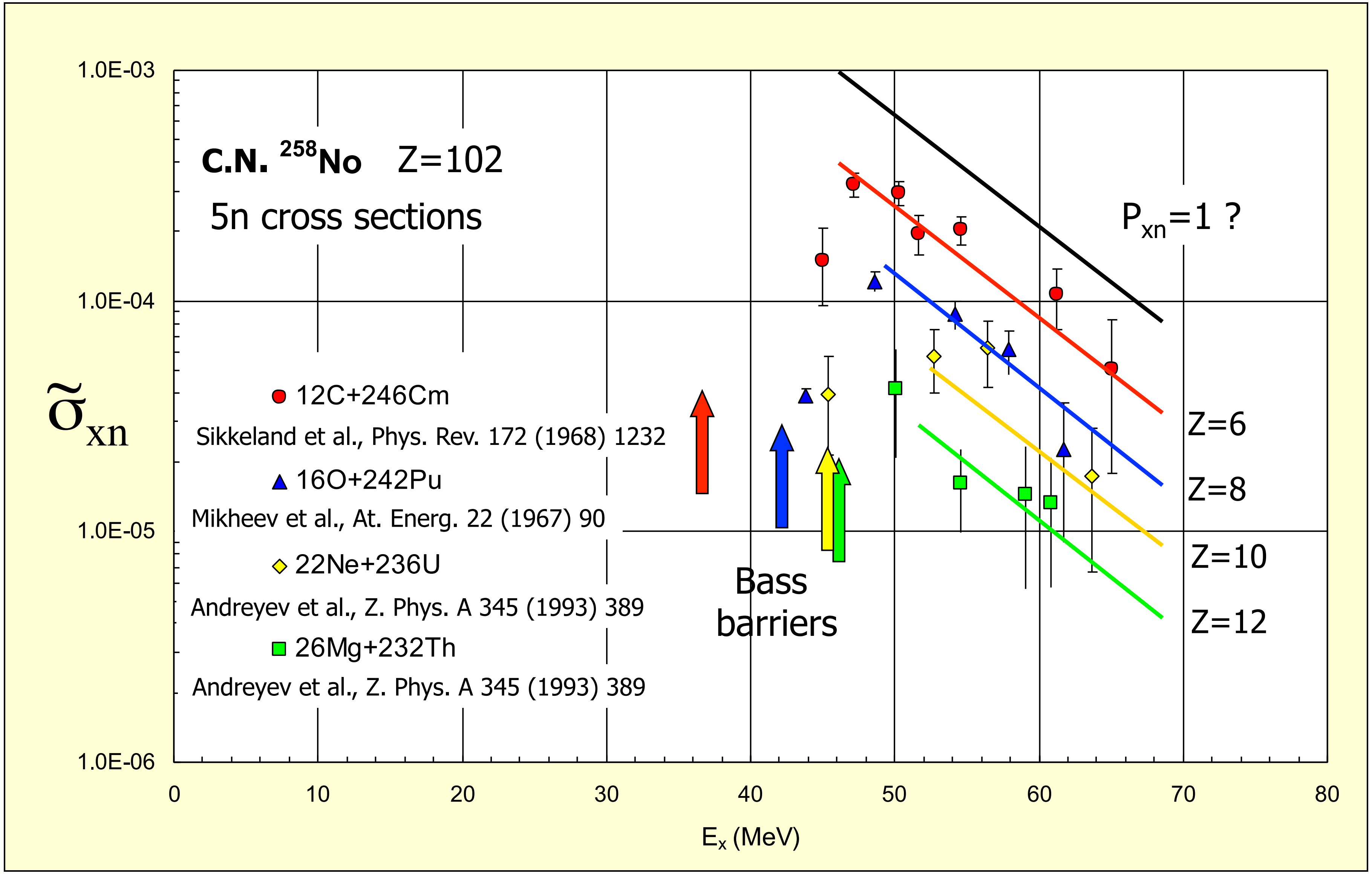
C.N. ^{258}No Z=102
5n cross sections
$\tilde{\sigma}_{xn}$
12C+246Cm
Sikkeland et al., Phys. Rev. 172 (1968) 1232
16O+242Pu
Mikheev et al., At. Energ. 22 (1967) 90
22Ne+236U
Andreyev et al., Z. Phys. A 345 (1993) 389
26Mg+232Th
Andreyev et al., Z. Phys. A 345 (1993) 389
Bass barriers
P_{xn}=1 ?
Z=6
Z=8
Z=10
Z=12
1.0E-03
1.0E-04
1.0E-05
1.0E-06
0
10
20
30
40
50
60
70
80
E_x (MeV)

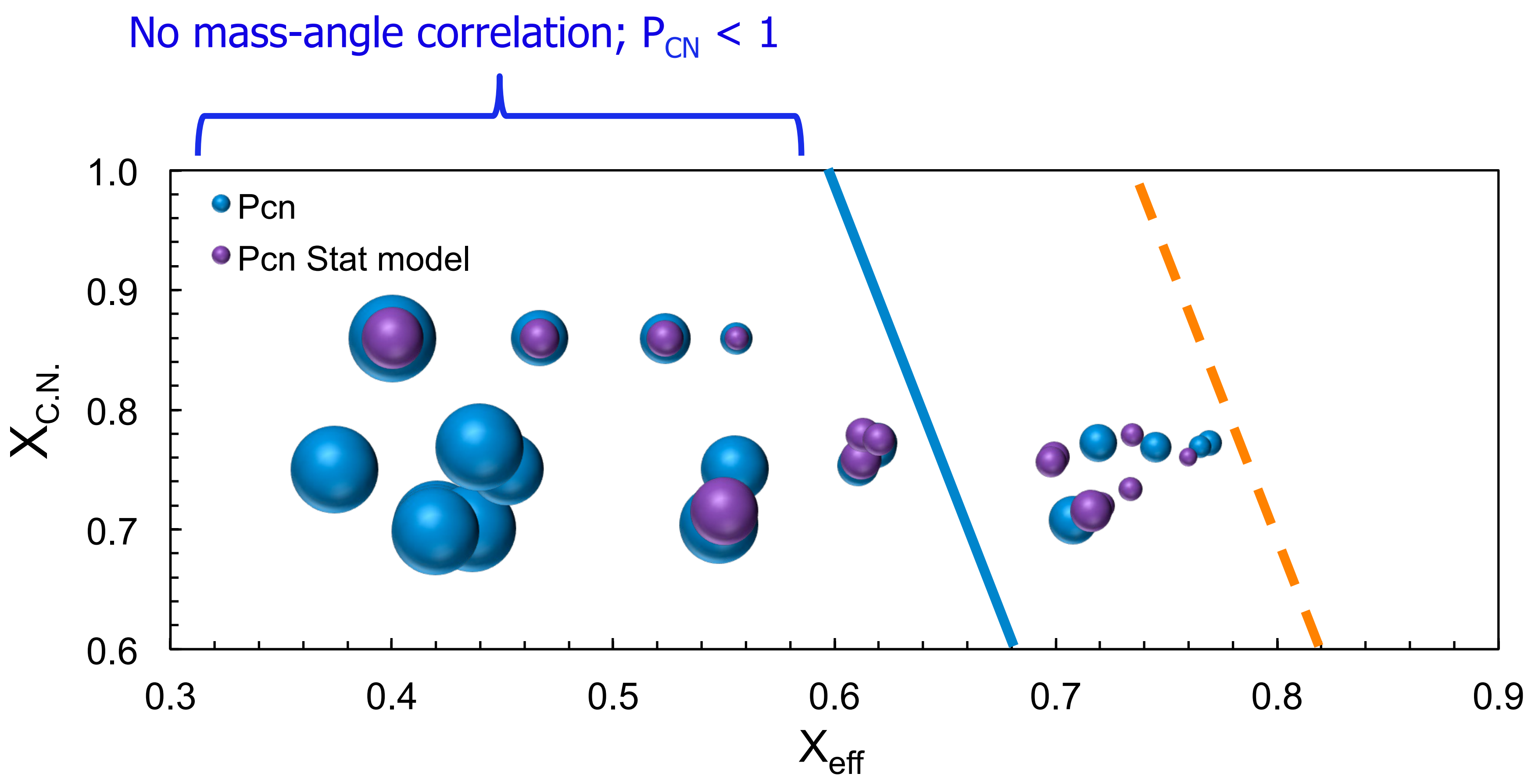

No mass-angle correlation; P_{CN} < 1
Pcn
Pcn Stat model
$X_{C.N.}$
X_{eff}
1.0
0.9
0.8
0.7
0.6
0.3
0.4
0.5
0.6
0.7
0.8
0.9

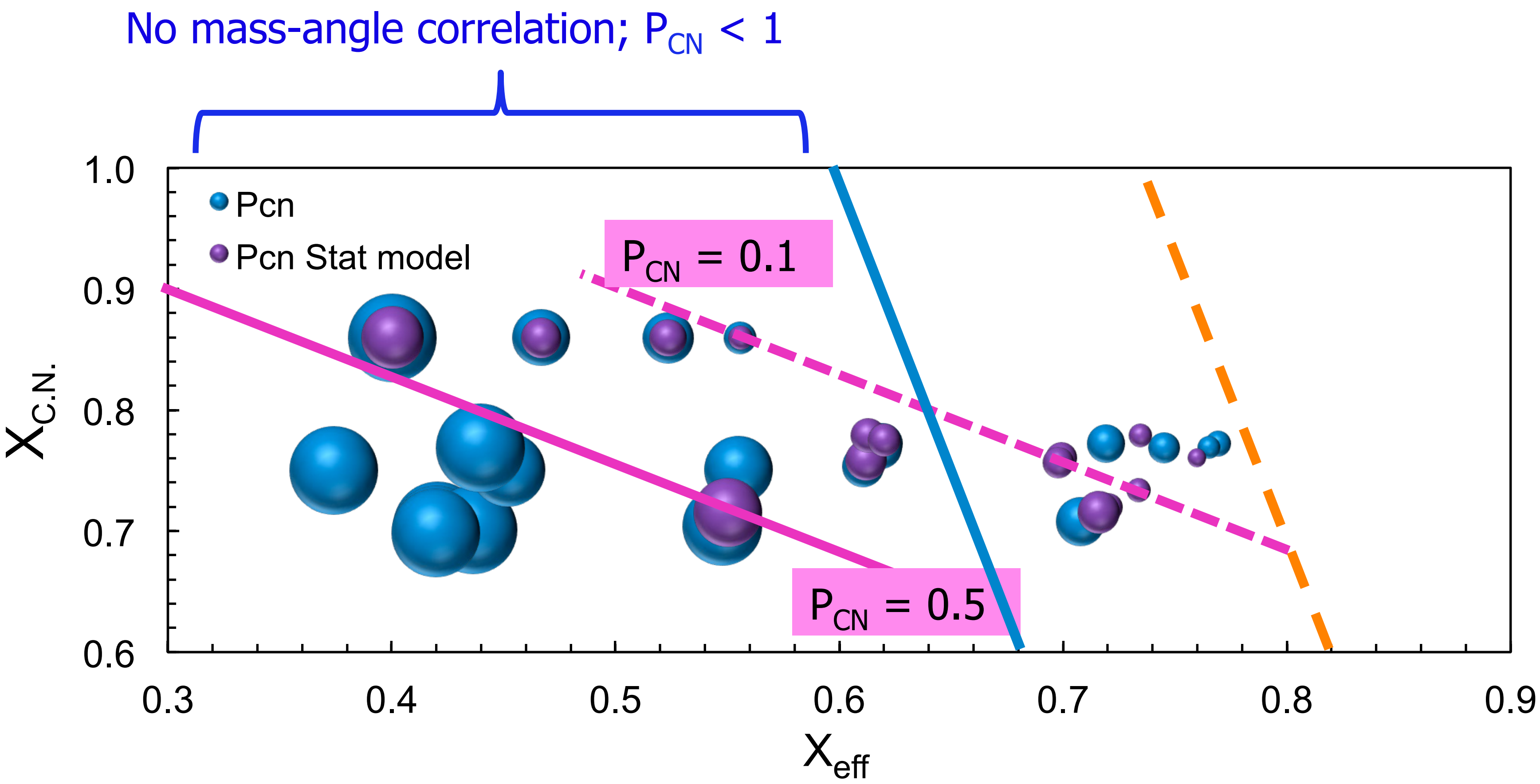

No mass-angle correlation; P_CN < 1
1.0
0.9
0.8
0.7
0.6
X_C.N.
Pcn
Pcn Stat model
P_CN = 0.1
P_CN = 0.5
0.3
0.4
0.5
0.6
0.7
0.8
0.9
X_eff

Different mean fissility X_m for P_{CN} compared with QF mass-angle distribution

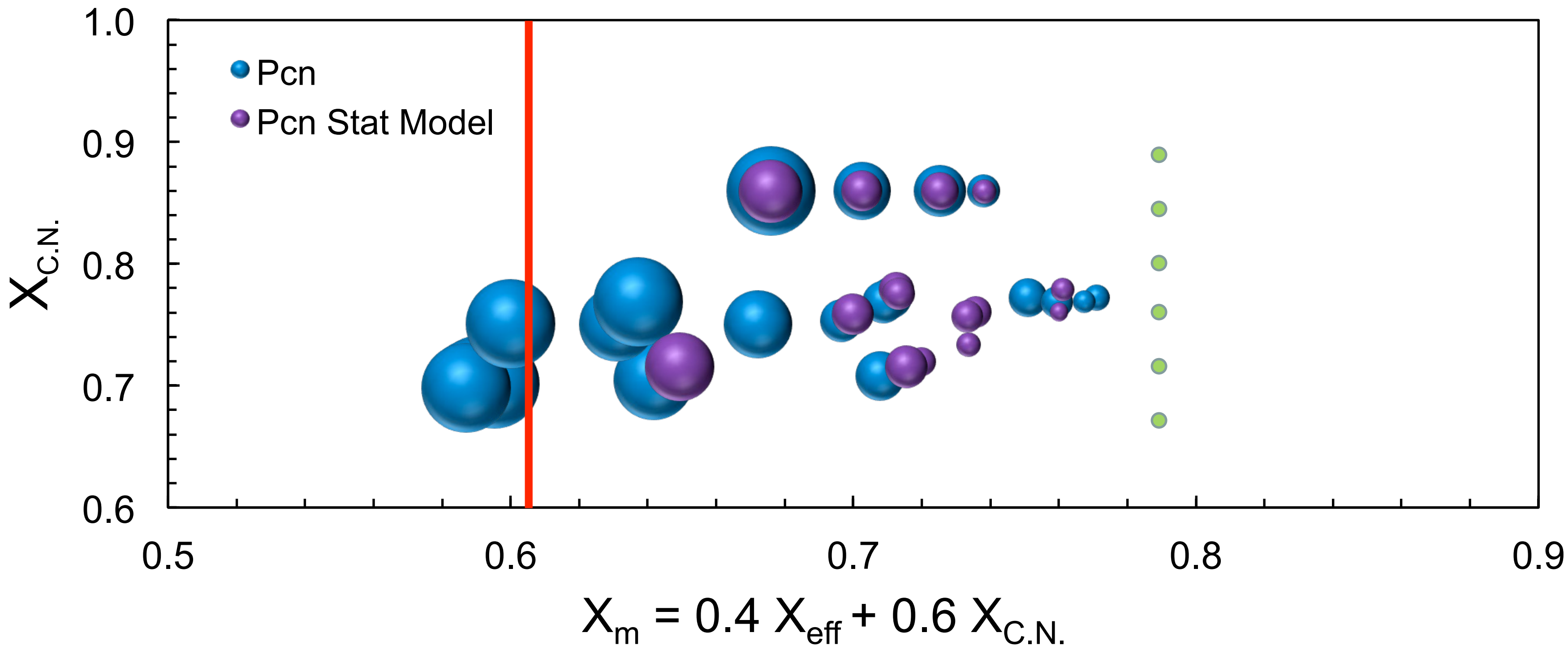

R. du Rietz et al., PRC **88** (2013) 054618

MAD Map

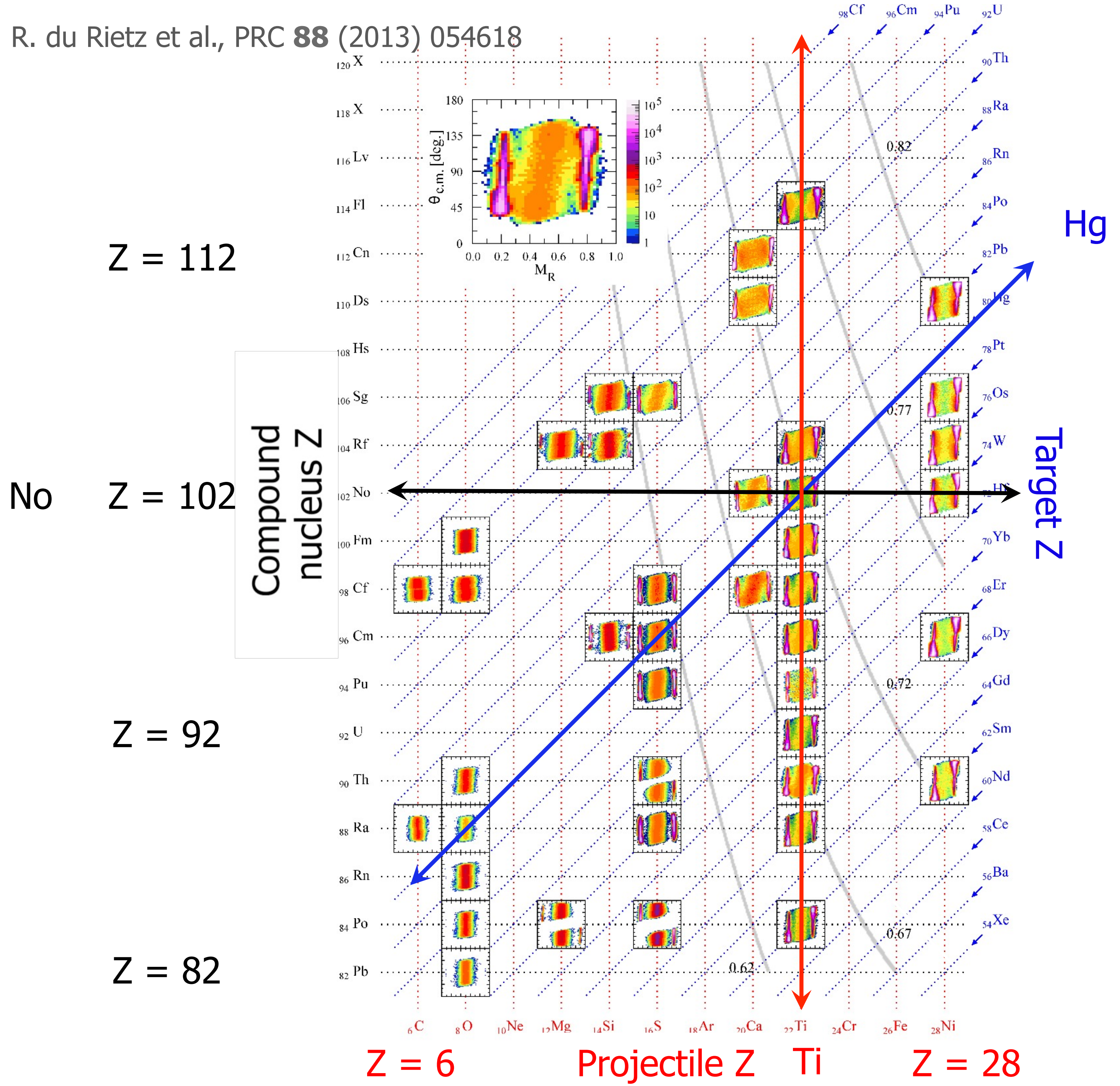

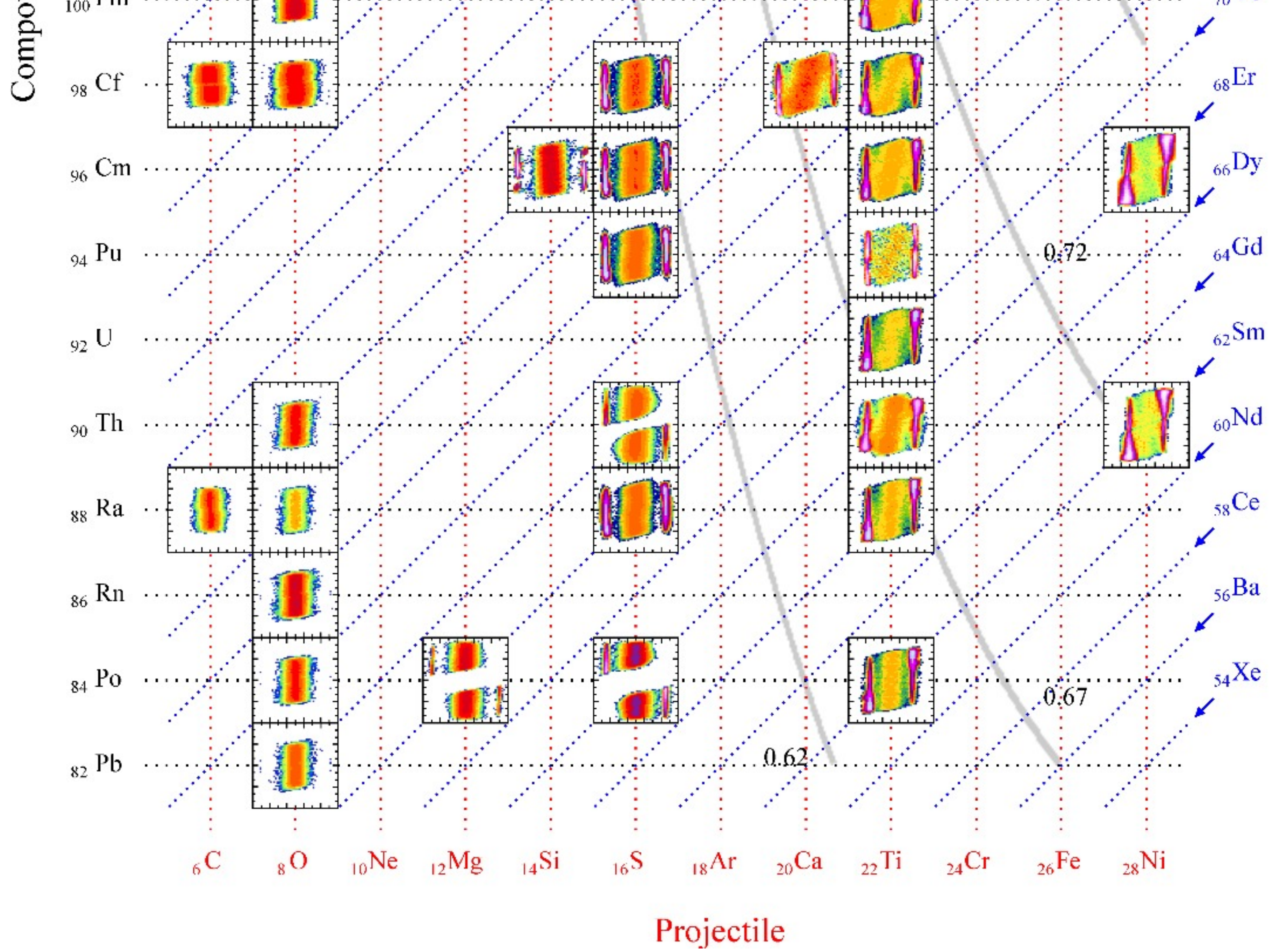

Compo
98 Cf
96 Cm
94 Pu
92 U
90 Th
88 Ra
86 Rn
84 Po
82 Pb
68 Er
66 Dy
64 Gd
62 Sm
60 Nd
58 Ce
56 Ba
54 Xe
0.72
0.67
0.62
6 C
8 O
10 Ne
12 Mg
14 Si
16 S
18 Ar
20 Ca
22 Ti
24 Cr
26 Fe
28 Ni
Projectile

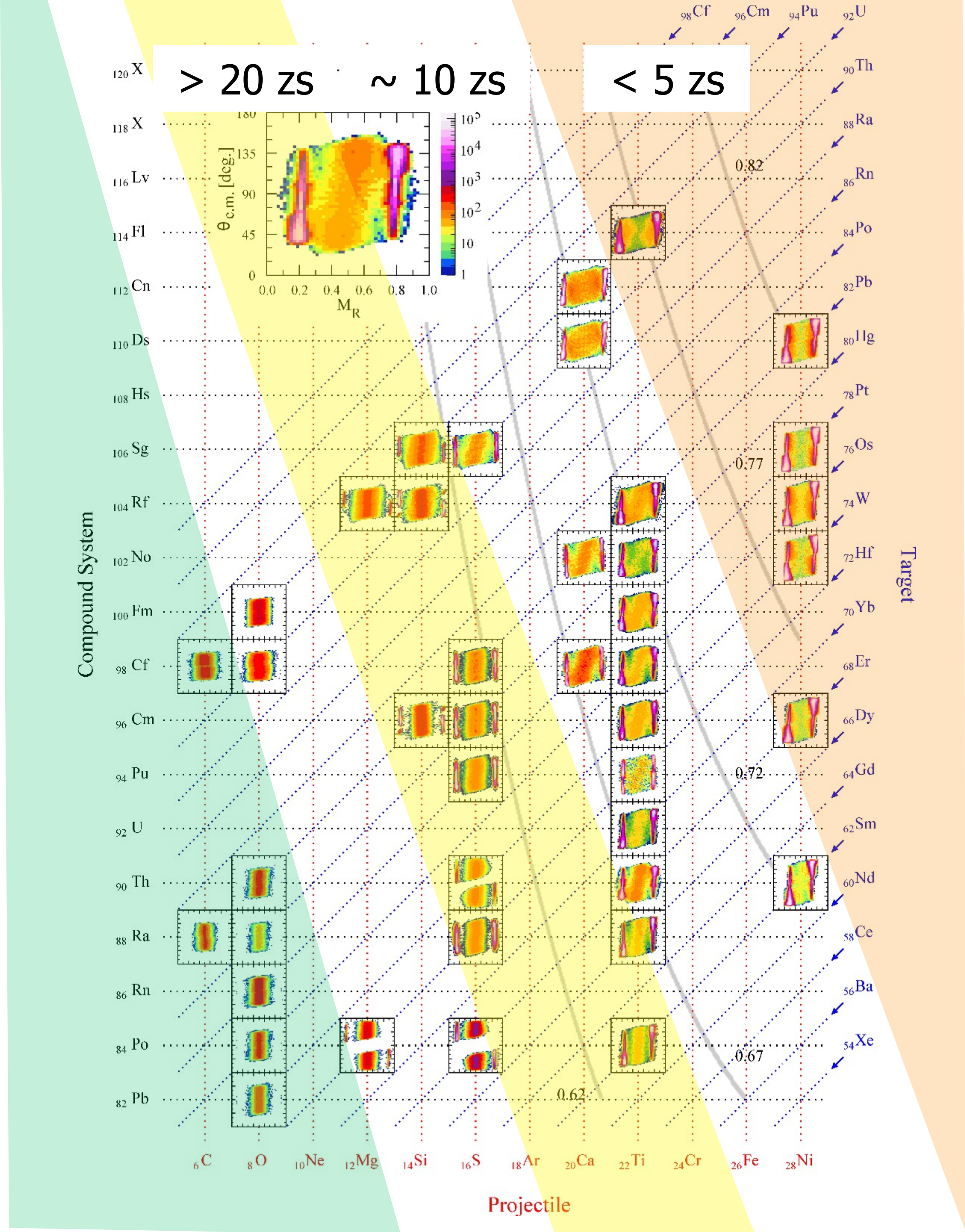

> 20 zs
~ 10 zs
< 5 zs
Compound System
Target
Projectile
θc.m. [deg.]
MR
0.82
0.77
0.72
0.67
0.62
120 X
118 X
116 Lv
114 Fl
112 Cn
110 Ds
108 Hs
106 Sg
104 Rf
102 No
100 Fm
98 Cf
96 Cm
94 Pu
92 U
90 Th
88 Ra
86 Rn
84 Po
82 Pb
6 C
8 O
10 Ne
12 Mg
14 Si
16 S
18 Ar
20 Ca
22 Ti
24 Cr
26 Fe
28 Ni
98 Cf
96 Cm
94 Pu
92 U
90 Th
88 Ra
86 Rn
84 Po
82 Pb
80 Hg
78 Pt
76 Os
74 W
72 Hf
70 Yb
68 Er
66 Dy
64 Gd
62 Sm
60 Nd
58 Ce
56 Ba
54 Xe

$^{34}S + ^{232}Th \longrightarrow ^{266}Sg$ (Z=106)

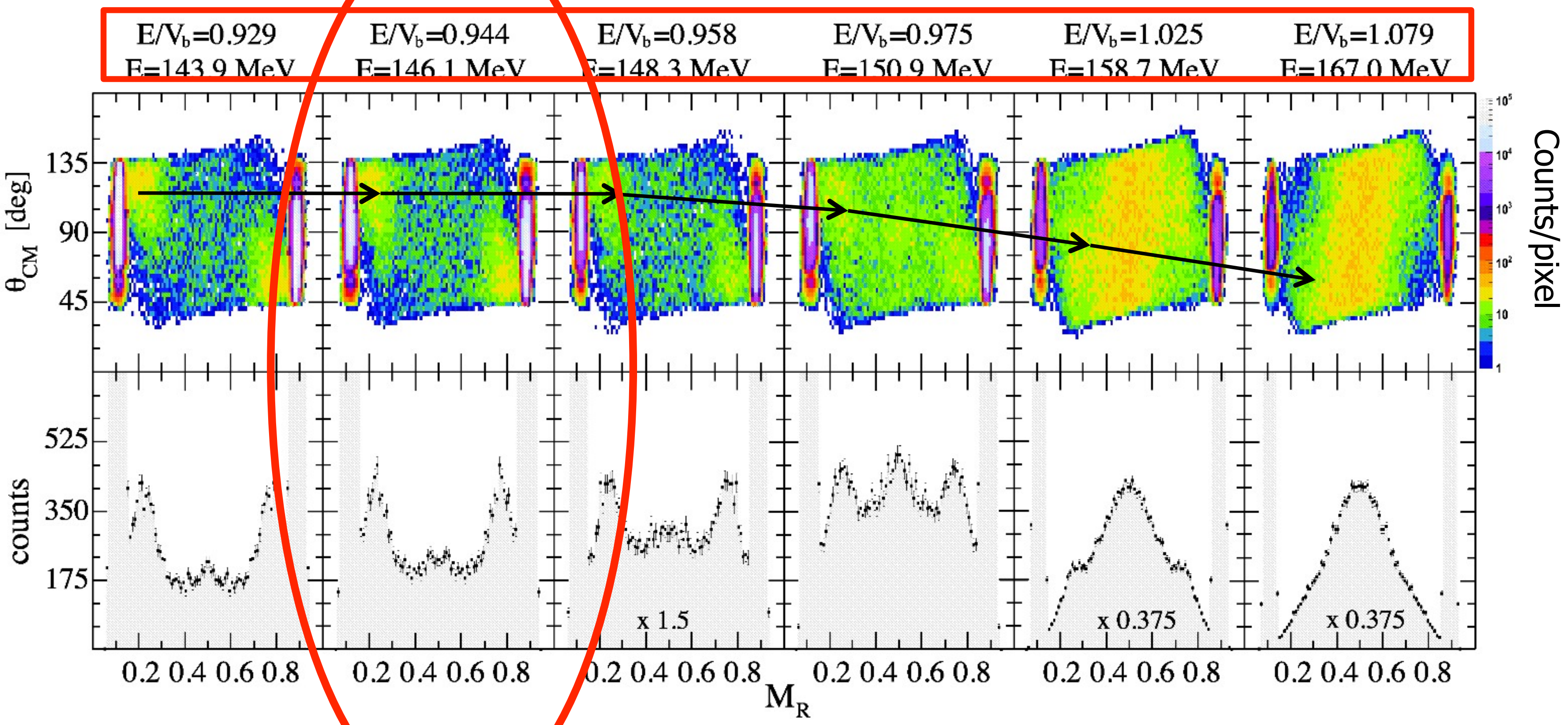

ANU, to be published

Two modes of quasi-fission – effect of deformation alignment

Hinde et al., PR **C53** (1996) 1290

$^{32}S + ^{232}Th$ (prolate)

^{232}Th: fissile – fission after peripheral collisions

Elimination of non-binary events: co-linear in c.m. frame

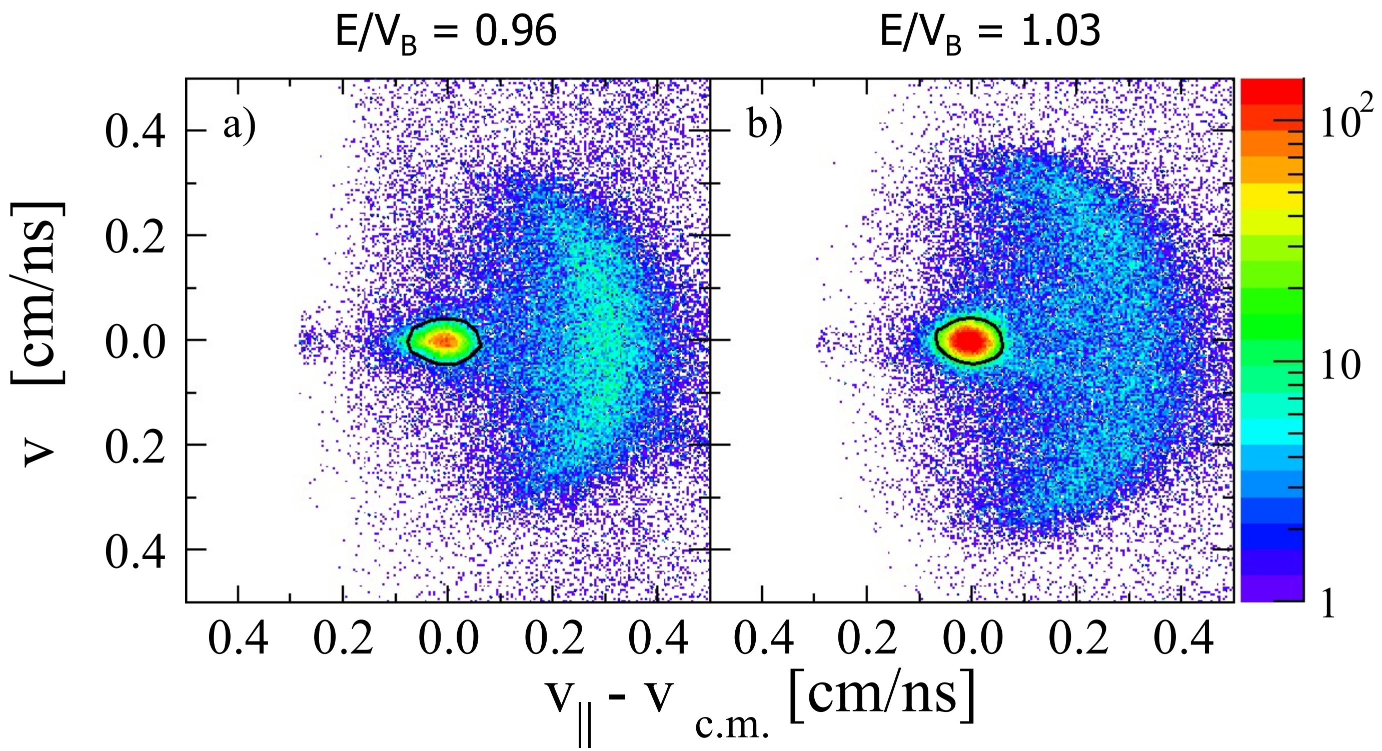

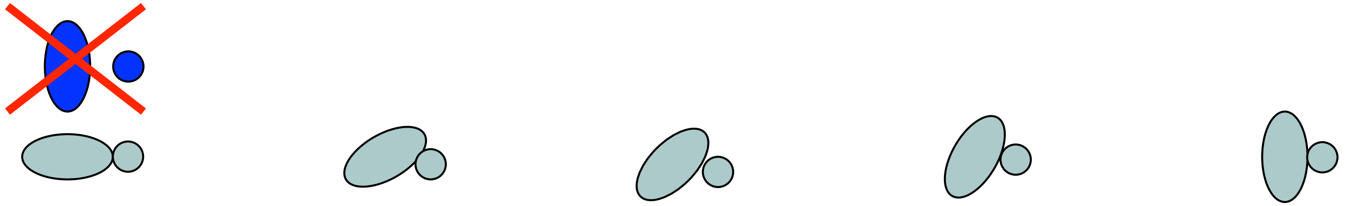

MAD: $^{32}S + ^{232}Th$

Hinde et al., PRL **101** (2008) 092702

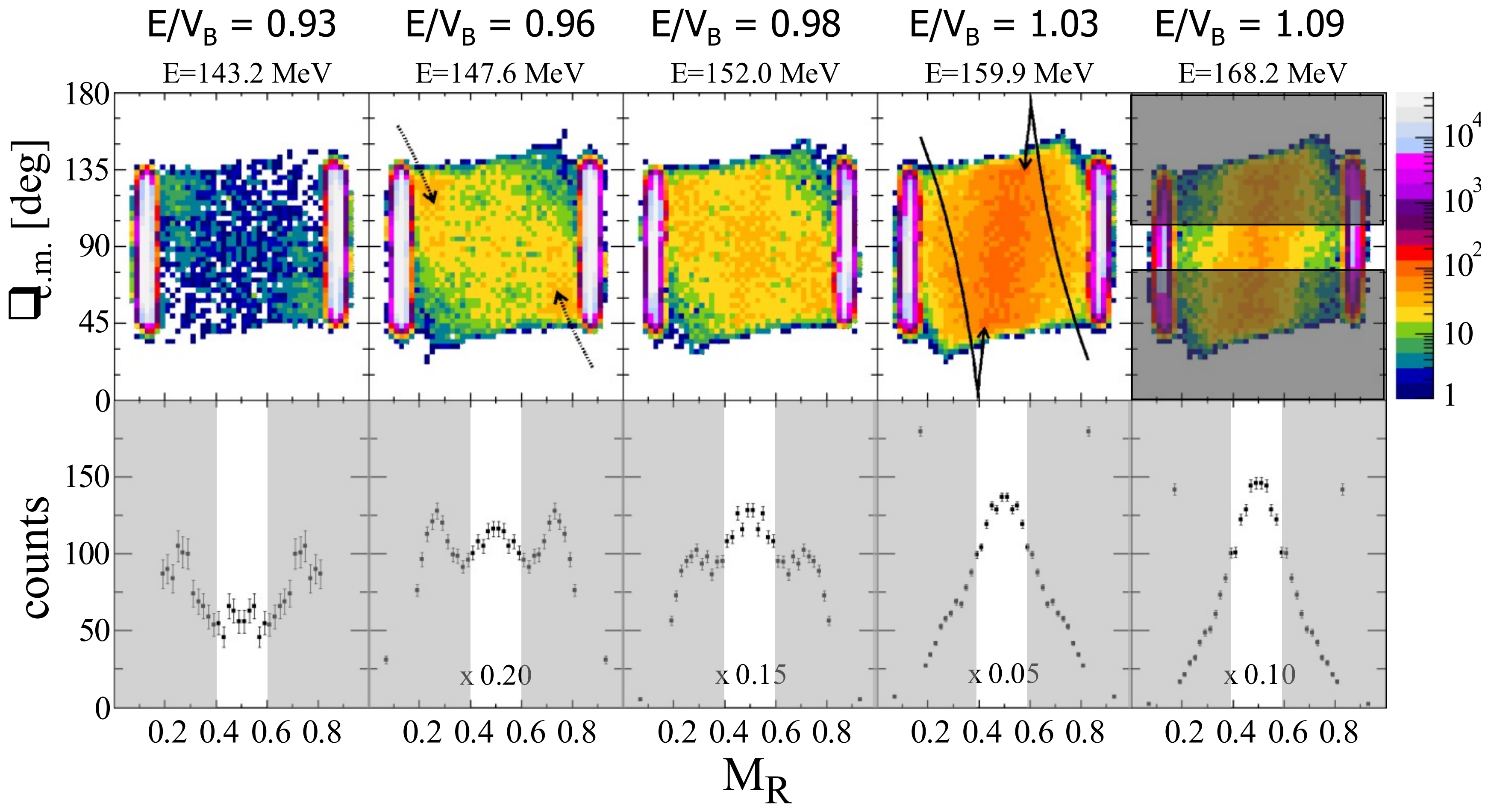

Mass-symmetric fragment angular anisotropies

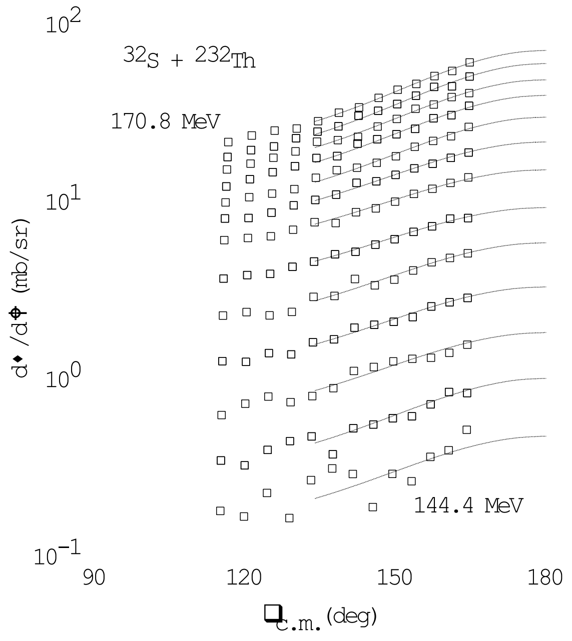

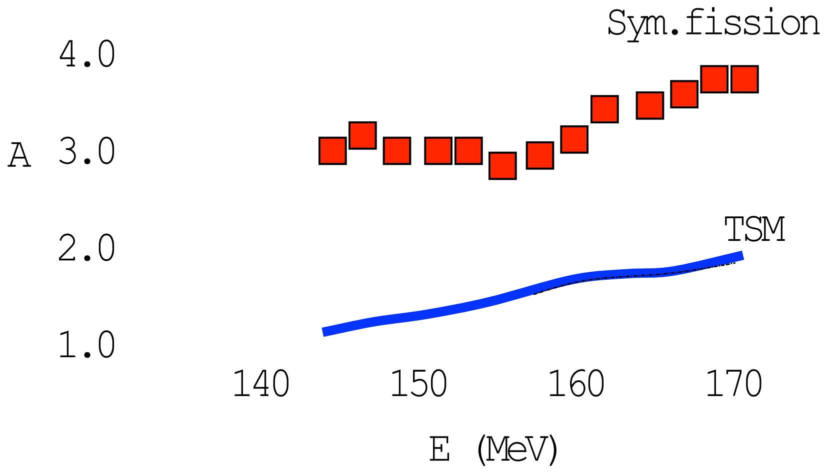

Hinde et al., J.Nucl.Radiochem.Sci. **3** (2002) 31
Hinde et al., PRL **101** (2008) 092702

- Mass-symmetric component shows large angular anisotropies – QF!

  Supports previous interpretation of deformation alignment effect on dynamics deduced from similar anisotropy results for $^{16}O + ^{238}U$

  Hinde et al., PRL **74** (1995) 1295; Hinde et al., PRC **53** (1996) 1290

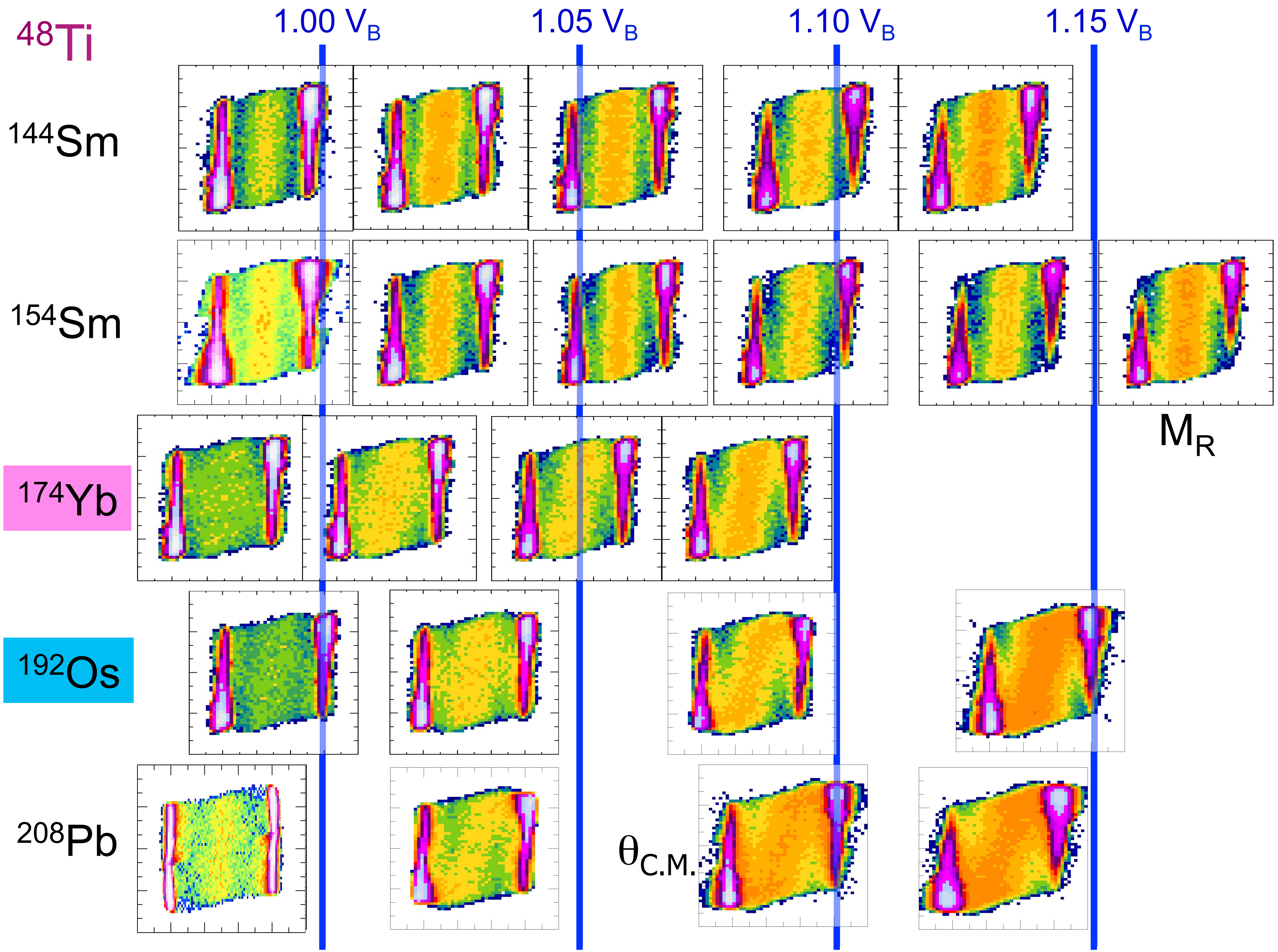
48Ti
1.00 VB
1.05 VB
1.10 VB
1.15 VB
144Sm
154Sm
174Yb
192Os
208Pb
MR
θC.M.

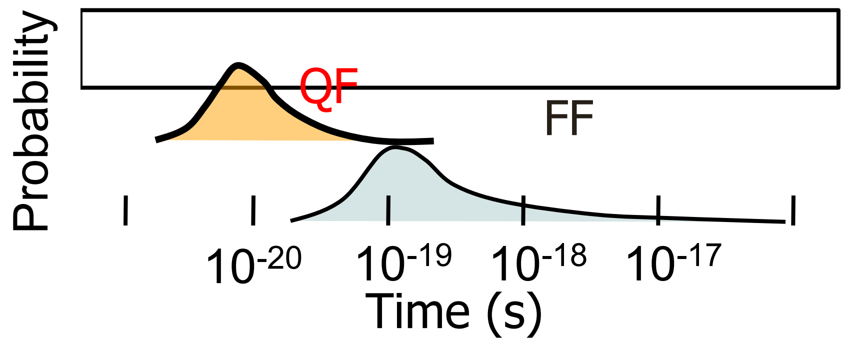
Probability
QF
FF
10^-20
10^-19
10^-18
10^-17
Time (s)

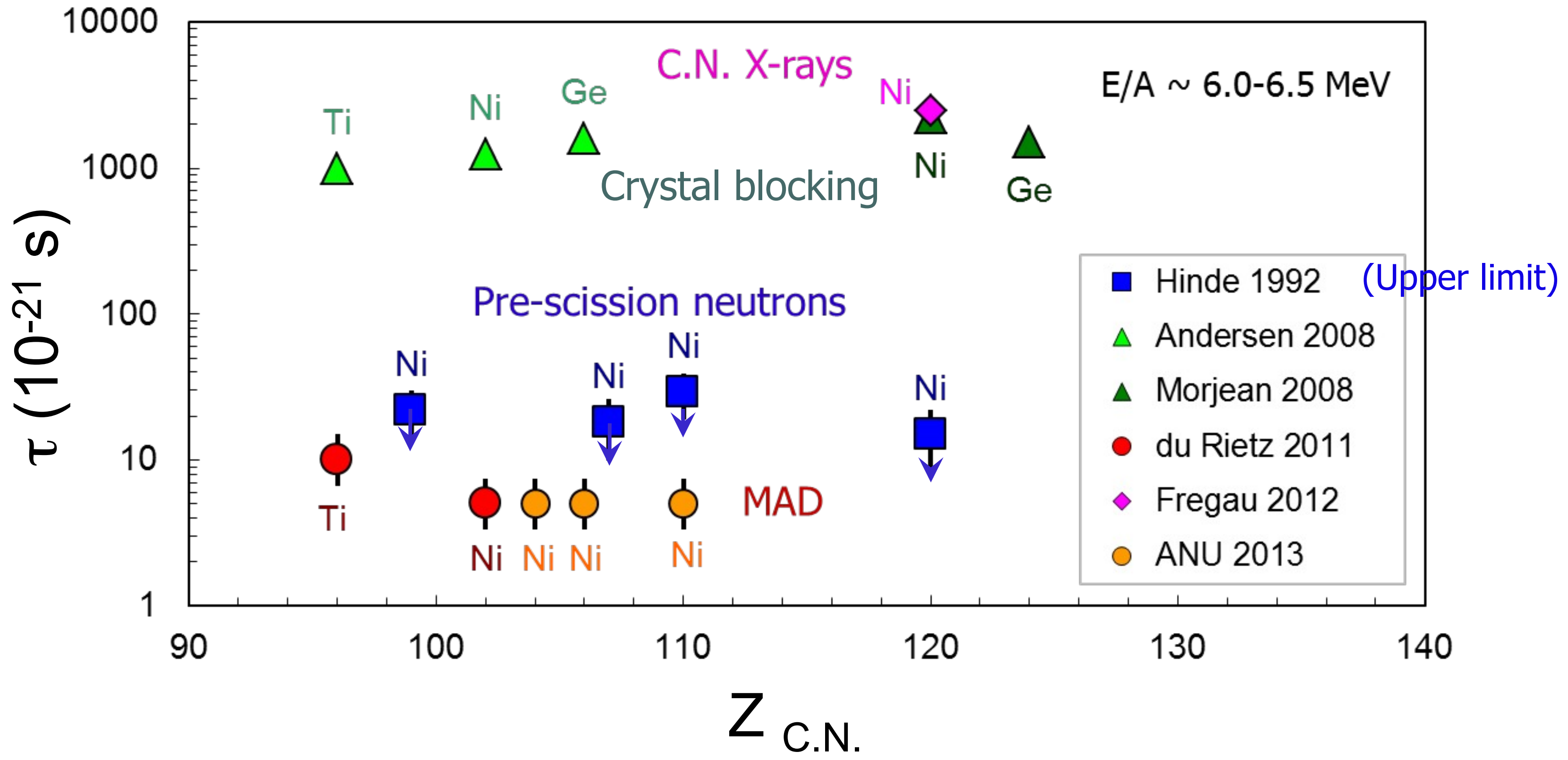
10000
1000
100
10
1
τ (10^-21 s)
90
100
110
120
130
140
Z C.N.
C.N. X-rays
E/A ~ 6.0-6.5 MeV
Ti
Ni
Ge
Ni
Ni
Ge
Crystal blocking
Pre-scission neutrons
Ni
Ni
Ni
Ni
Ti
Ni
Ni
Ni
Ni
MAD
Hinde 1992
(Upper limit)
Andersen 2008
Morjean 2008
du Rietz 2011
Fregau 2012
ANU 2013

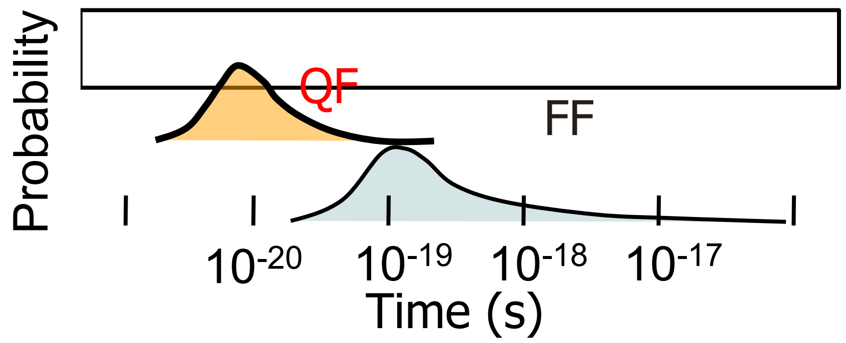
Probability
QF
FF
10-20
10-19
10-18
10-17
Time (s)

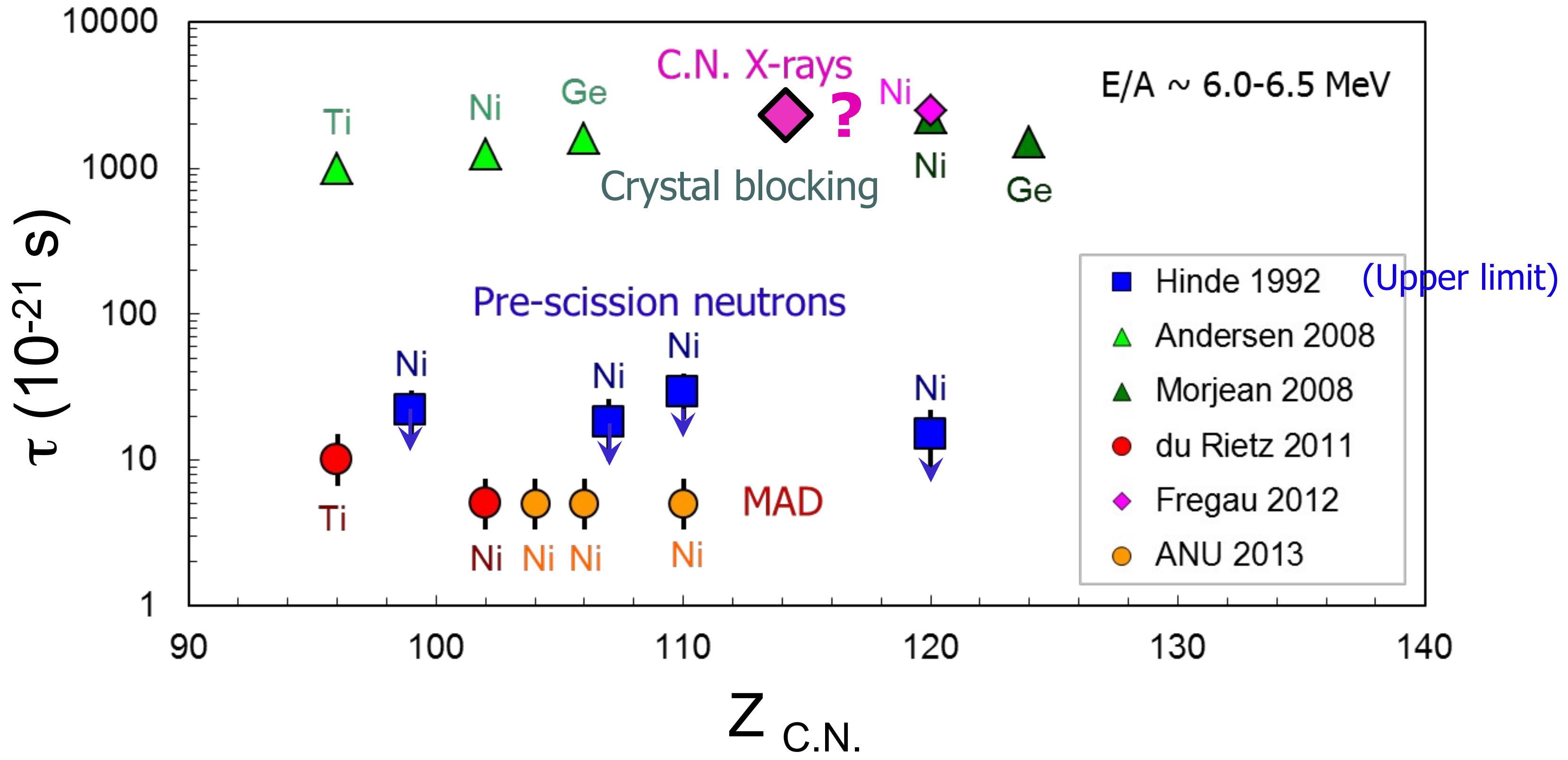
C.N. X-rays
?
Crystal blocking
E/A ~ 6.0-6.5 MeV
Ti
Ni
Ge
Ni
Ni
Ge
Pre-scission neutrons
Ni
Ni
Ni
Ni
MAD
Ti
Ni
Ni
Ni
Ni
Hinde 1992
(Upper limit)
Andersen 2008
Morjean 2008
du Rietz 2011
Fregau 2012
ANU 2013
τ (10-21 s)
10000
1000
100
10
1
90
100
110
120
130
140
Z C.N.

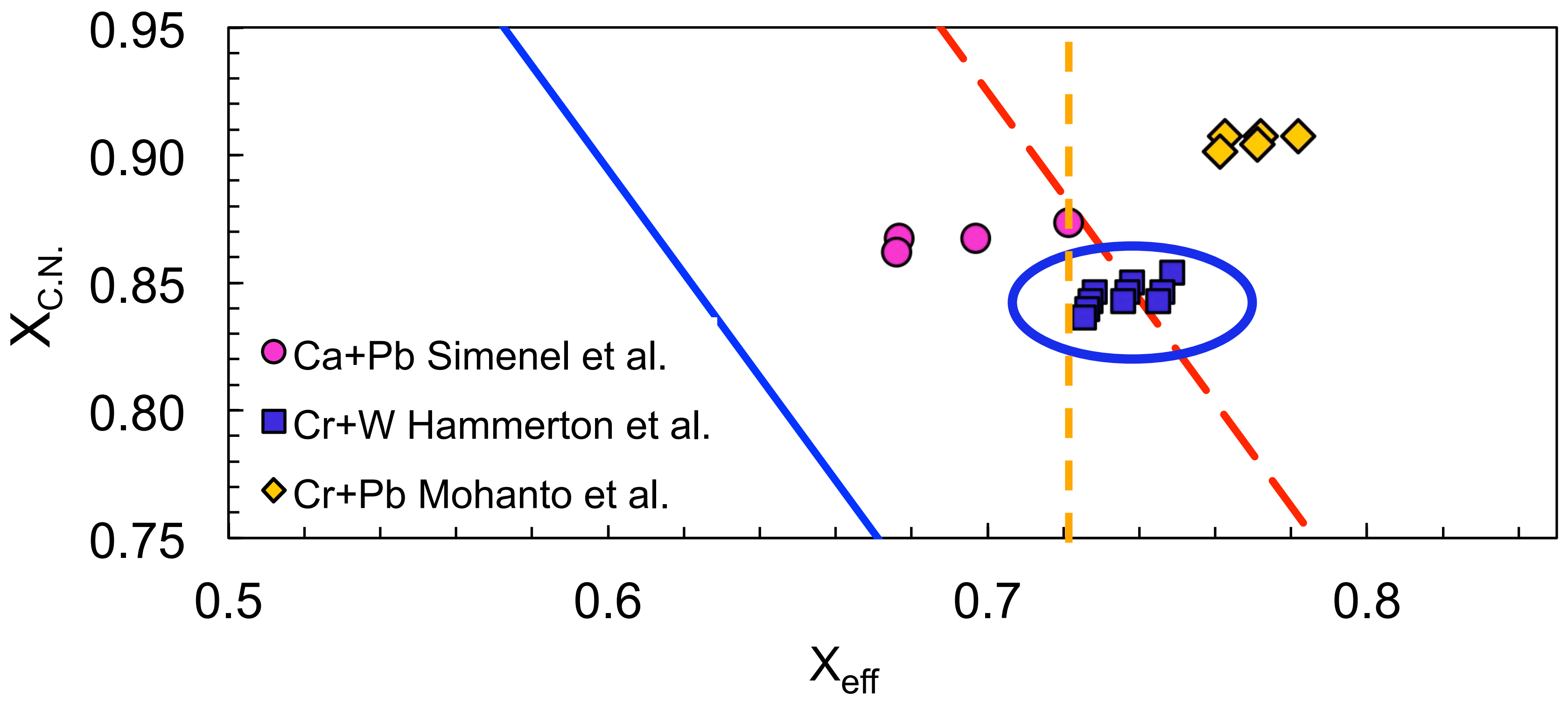

C. Simenel et al., PLB **710** (2012) 607

K. Hammerton et al., PRC **91** (2015) 041602

G. Mohanto et al., ANU, in preparation

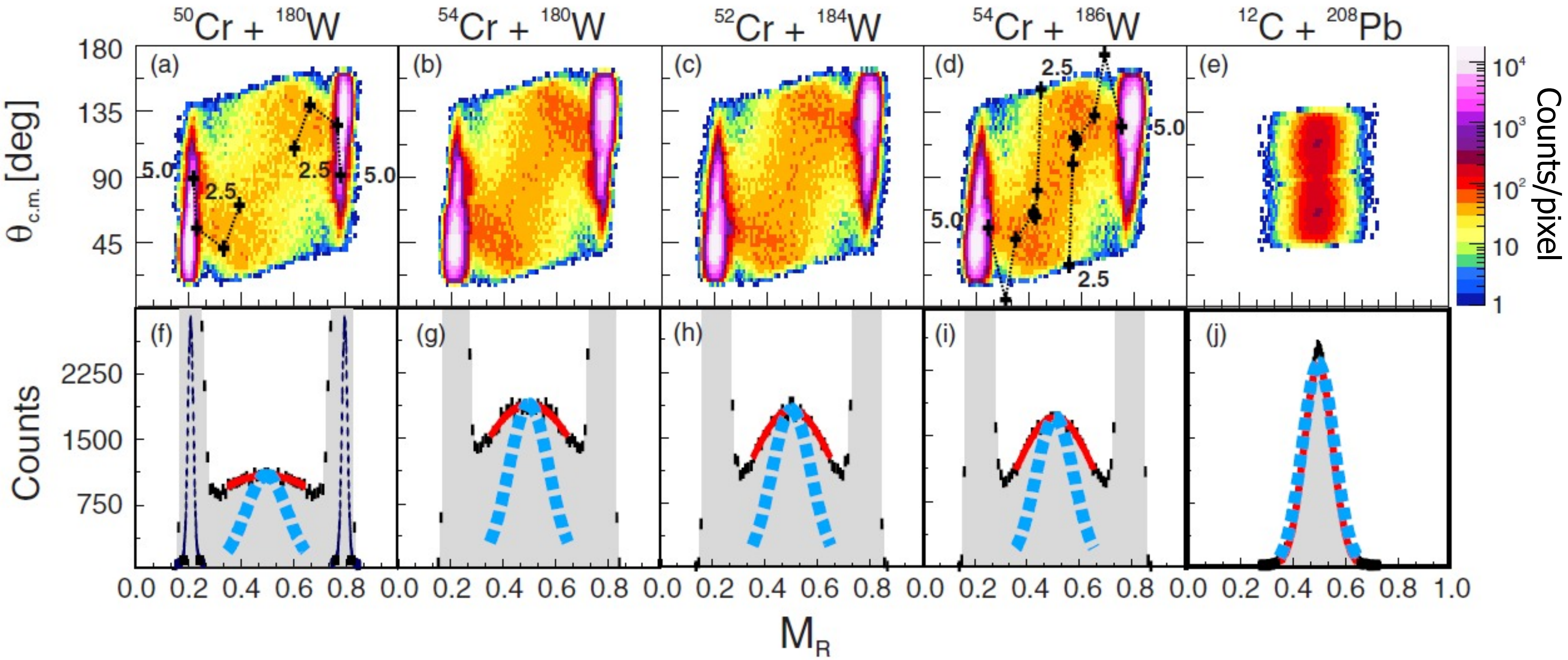

E/V_B = 1.13

Smooth change in mass width with neutron number

K. Hammerton et al., PRC **91** (2015) 041602

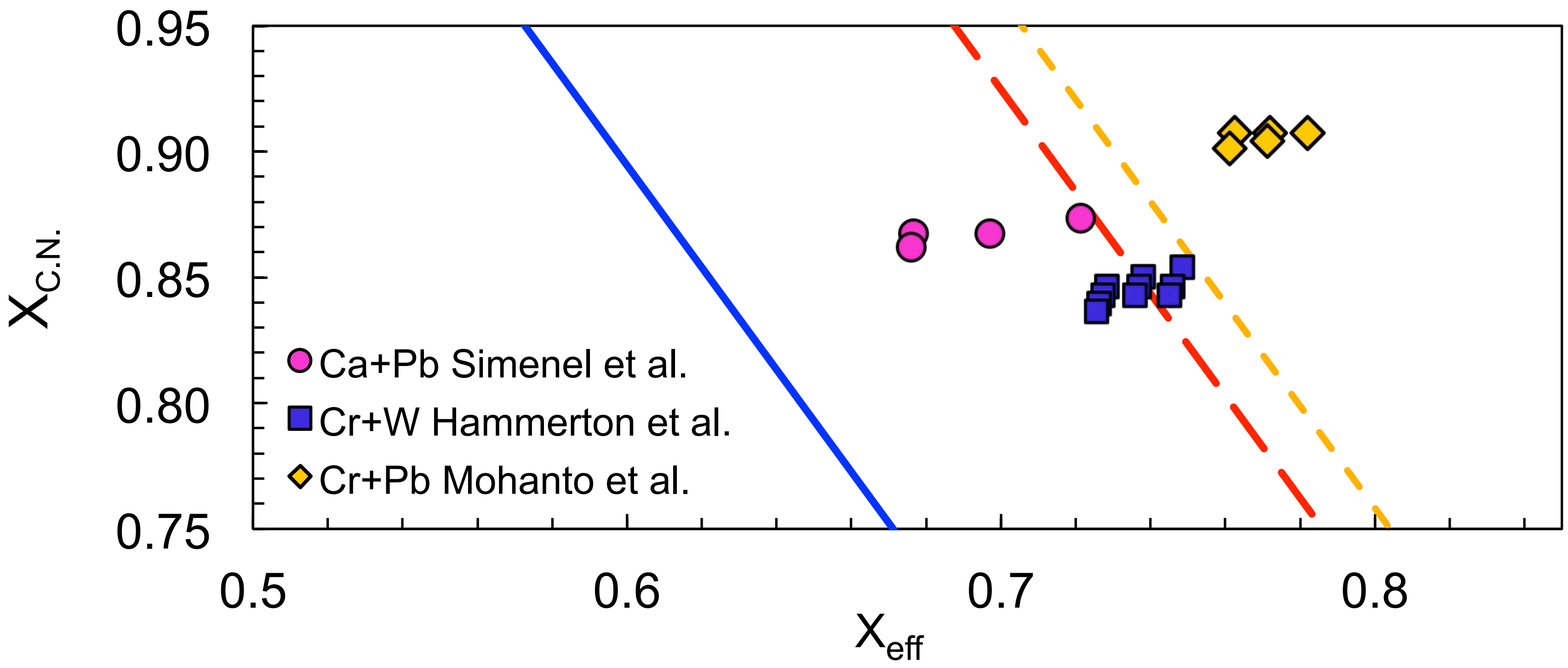

C. Simenel et al., PLB **710** (2012) 607

K. Hammerton et al., PRC **91** (2015) 041602

G. Mohanto et al., ANU, in preparation

Spherical nuclei

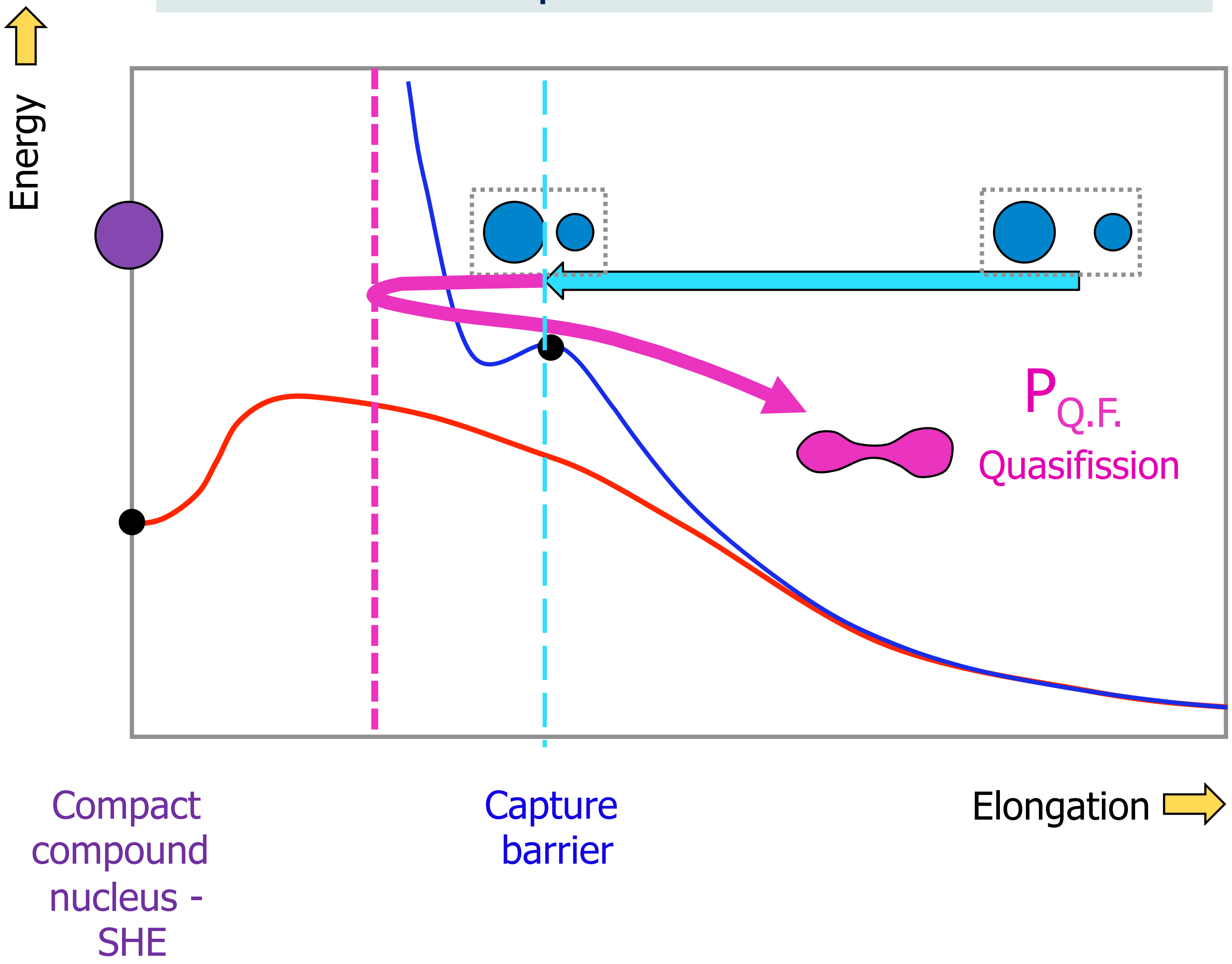

Collisions of magic nuclei

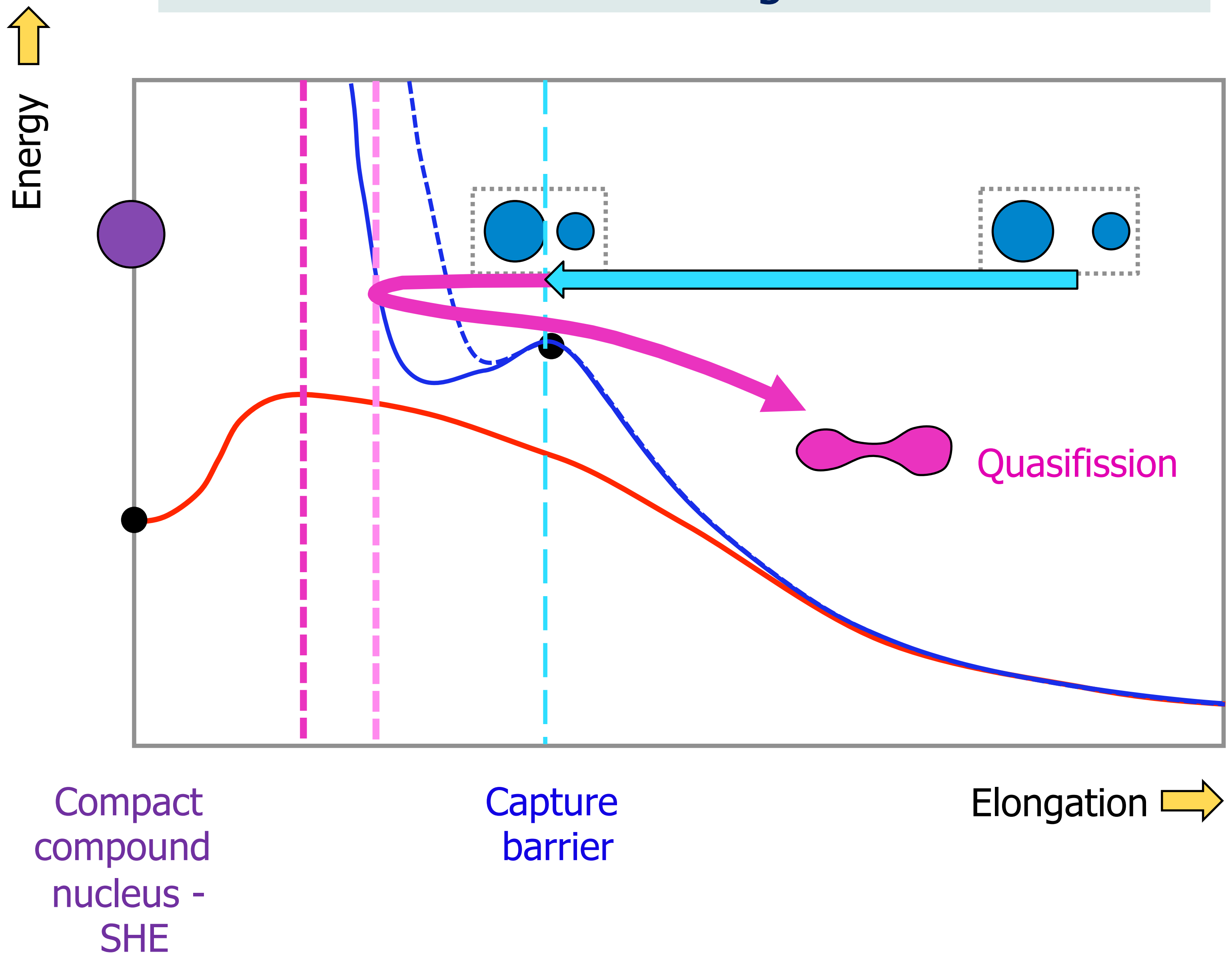

Collisions of magic nuclei

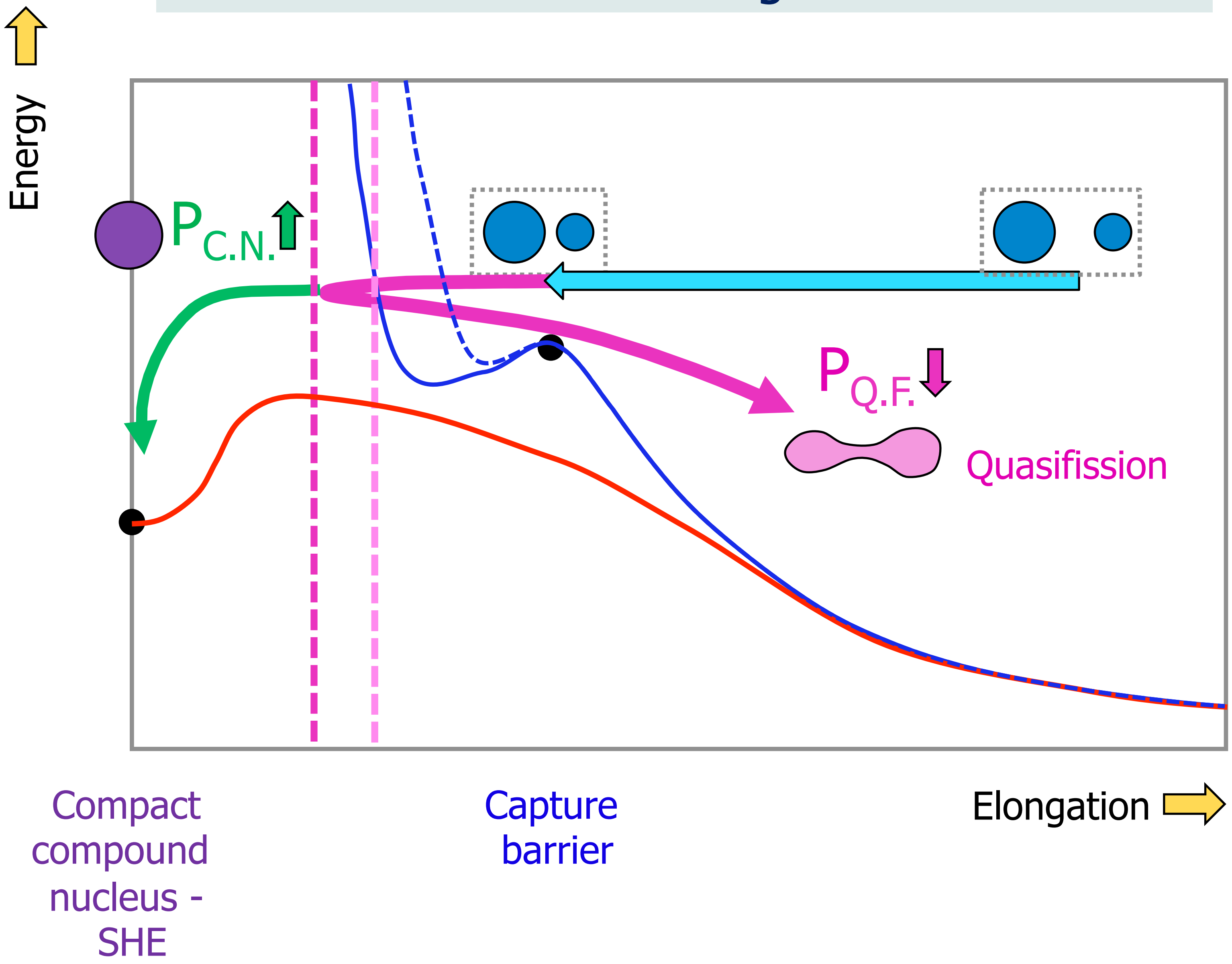

Berriman et al., Nature 413 (2001) 144

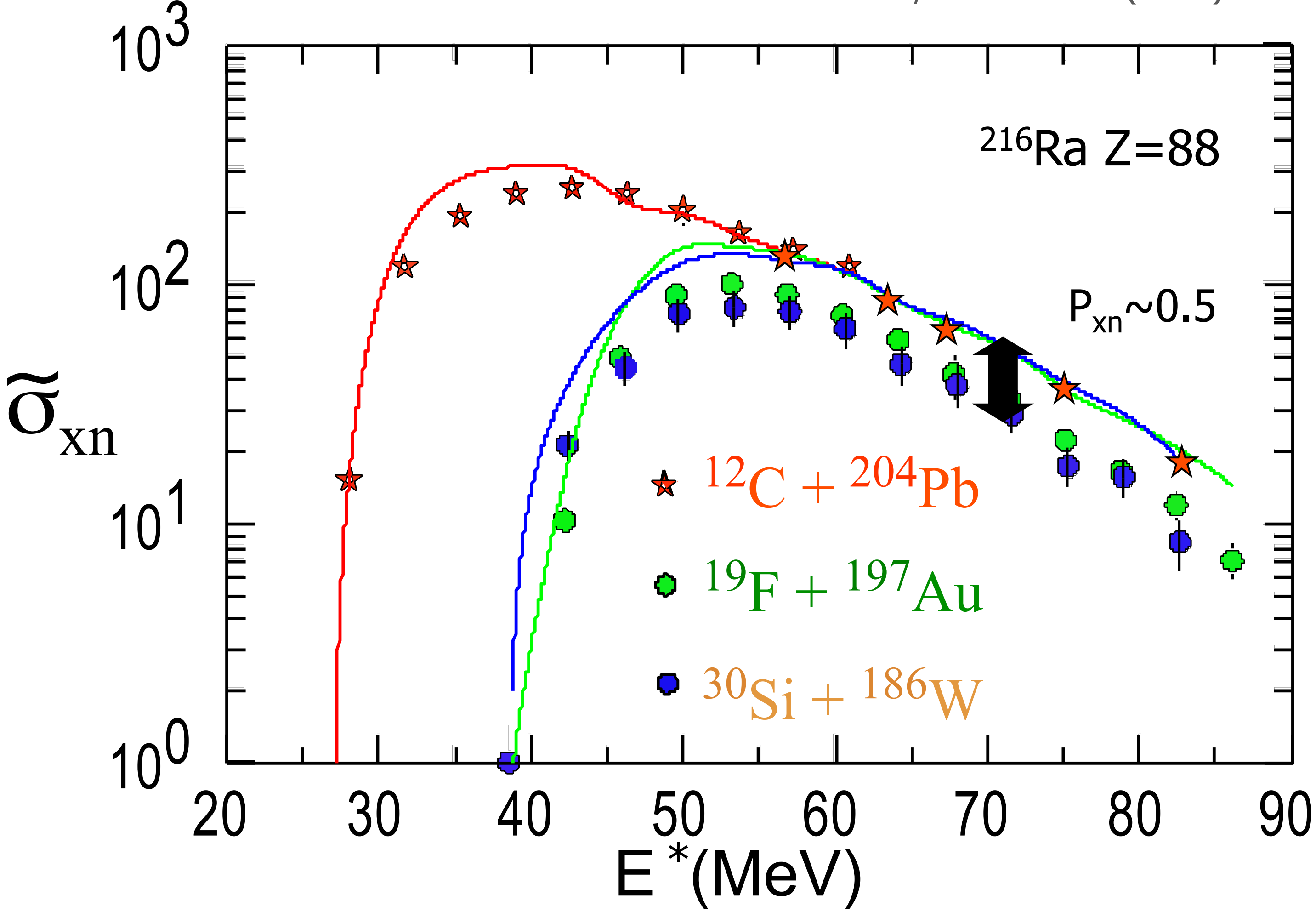

Systematic difference - largest saturated ER yield for the lightest projectile

Unexpected: $P_{xn}<1$ for asymmetric reactions forming Ra

Towards a true understanding of superheavy element synthesis:

- Make unambiguous measurements of P_{CN} from xn ERs – X-bomb.
- Measurements of all observables for selected systems:

  Resolve discrepancies between different observables

  MAD, crystal blocking, CN X-rays, ν_{pre}
- Include important degrees of freedom in models

  and calculate all observables:

  Fission Mass-Angle-Distributions (MAD)

  Fission Mass-TKE-Distributions (MED)

  Scission time distributions, n angular correlations

  Heavy element yields

$^{28}Si + ^{238}U \longrightarrow ^{266}Sg$

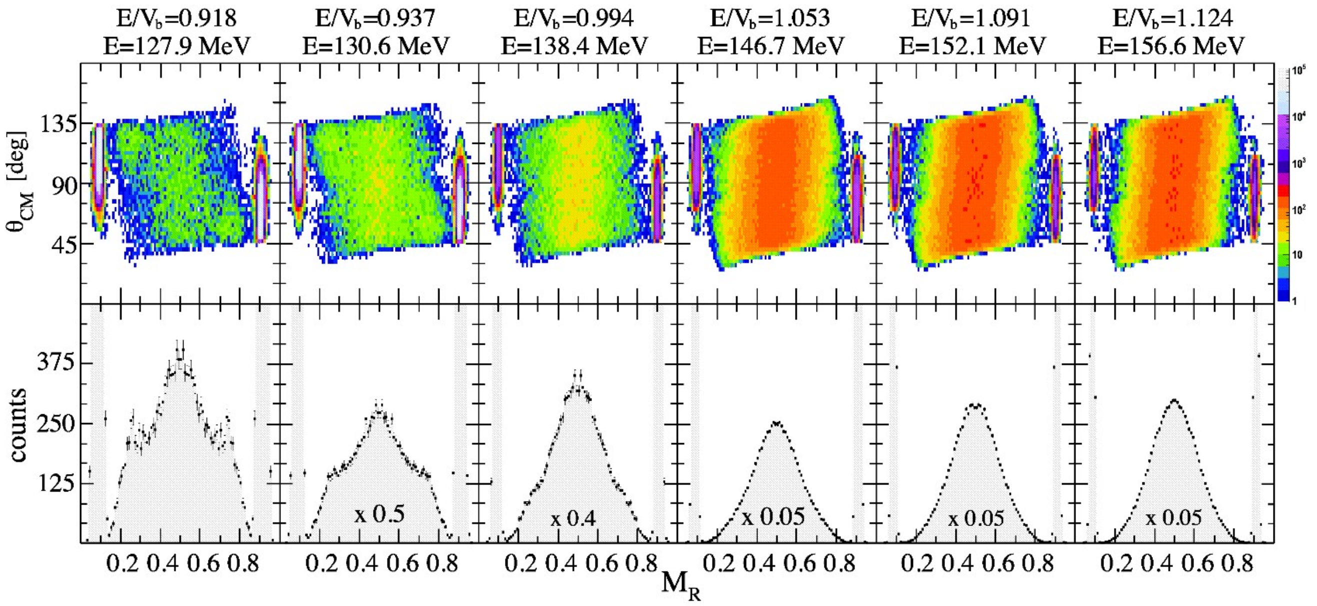

$^{34}S + ^{232}Th \longrightarrow ^{266}Sg$

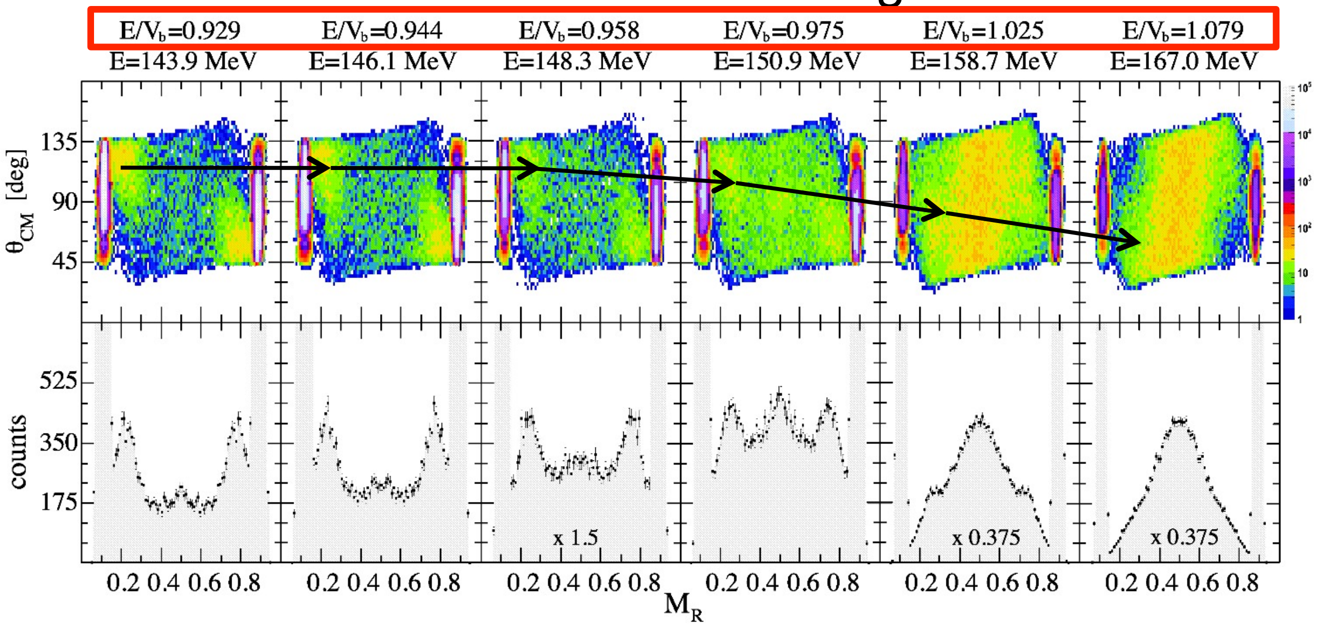

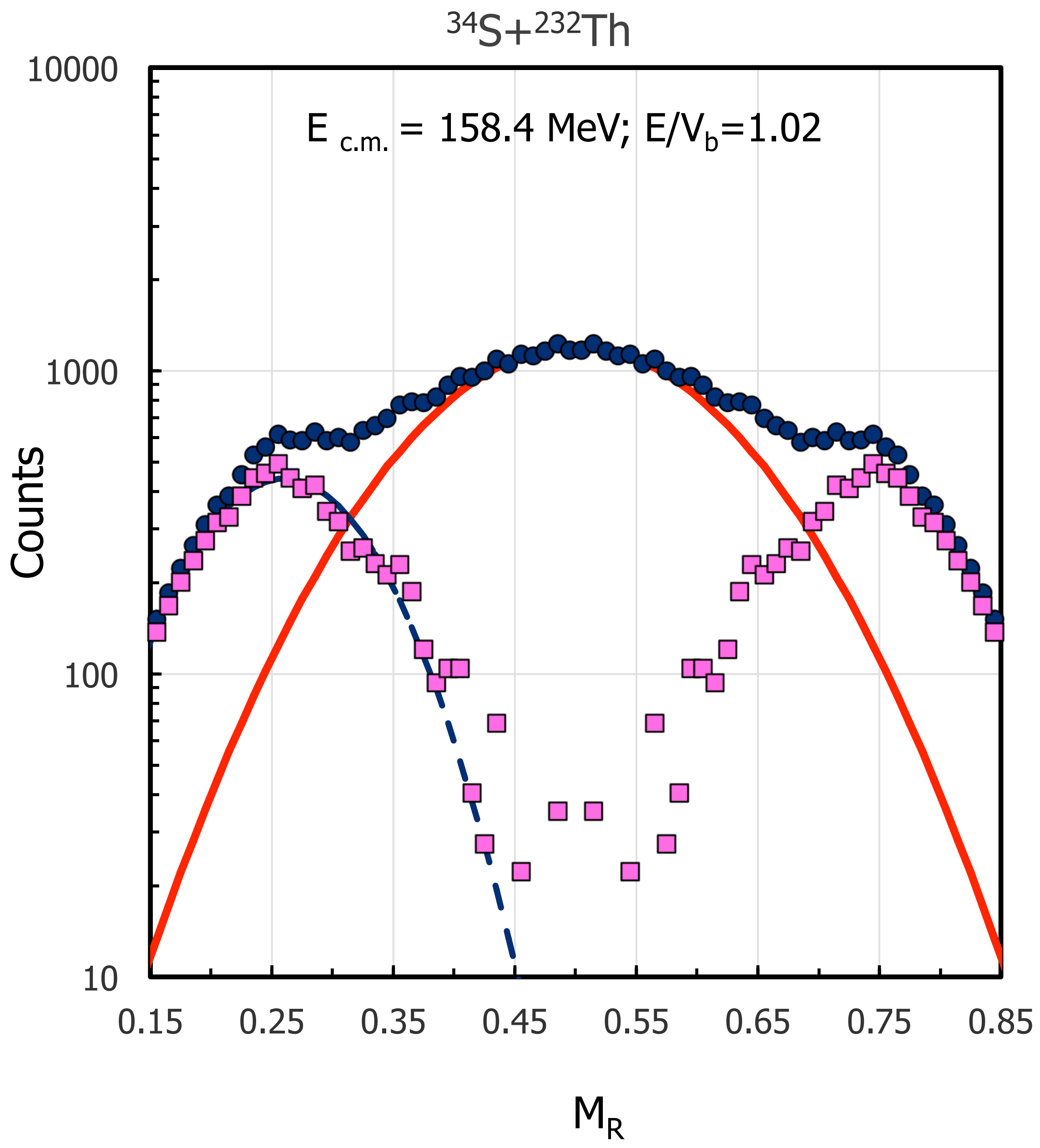

34S+232Th
E c.m. = 158.4 MeV; E/Vb=1.02
Counts
10000
1000
100
10
0.15 0.25 0.35 0.45 0.55 0.65 0.75 0.85
MR

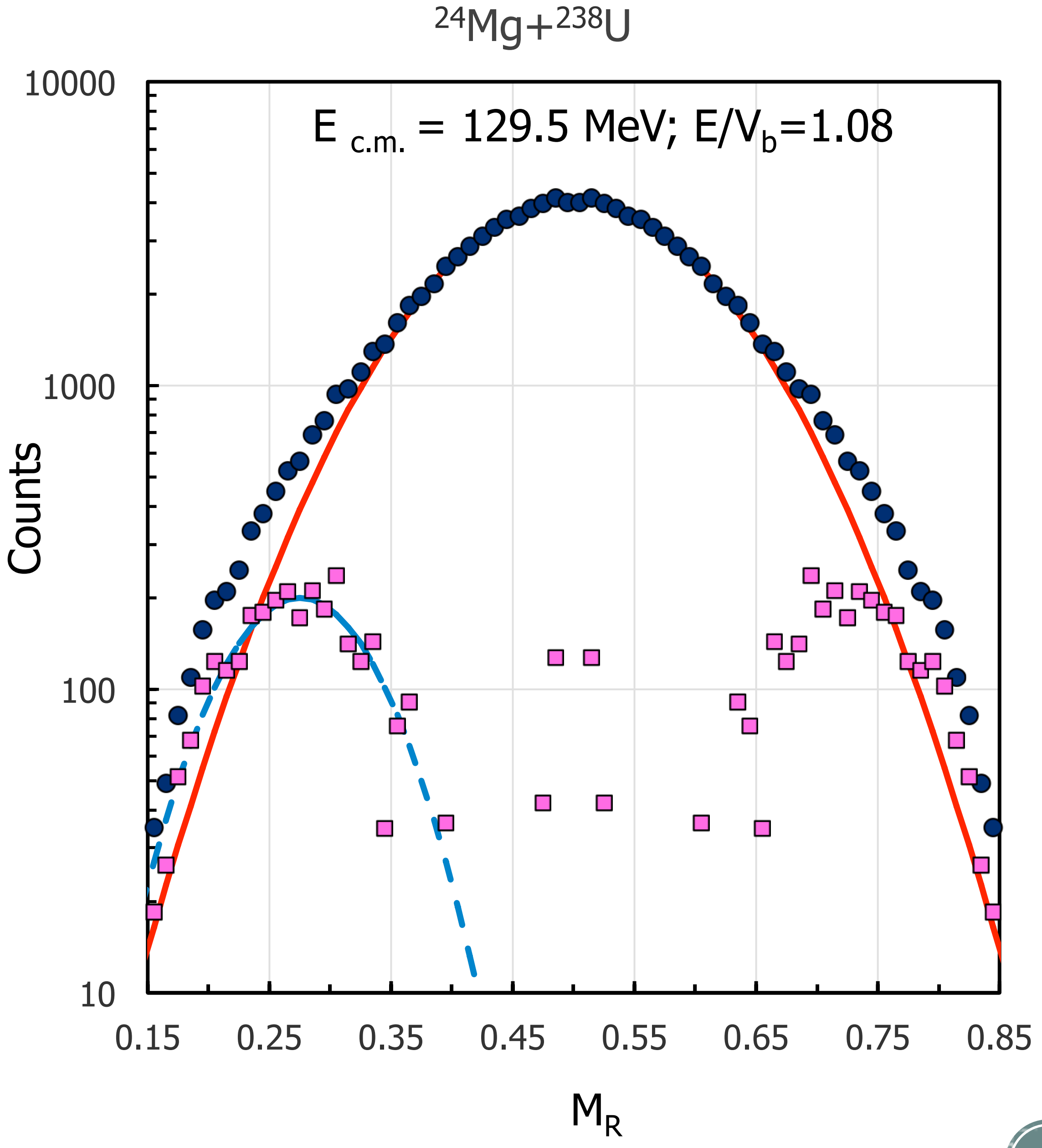

24Mg+238U
E c.m. = 129.5 MeV; E/Vb=1.08
Counts
10000
1000
100
10
0.15 0.25 0.35 0.45 0.55 0.65 0.75 0.85
MR

Sum CC calculations of l-distributions for each classical orientation angle

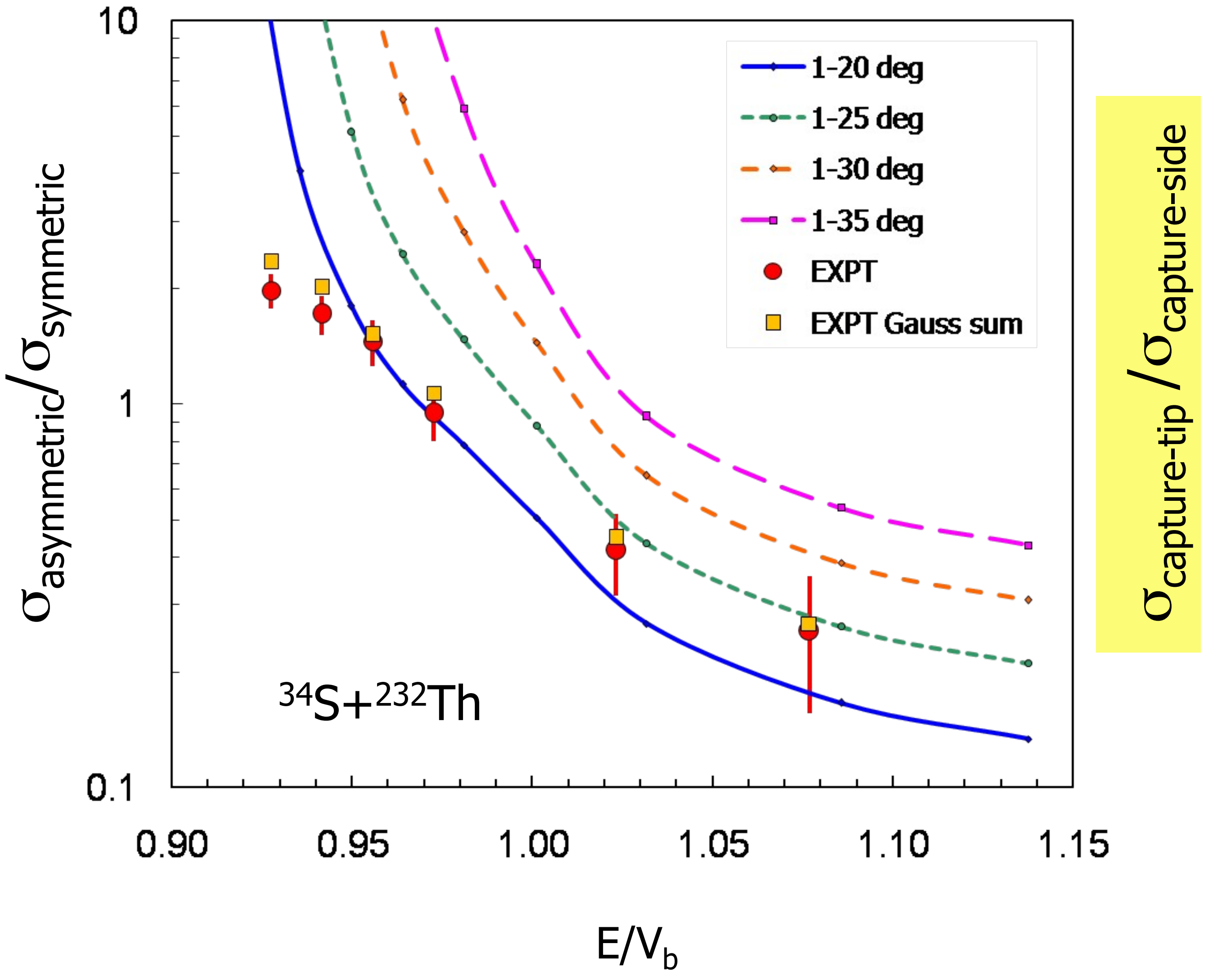

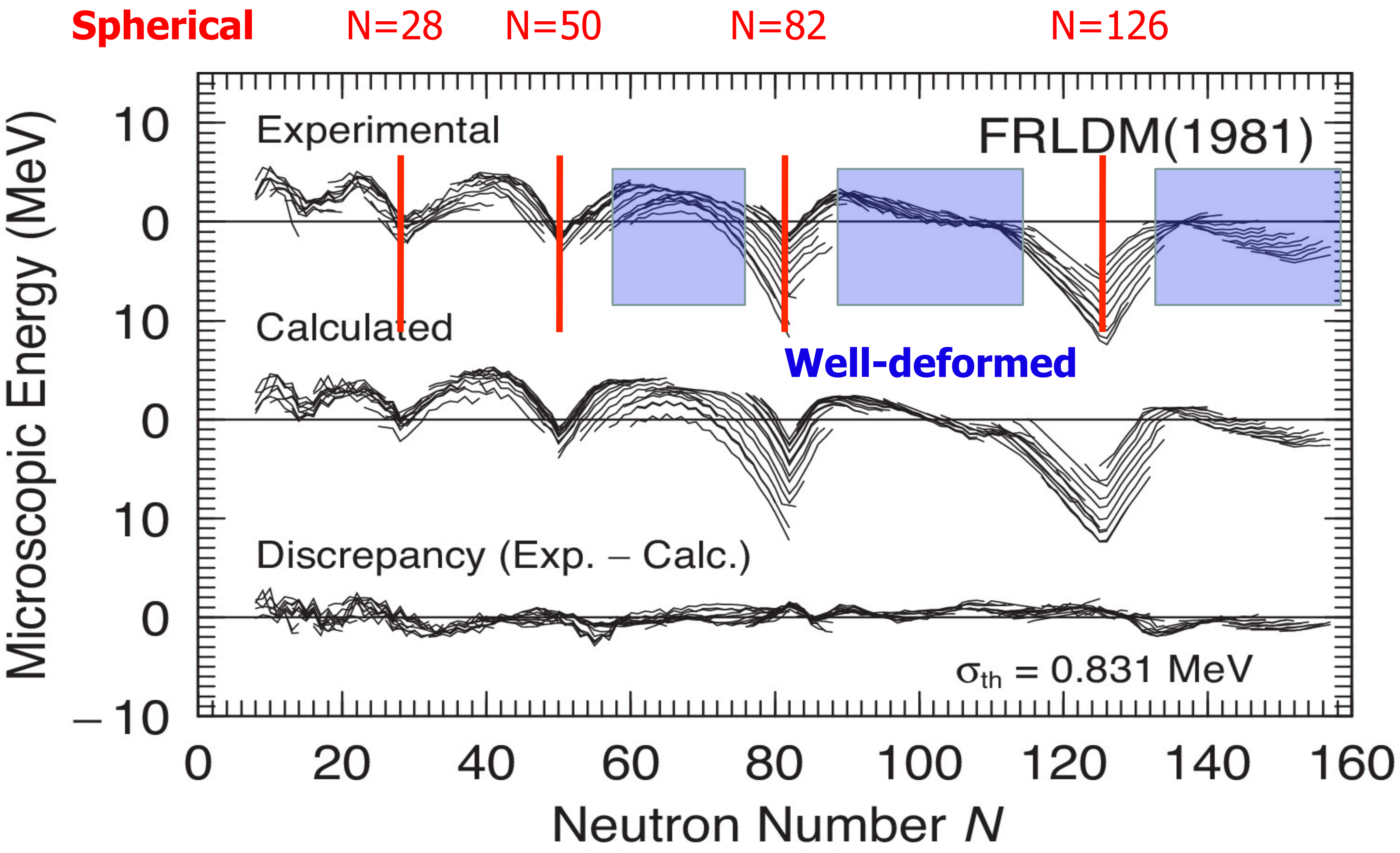

Fig. 1 Differences between experimental masses and a recent macroscopic (semiempirical) mass model as a function of neutron number (top section). Isotopes are connected by lines. The large

80 Years of the liquid drop—50 years of the macroscopic–microscopic model

P. Möller , A.J. Sierk

International Journal of Mass Spectrometry, Volumes 349–350, 2013, 19 - 25